A search for charged Higgs bosons in multilepton final states and a measurement of pp → WZ → lνl'l' with the CMS detector at the LHC

Devin Taylor, UW-Madison

Final Oral Committee:

Sridhara Dasu

Mark Eriksson

Lisa Everett

Matt Herndon

Wesley Smith

1

Rice University

- Fall 2008: Matriculated
  - Hanszen College
- Spring 2012: Bachelor of Science in Physics
- Research
  - Electron-positron pair production from high intensity laser irradiating solid targets
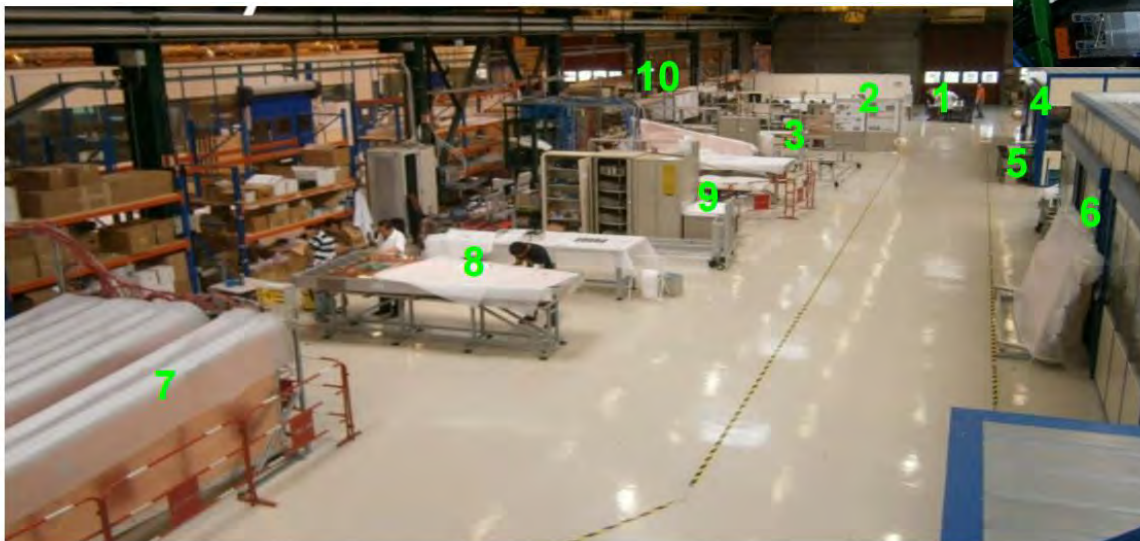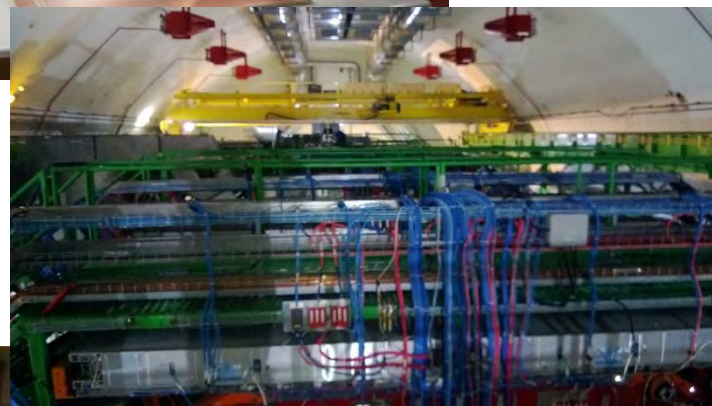 - Petawatt laser at UT Austin

E. Liang et al. "High e+/e− Ratio Dense Pair Creation with 10^{21} W.cm^{-2} Laser Irradiating Solid Targets" *Scientific Reports* 5, 13968 (2015) doi:10.1038/srep13968

UW—Madison

- Fall 2012: Matriculated
- Summer 2013: CERN
  - Assembly of new muon endcap detectors
    - CSC ME4/2

1) Cleaning and Inspection
2) Anode and Cathode gluing
3) Anode thick wire soldering
4) Anode winding and automatic soldering
5) Electrical component hand soldering
6) High voltage test and chamber assembly
7) Long term HV test
8) Electronics Integration
9) FAST site (cosmic tests)
10) Long term storage

CERN

- Summer 2014: Move to CERN
- June 2015: First 13 TeV collisions
- December 2016: Back to US
- Activities
  - CSC DOC (Detector on call expert)
  - CSC offline performance monitoring
  - CMS reconstruction monitoring
  - 13 TeV WZ cross section measurement
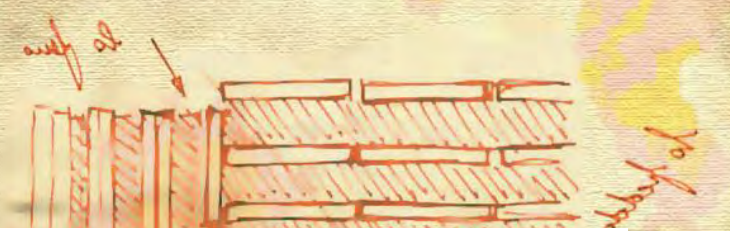 - Doubly-charged Higgs search (8+13 TeV)

Outline

- Theoretical motivation
- The LHC and the CMS detector
- Simulation
- Object reconstruction
- WZ cross section measurement
- Search for doubly-charged Higgs boson
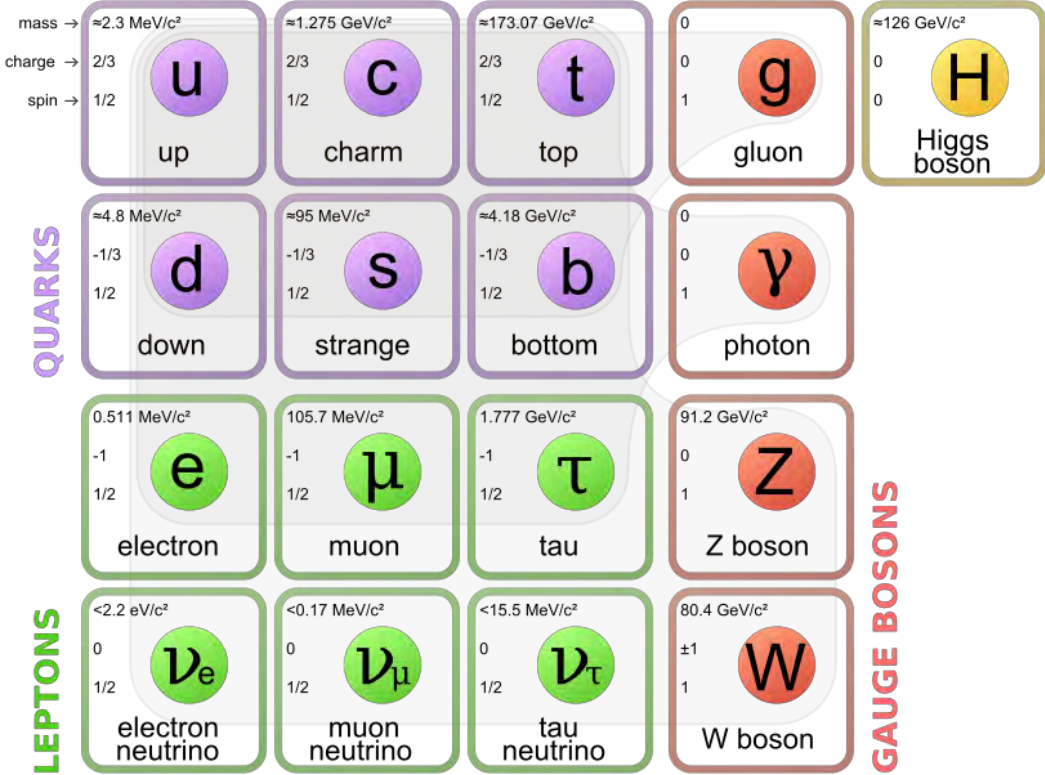- Conclusions and future outlook

THEORETICAL MOTIVATION

The Standard Model

- Fermions
  - Spin-1/2
  - Quarks and leptons in three generations
  - Each has associated antiparticle with opposite charge
- Gauge bosons
  - Spin-1 mediators of Standard Model (SM) interactions
- Higgs boson
  - Scalar boson

Particle Interactions

- Quantum Chromodynamics (QCD)
  - Interactions between color charges
  - Mediated by the gluon
  - Strong force
- Electroweak interaction (EWK)
  - Electrodynamics
    - Charge conservation
    - Mediated by the photon
  - Weak interaction
    - Three massive gauge bosons mediate
- Higgs mechanism
  - Higgs boson couples to mass
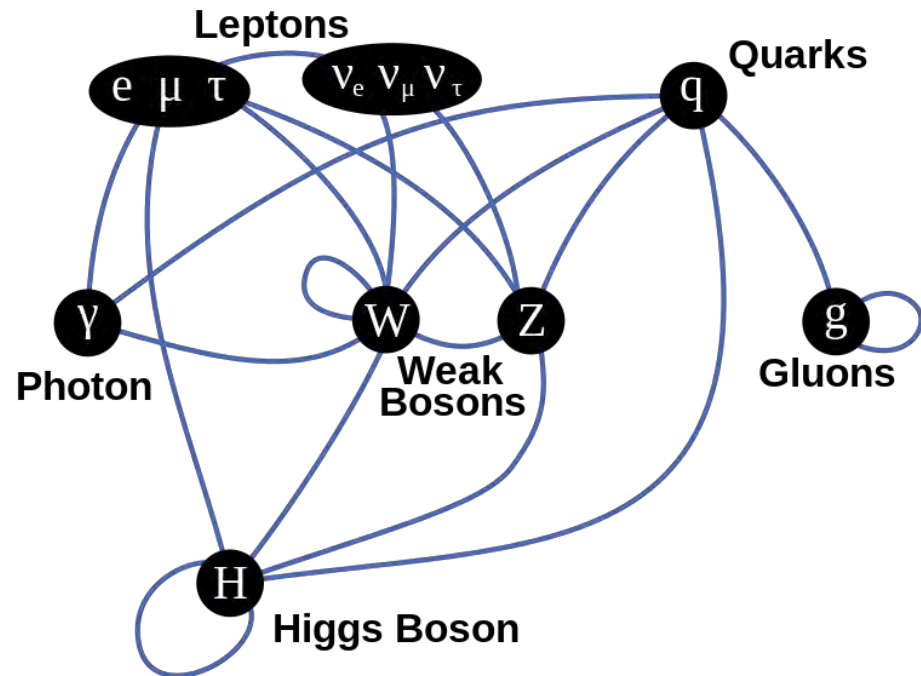
Electroweak Symmetry Breaking

- Electroweak symmetry group
  - SU(2)$_L$ X U(1)$_Y$
  - Gives four massless gauge bosons
- Electroweak symmetry breaking
  - Add Higgs doublet (two complex scalar fields)
  - Three free parameters give rise to mass of W/Z
  - Fourth becomes Higgs boson
  - Vacuum expectation value (VEV): 246 GeV
- Fermion mass arises through Yukawa coupling

$$\phi = \begin{pmatrix} \phi^+ \\ \phi^0 \end{pmatrix}$$

$$M_W = \frac{vg}{2}$$

$$M_Z = \frac{v\sqrt{g^2 + g'^2}}{2}$$

$$M_Z = \frac{M_W}{\cos\theta_W}$$
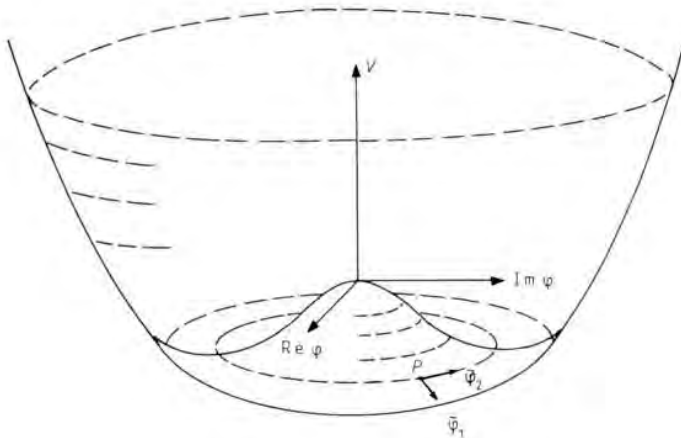
$$\mathcal{L}_{YUK} = \frac{\sqrt{2}m_f}{v}(\bar{f}_L f_R + \bar{f}_R f_L)$$
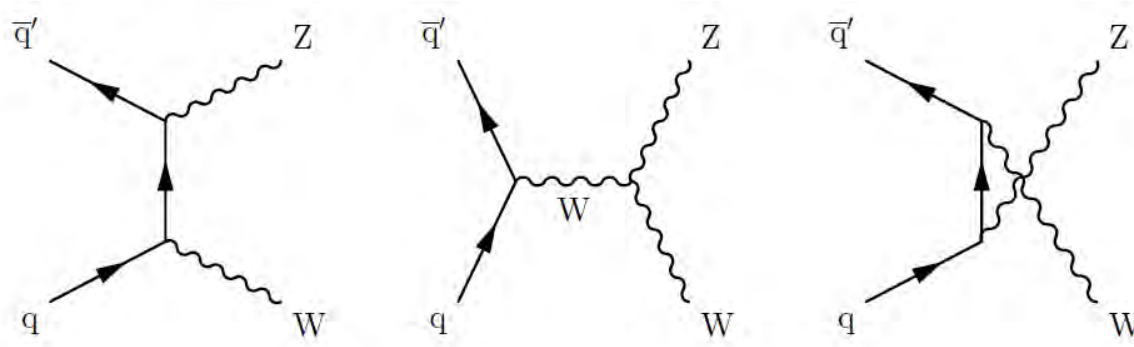
WZ Production

- The measurement of the WZ cross section at proton-proton colliders has the ability to probe both QCD and the EWK triple and quartic gauge couplings (TGC and QGC)

  - The measurement discussed here probes QCD and EWK TGC
  - Deviations from SM prediction expected in models with additional gauge or Higgs bosons

Tree level
diagrams

Vector boson
scattering (VBS)
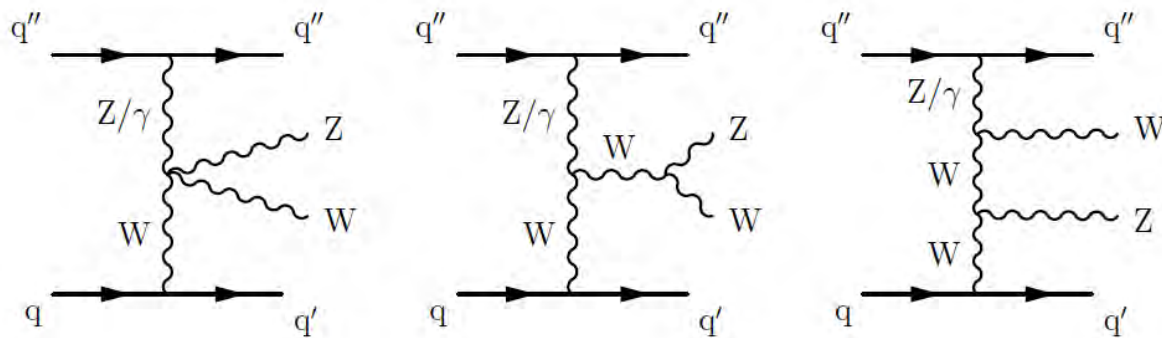
Φ^{++} Type II Seesaw Mechanism

- Includes a Higgs triplet, Φ
- Gives rise to a new interaction term that allows lepton flavor violation

$$\mathcal{L} = i\bar{l}^c_{Li}\tau_2 Y^{ij}_\Phi (\tau \cdot \Phi) l_{Lj} + h.c.$$

$$\Phi = \begin{pmatrix} \frac{\Phi^+}{\sqrt{2}} & \Phi^{++} \\ \Phi^0 & \frac{-\Phi^+}{\sqrt{2}} \end{pmatrix} \qquad (m_\nu)_{ij} = 2 (Y_\Phi)_{ij} v_\Phi$$

- Φ vacuum expectation value arises from the neutral component coupling to the standard model Higgs doublet (not symmetry breaking)
- The decay to W^+W^+ is suppressed with the assumption that the VEV is small
  - Natural assumption from non-observation in precision data and small neutrino masses
- Neutrino masses (in flavor basis) could then be extracted from the Φ^{++} lepton Yukawa coupling strengths

CMS

Pair and Associated Production

- Pair production (PP)
  - 4 lepton final states
  - Primary search channel for Tevatron and LHC (also LEP in addition to modification to Bhabha scattering)
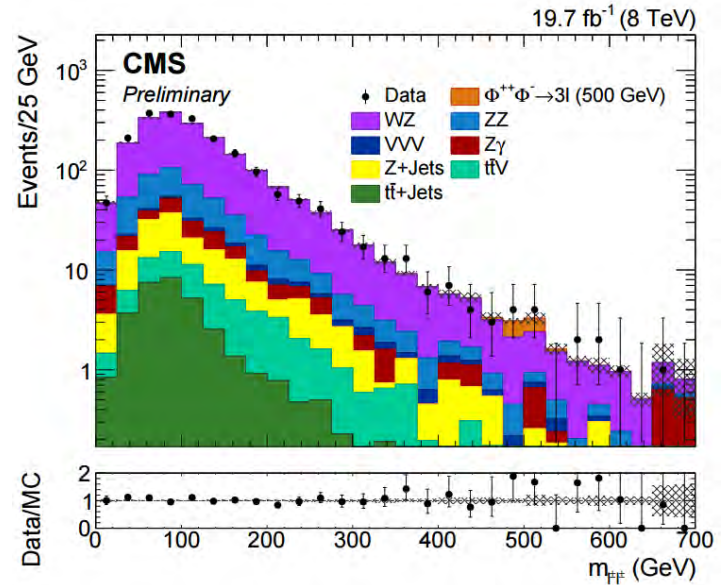
- Associated production (AP)
  - 3 lepton final states
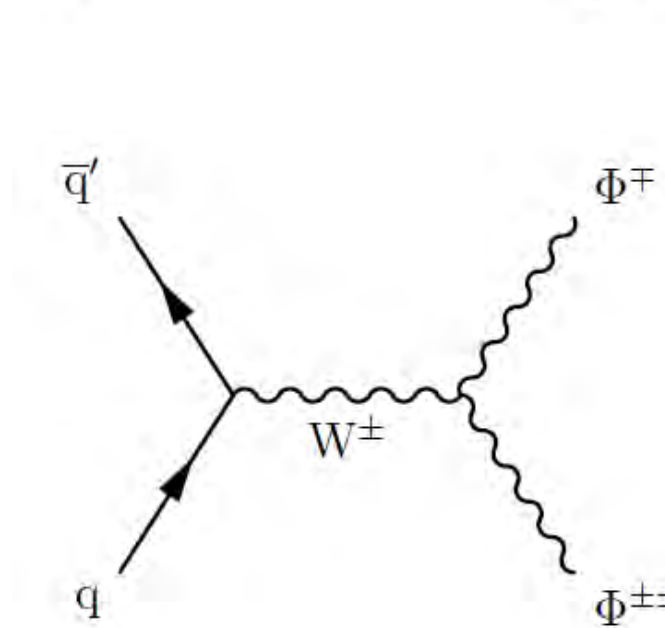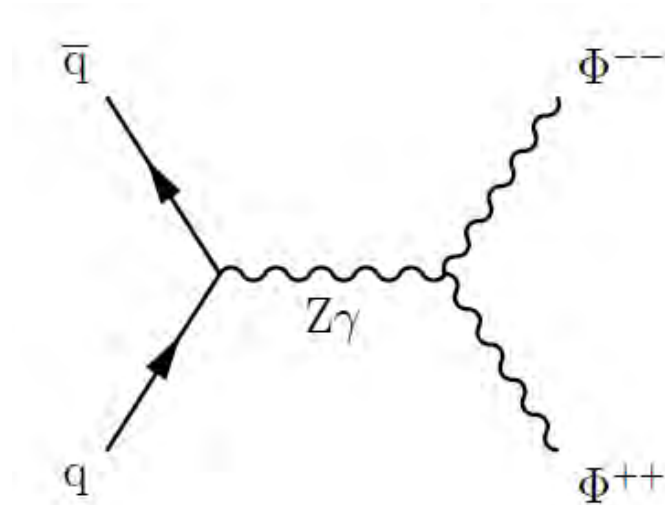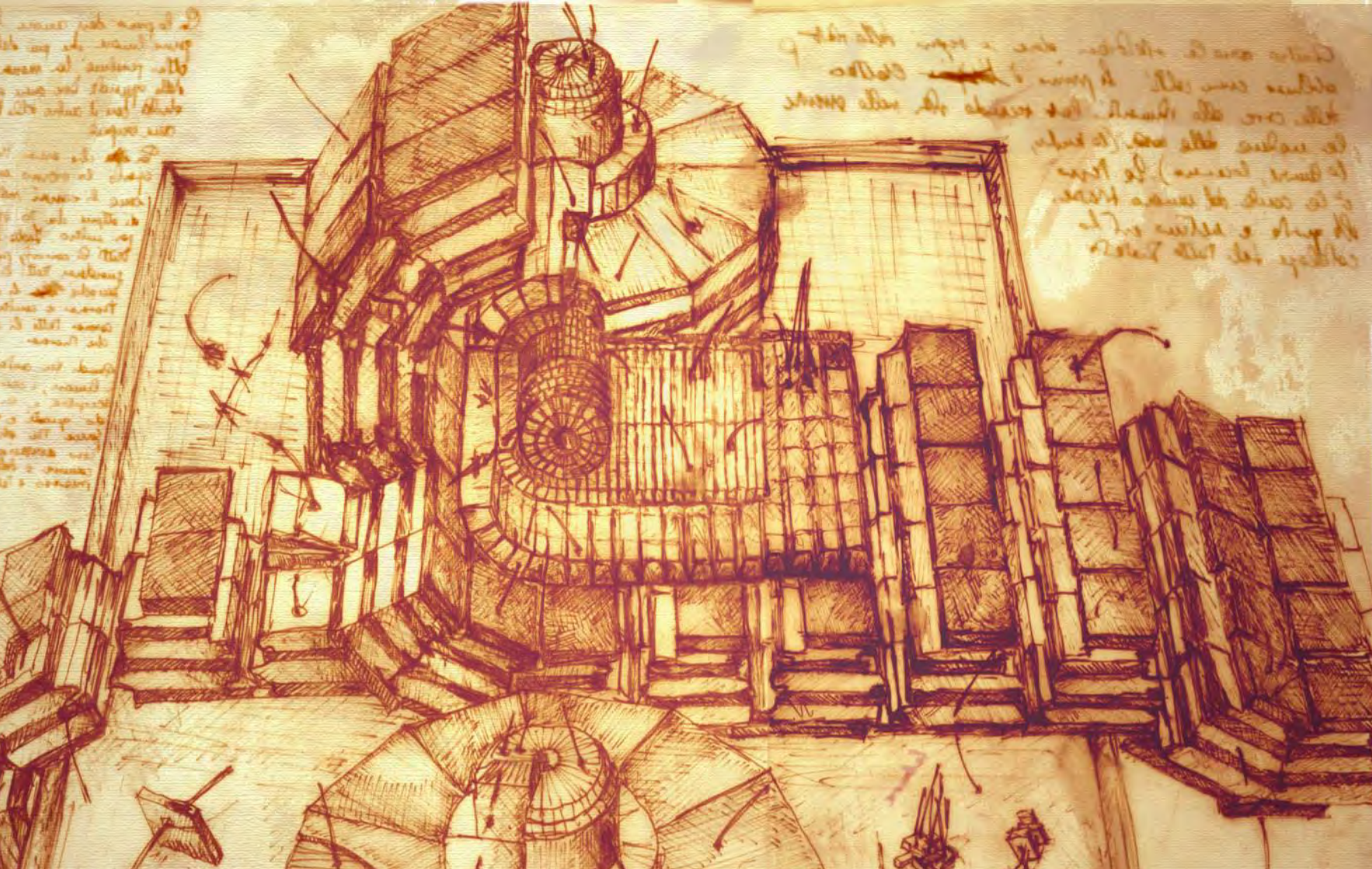
Φ^{++} Current Experimental Limits

- CMS
  - e, μ, τ with 4.9 fb^{-1} (7 TeV)*
  - e, μ with 19.7 fb^{-1} (8 TeV)
  - 3 and 4 lepton final states
- ATLAS
  - e, μ with 20.3 fb^{-1} (8 TeV)
  - 2 lepton final state

Scenario	CMS PP	ATLAS PP	CMS AP
$BR(\Phi^{\pm\pm} \to e^{\pm}e^{\pm}) = 100\%$	550 (550)	551 (553)	517 (517)
$BR(\Phi^{\pm\pm} \to e^{\pm}\mu^{\pm}) = 100\%$	569 (568)	468 (487)	521 (521)
$BR(\Phi^{\pm\pm} \to e^{\pm}\tau^{\pm}) = 100\%$	353 (395)	–	312 (336)
$BR(\Phi^{\pm\pm} \to \mu^{\pm}\mu^{\pm}) = 100\%$	576 (575)	516 (543)	526 (526)
$BR(\Phi^{\pm\pm} \to \mu^{\pm}\tau^{\pm}) = 100\%$	381 (418)	–	316 (352)
$BR(\Phi^{\pm\pm} \to \tau^{\pm}\tau^{\pm}) = 100\%$	169 (155)*	–	130 (120)*

13

THE LHC AND CMS DETECTOR

14

CMS

The Large Hadron Collider

- Proton-proton collider near Geneva, Switzerland
  - 27 km circumference
  - Design center of mass energy of 14 TeV
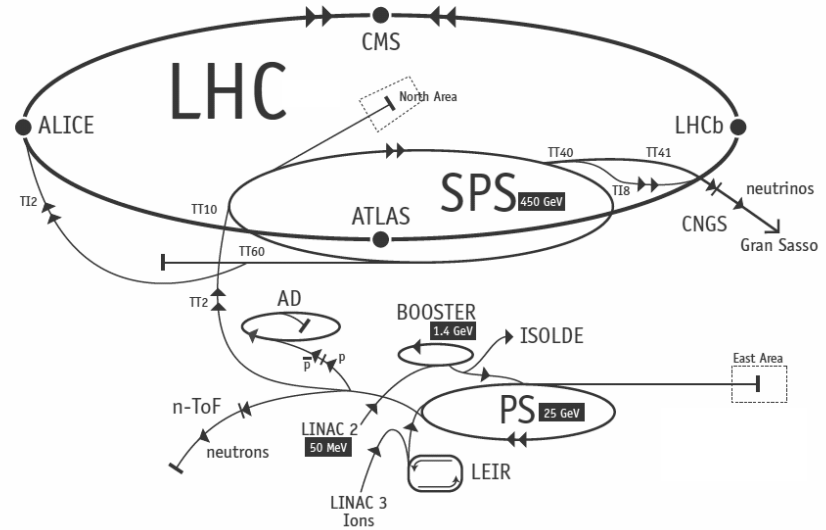
CMS Integrated Luminosity, pp
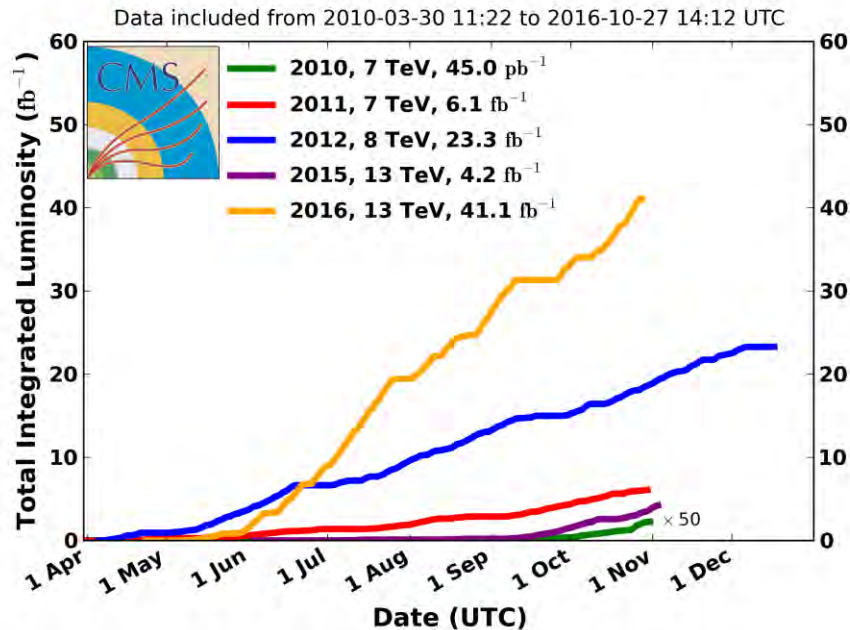
The CMS Detector

- The central feature of CMS is the large 3.8 T solenoid magnet
  - Length: 12.5 m, diameter: 6.3 M
  - Cooled to 4.7 K
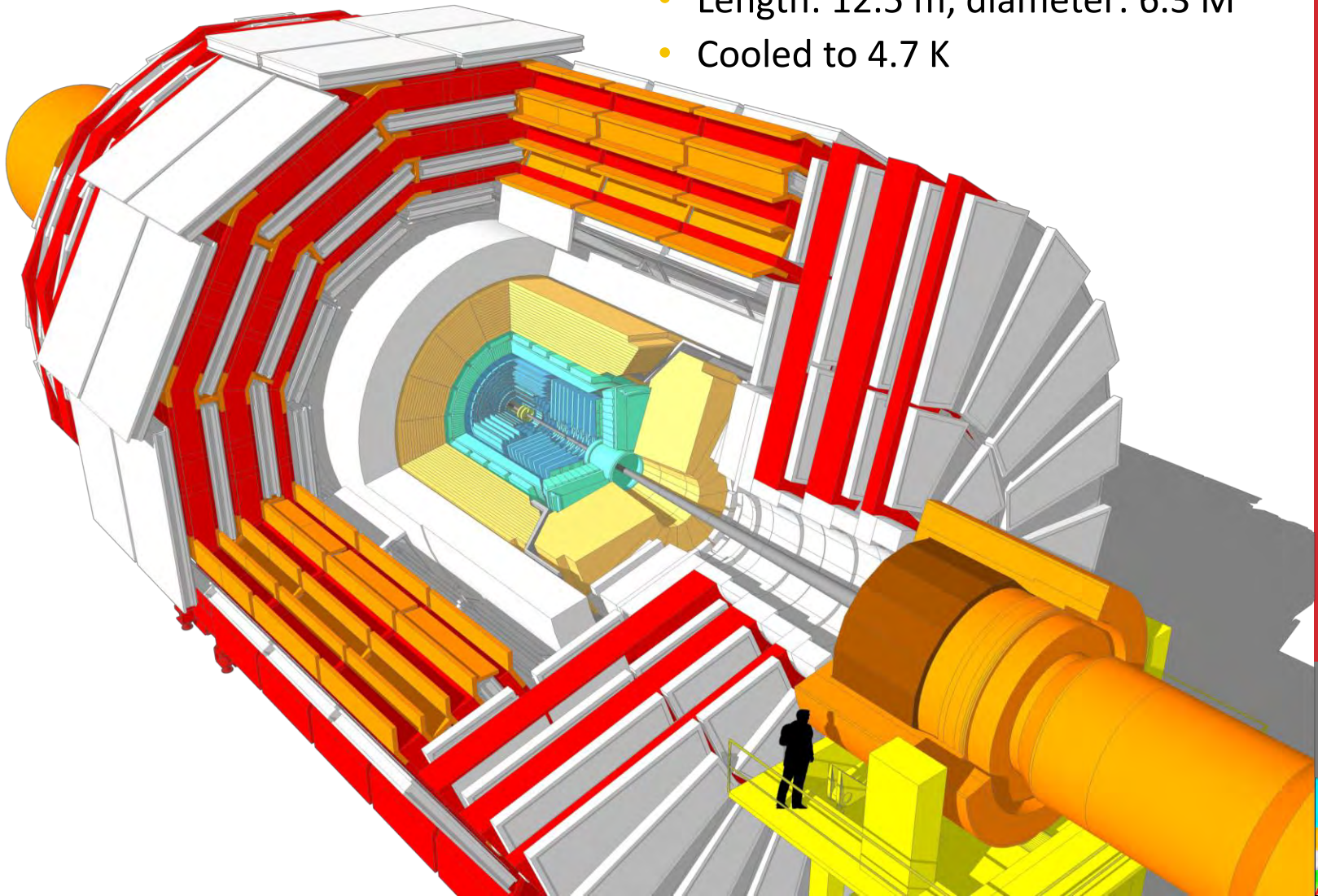
Pixel and Silicon Tracker

- Silicon Pixel Detector
  - 3 barrel layers, 2 disks each endcap
- Silicon Strip Detector
  - Outside pixel detector
  - Inner and outer barrel and endcap
- Coverage: |η| < 2.5
- Resolution (in barrel): $\frac{\delta p_T}{p_T} = \left(15 \frac{p_T}{TeV} \oplus 0.5\right) \%$
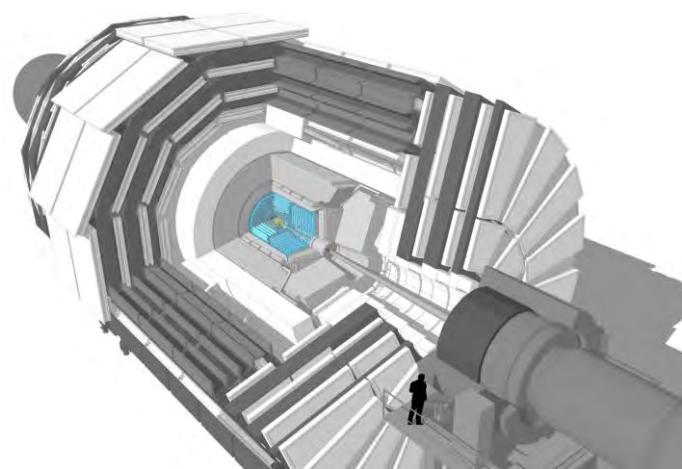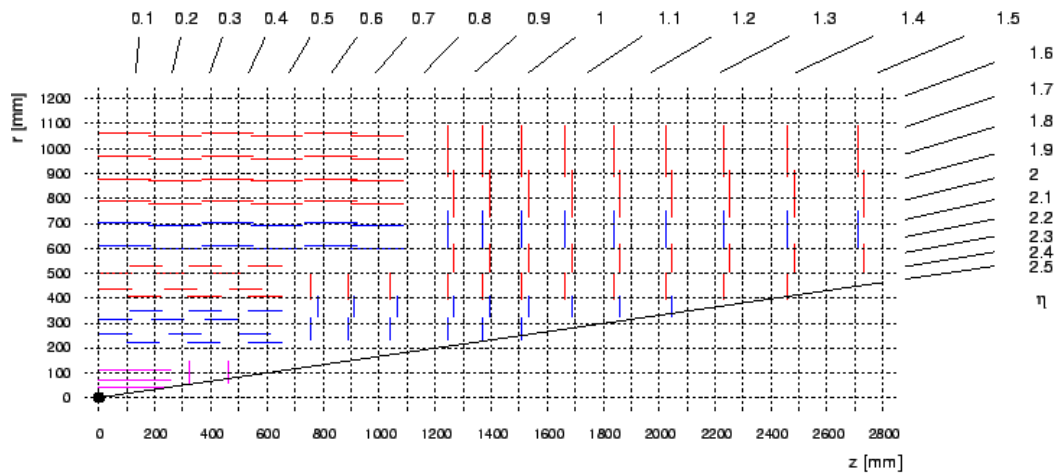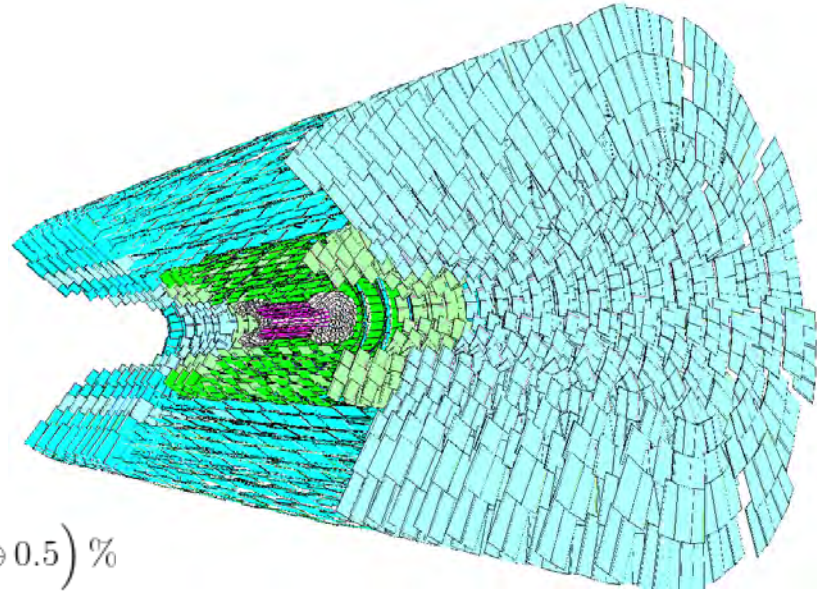
Electromagnetic Calorimeter

- PbWO$_4$ Crystals with photodetectors
  - Barrel Region, $|\eta| < 1.479$
    - Length 230 mm, 25.8 X$_0$
  - Endcap Region, $1.479 < |\eta| < 3.0$
    - Length 220 mm, 24.7 X$_0$
- Preshower detector
  - $1.653 < |\eta| < 2.6$
  - Silicon strips
- Resolution: $\left(\dfrac{\sigma}{E}\right)^2 = \left(\dfrac{2.8\%}{\sqrt{E}}\right)^2 + \left(\dfrac{0.12}{E}\right)^2 + (0.3\%)^2$

Barrel ECAL (EB)

$= 1.479$

$= 1.653$

Preshower (ES)

$= 2.6$

$= 3.0$

Endcap ECAL (EE)
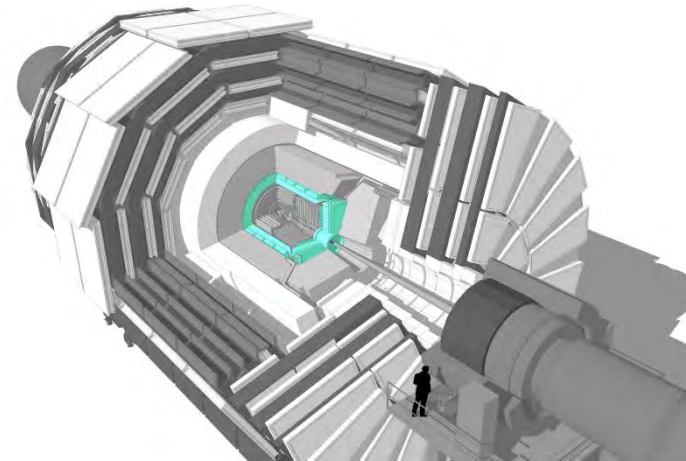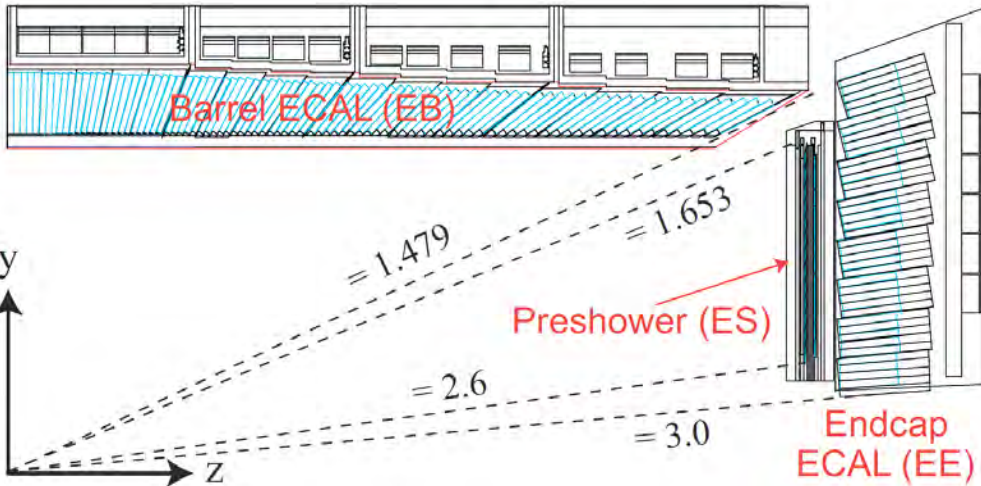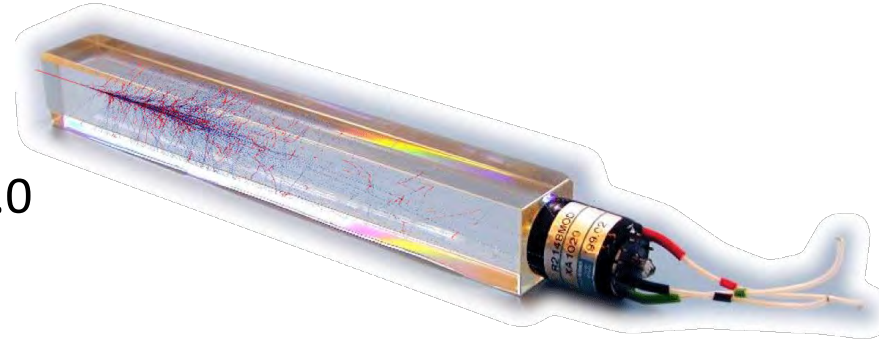
Hadronic Calorimeter

- Brass and steel absorbers
  - Steel outer and inner absorber layers
  - 14 brass absorber layers
- Scintillator
  - Between absorber layers
- HCAL Barrel (HB)
  - |η| < 1.3
  - 5.8-10.6 λ (+1.1 λ from ECAL)

$$\left(\frac{\sigma}{E}\right)^2 = \left(\frac{115\%}{E}\right)^2 + (5.5\%)^2$$

- HCAL Endcap (HE)
  - 1.3 < |η| < 3.0
  - ~10 λ (including ECAL)

$$\left(\frac{\sigma}{E}\right)^2 = \left(\frac{280\%}{E}\right)^2 + (11\%)^2$$

- HCAL Outer (HO)
  - 5 rings outside the solenoid
- HCAL Forward (HF)
  - 3.0 < |η| < 5.2
  - Cherenkov-based detector
  - Quartz fibers with steel absorber
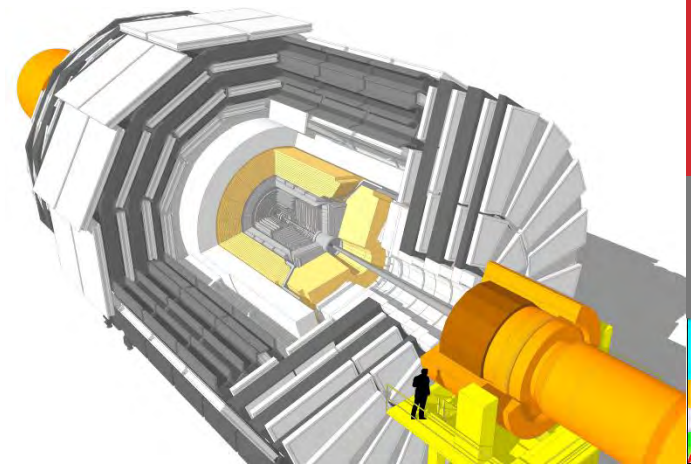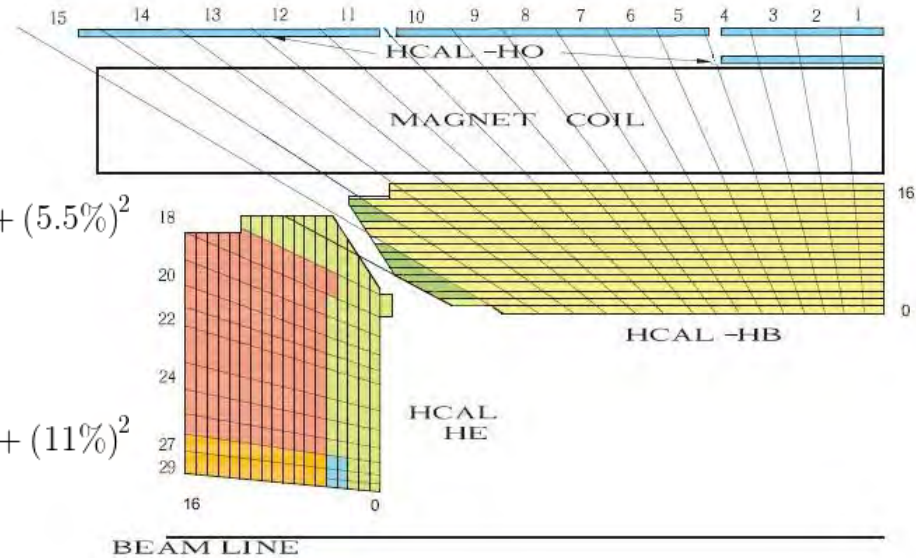
The Muon System

- Embedded in CMS solenoid return yoke
  - 2 T magnetic field
- Drift Tubes
  - Barrel region, $|\eta| < 1.2$
- Cathode Strip Chambers
  - Endcap region, $0.9 < |\eta| < 2.4$
- Resistive Plate Chambers
  - Barrel and Endcap, $|\eta| < 1.8$
- Relative p_T resolution (with tracker)
  - 2% in barrel
  - 6% in endcap

6 layers

20
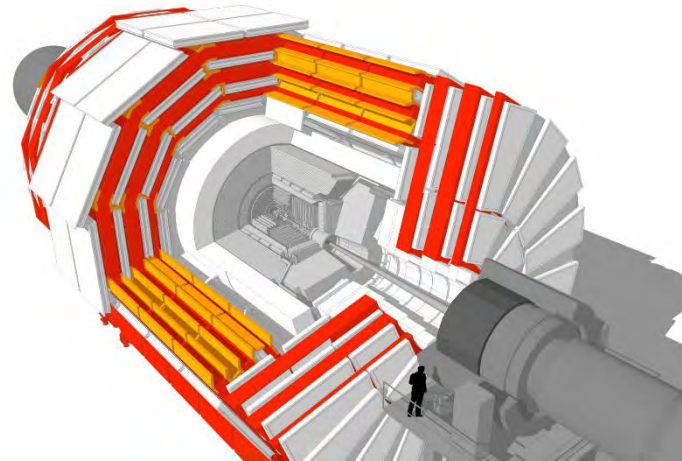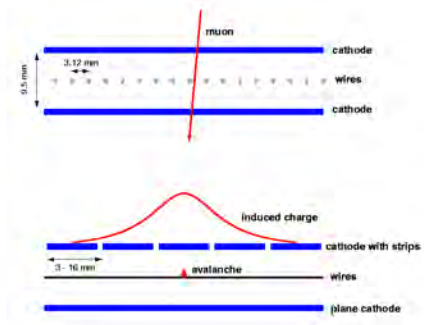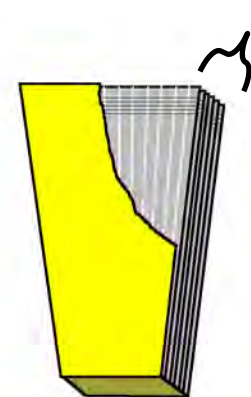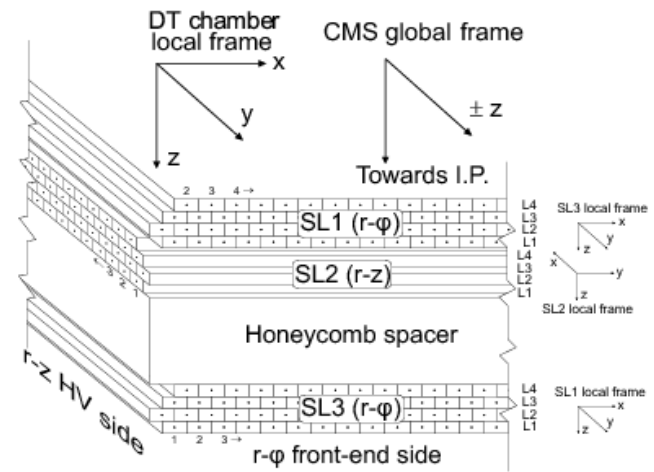
Muon System Diagram

21
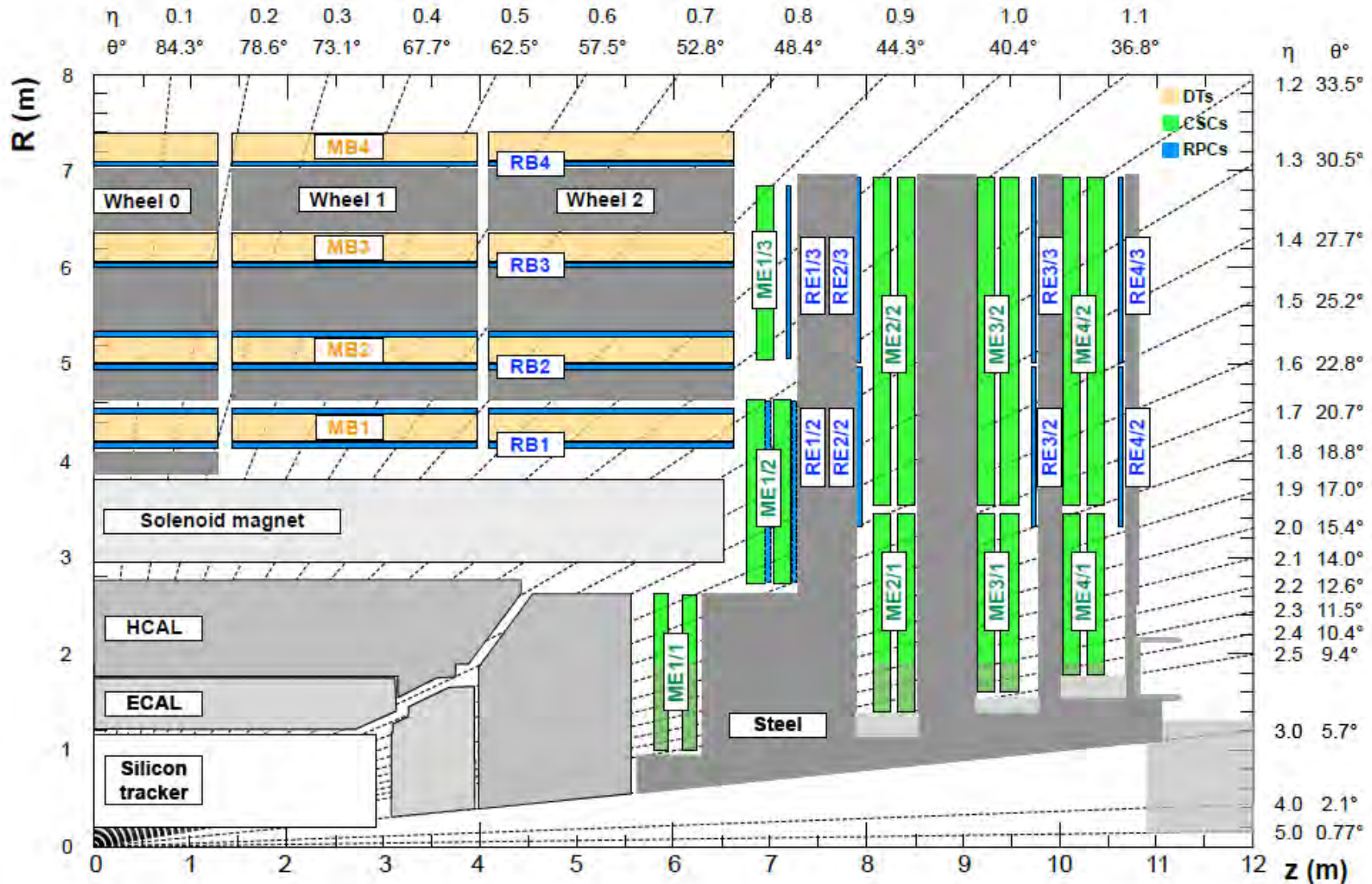
CMS Trigger System

- Level 1 Trigger
  - Separate calorimeter and muon trigger paths
  - Dedicated on detector and peripheral electronics
  - At 25 ns bunch spacing, must reduce 40 MHz event rate to 100 kHz
  - Upgraded from Run-1 in two steps
    - Different trigger systems between 2015 and 2016
- High Level Trigger (HLT)
  - Large, dedicated computer farm
  - Combine information from all detector systems
  - Allows easily programmable trigger paths similar to offline reconstruction
  - Further reduce rate to ~1 kHz

The Trigger Menu

- The trigger is designed to be easily programmable to adapt to changing LHC conditions
  - Between 2015 and 2016, the peak instantaneous luminosity more than doubled
  - New beam mode operation: Bunch Compression Merging and Splitting (BCMS)
  - Higher pileup (overlapping vertices)
- In the table below, the trigger thresholds for the HLT (L1 trigger) for the two run periods are compared for trigger paths relevant to this analysis
  - 2015: 2.3 fb^{-1} (WZ dataset)
  - 2016 partial: first 12.9 fb^{-1} (Φ^{++} dataset)
  - 2016 full: 36.5 fb^{-1}

Trigger Path	2015	2016 (partial)	2016 (full)
Single electron	**23** (20)	**27** (24)	**27** (24)
Single muon	**20** (16)	**22** (20)	**24** (22)
Double electron	**17/12** (15/10)	**23/12** (15/10)	**23/12** (15/10)
Double muon	**17/8** (10/3.5)	**17/8** (11/4)	**17/8** (11/4)
Electron-muon	**17/8** and **12/17** (15/5 and 10/12)	**17/8** and **12/17** (15/5 and 10/12)	**23/8** and **12/23** (20/5 and 10/20)
Double tau	**35/35** (28/28)	**35/35** (26/26)	35/35 (28/28)

SIMULATION

24
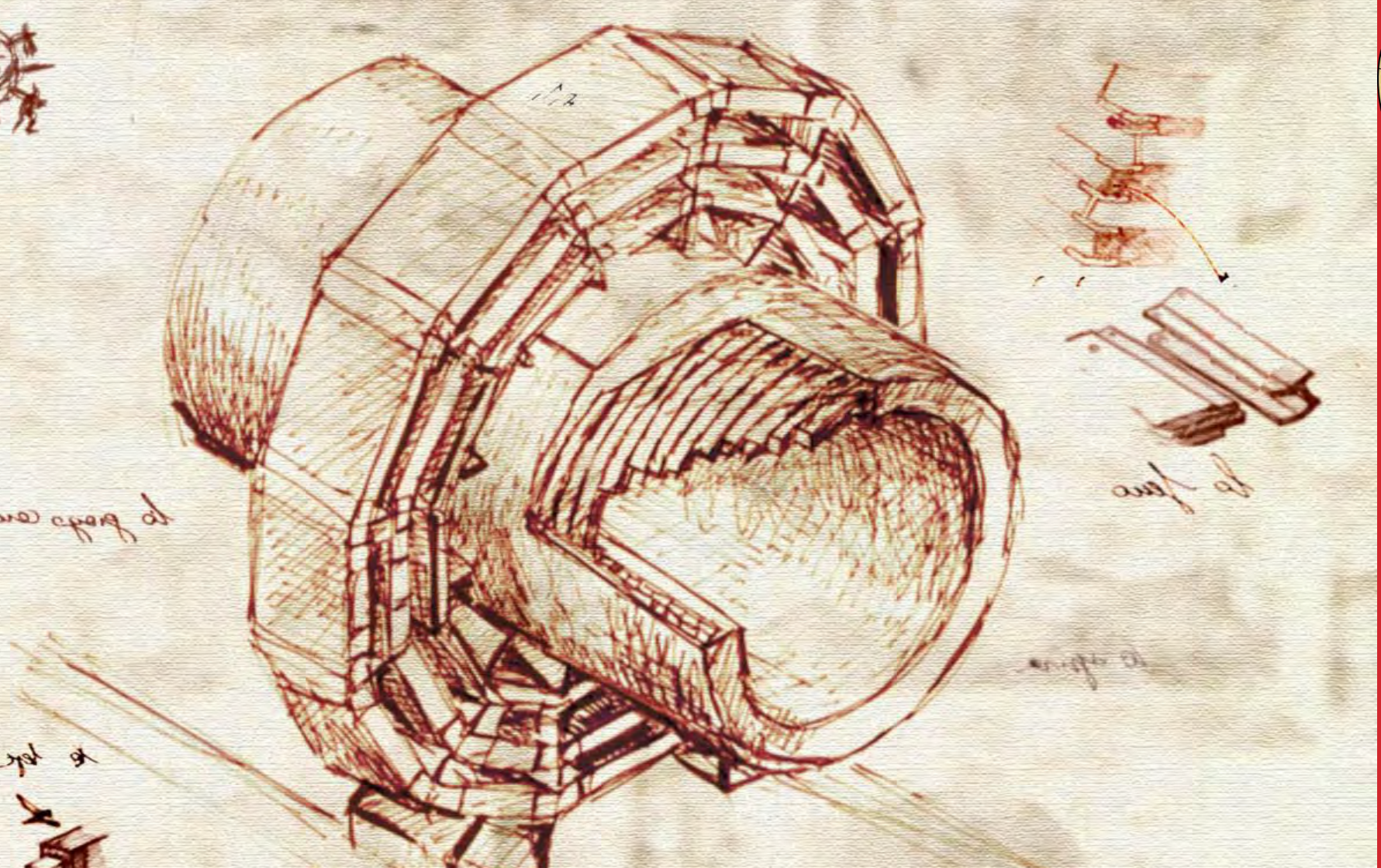
Monte Carlo Generation

- Events are simulated using the MC method
- Underlying vertex first produced in matrix element generator
- Parton distribution functions (PDFs) describe the structure of a particle
  - NNPDF3.0 proton PDF is used
- The underlying event is then passed to PYTHIA for showering and hadronization
- The primary interaction is combined with minimum bias events to simulate pile-up effects (overlapping vertices)
- Finally, the event is passed to a detailed GEANT4 simulation of the CMS detector to simulate the particle interaction
- Simulated events are then digitized and follow the same event reconstruction chain as data

protons   protons
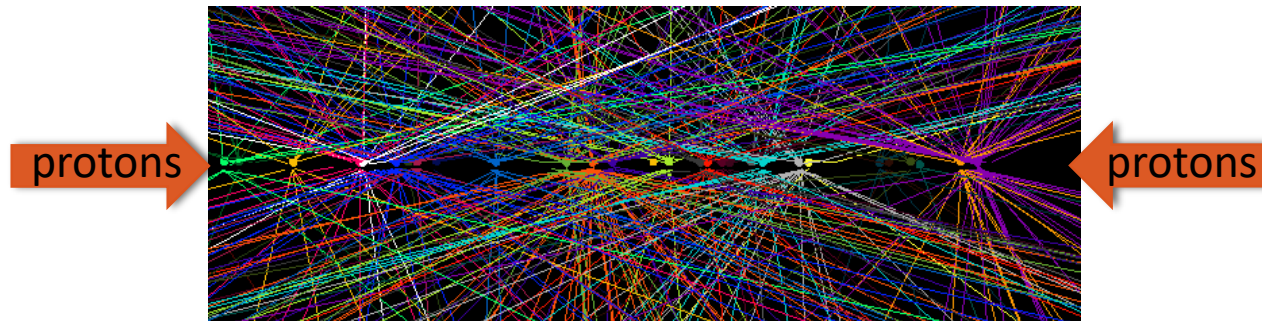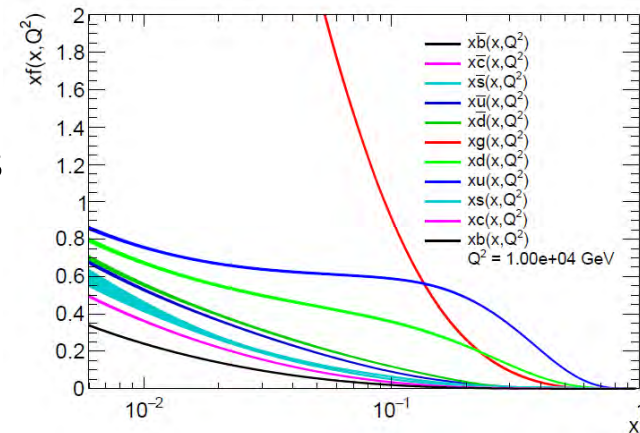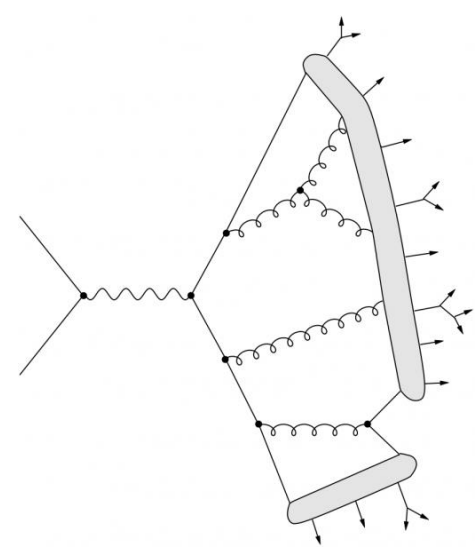
Event Generators

- Several generators used throughout this analysis
- MadGraph5_amc@NLO
  - Next-to-leading order (NLO) generic event generator
  - NLO through addition of real emission and loop
- POWHEG2.0
  - NLO generator with processes implemented separately
  - Generates hardest radiation
  - WZ signal sample
- MCFM
  - NLO cross section calculator
  - Used for comparison to POWHEG WZ cross section calculation
- PYTHIA8
  - LO matrix element generator (doubly-charged Higgs signal sample)
  - Primarily used for hadronization
- CalcHEP
  - Doubly-charged Higgs signal sample
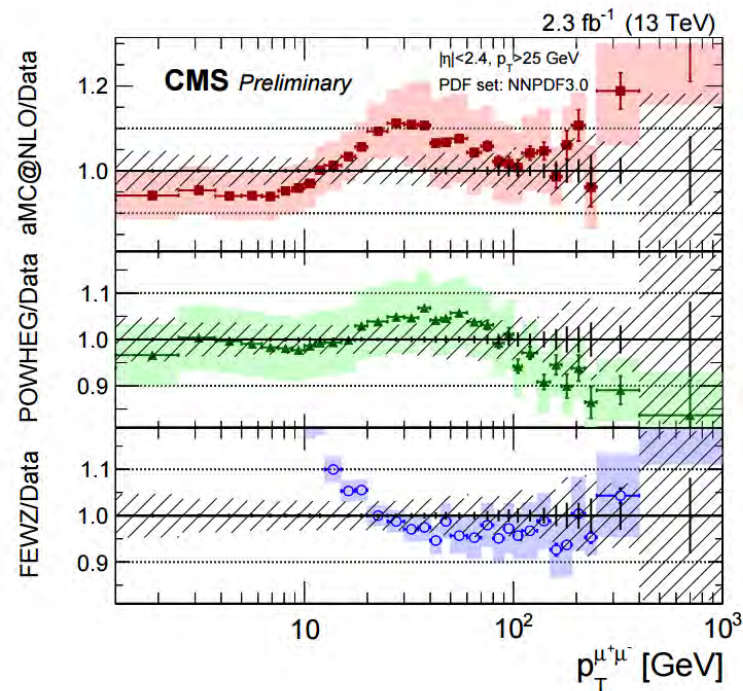
- MATRIX
  - NNLO cross section
  - Used as a comparison in the WZ cross section calculation
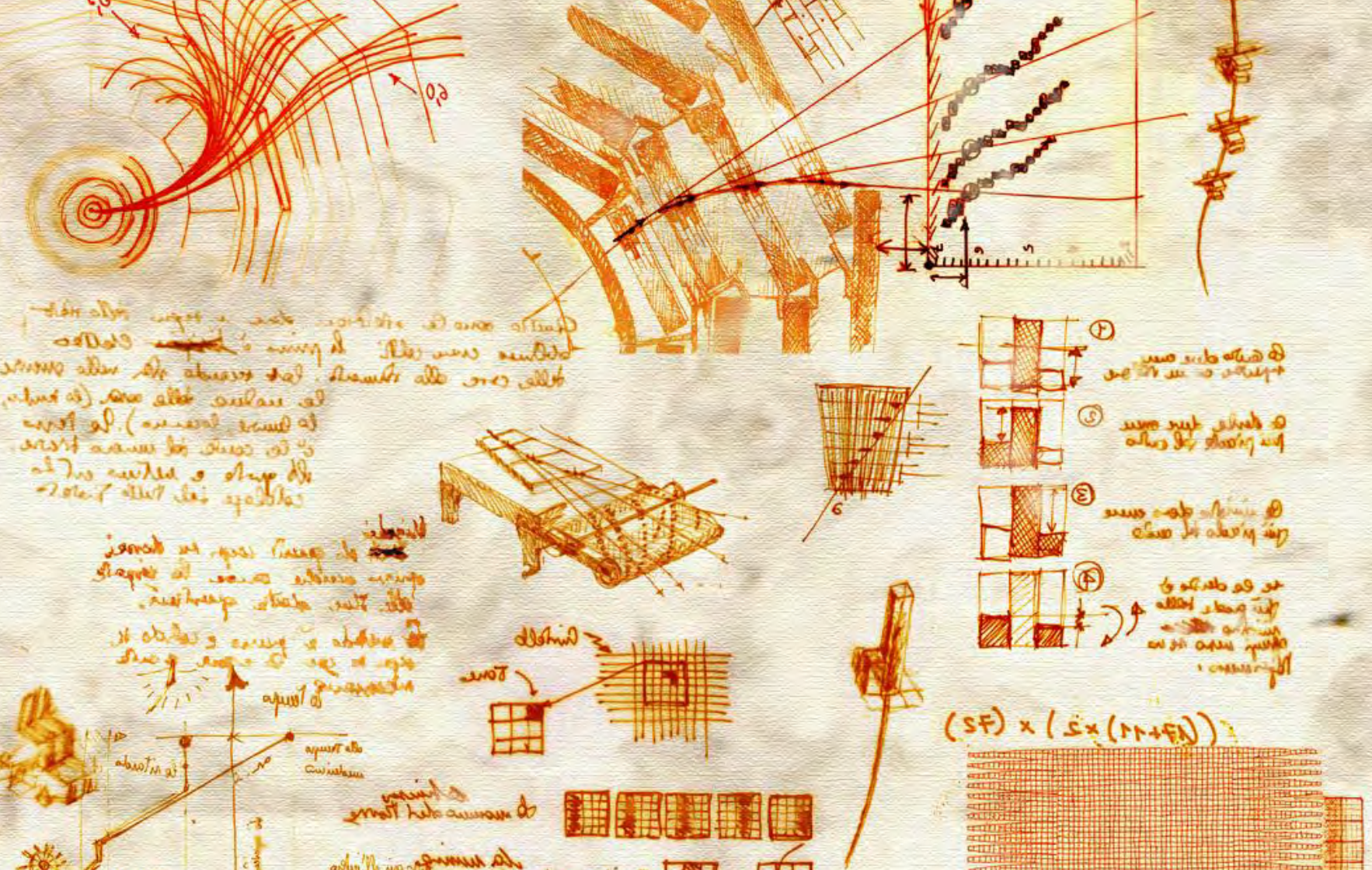
OBJECT RECONSTRUCTION

Event Reconstruction

- CMS uses Particle Flow (PF) to combine information from each detector and select physics objects
  - Improves resolution and identification
  - Charged and neutral hadrons, photons, electrons, and muons
- Algorithm
  - First muon detector tracks are matched to tracks in the inner tracker
  - Remaining tracks are then associated with energy deposits in ECAL (electrons) and HCAL (charged hadrons)
  - Remaining energy deposits are called photons (ECAL) or neutral hadrons (HCAL)
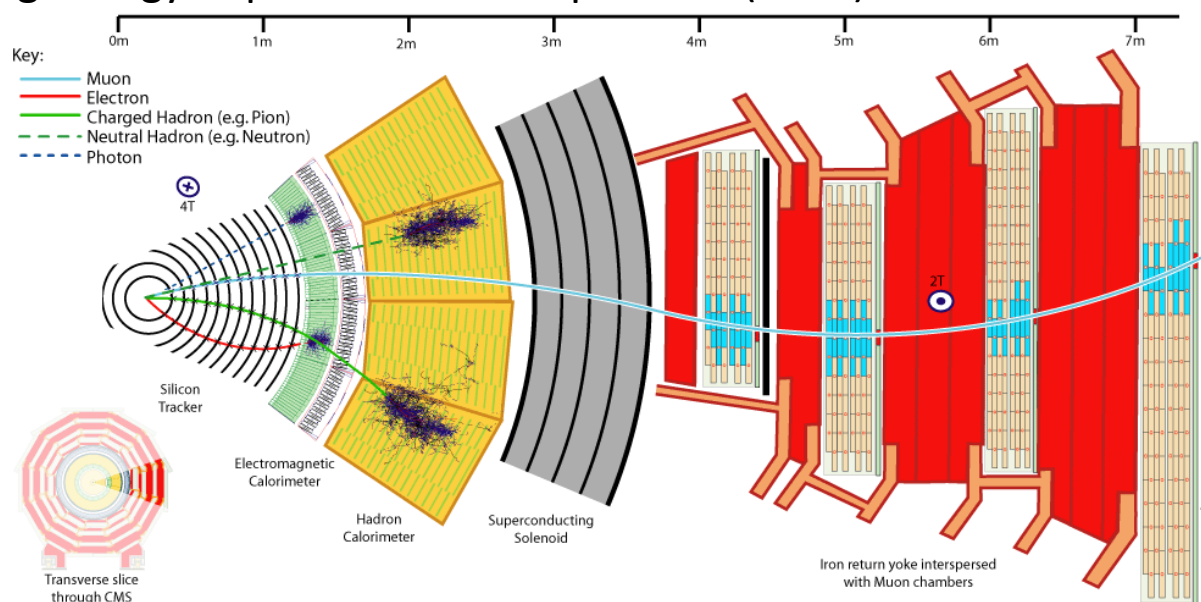
Object Isolation

- Isolation is defined using PF objects within a cone of ΔR < 0.4

$$I^\ell = \left(\sum p_\mathrm{T}^\mathrm{charged} + \max\left[0, \sum p_\mathrm{T}^\mathrm{neutral} + \sum p_\mathrm{T}^\gamma - p_\mathrm{T}^\mathrm{PU} \right] \right) / p_\mathrm{T}^\ell$$

- Pileup correction is object dependent
  - Muons use a delta beta correction which use the ratio of charged to neutral hadrons in a jet (2:1)

$$p_\mathrm{T}^\mathrm{PU} \equiv 0.5 \sum_i p_\mathrm{T}^{\mathrm{PU},i}$$

  - Electrons use an effective area method

$$p_\mathrm{T}^\mathrm{PU} \equiv \rho \, A_\mathrm{eff}$$

Muon Reconstruction

- Combine muon system for identification and tracker for better p_T assignment
  - Muon subdetectors able to function as a standalone system
  - Reconstruction requires a standalone muon track to match with a tracker track to produce a "global" muon
- *Tight* muon identification
  - Vertex requirements: d_{xy} < 0.01 (0.02) cm for p_T < (>) 20 GeV, d_z < 0.1 cm
  - Hits in muon system (>1 chambers)
  - Track quality requirements
  - PF isolation < 0.15
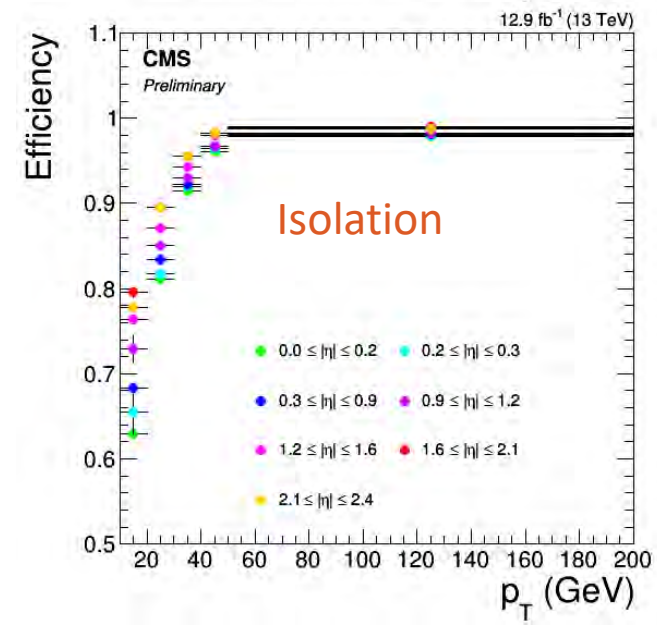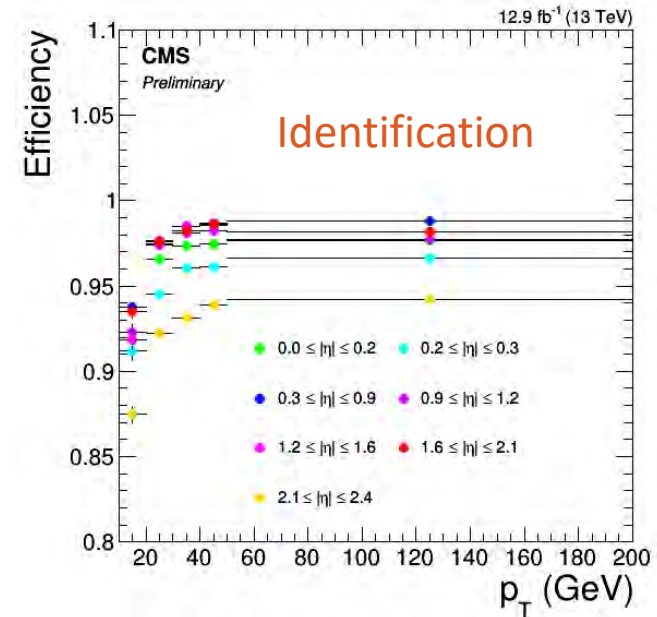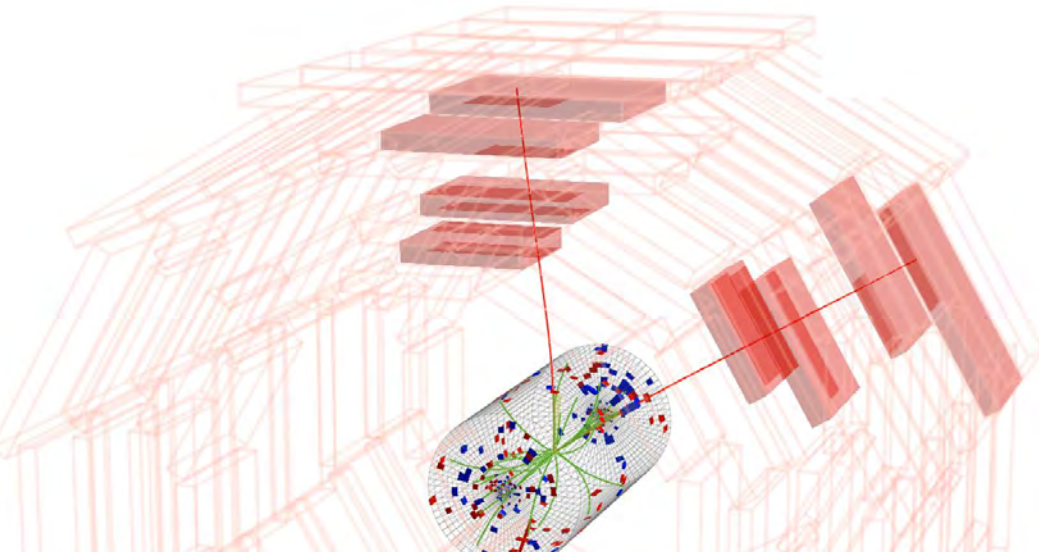
Electron Reconstruction

- Use energy deposits in ECAL and tracker for p_T assignment

- Cut based identification
  - Shower shape and HCAL and ECAL energy requirements
  - Photon conversion rejection
  - Vertex requirements for barrel (endcap)
    - *Tight*: $d_{xy} < 0.01$ (0.07) cm, $d_z < 0.4$ (0.6) cm
    - *Very tight*: $d_{xy} < 0.01$ (0.04) cm, $d_z < 0.05$ (0.4) cm
  - At most one missing inner tracker hit
  - PF Isolation
    - *Tight*: < 0.08 (0.07)
    - *Very tight*: < 0.04 (0.06)
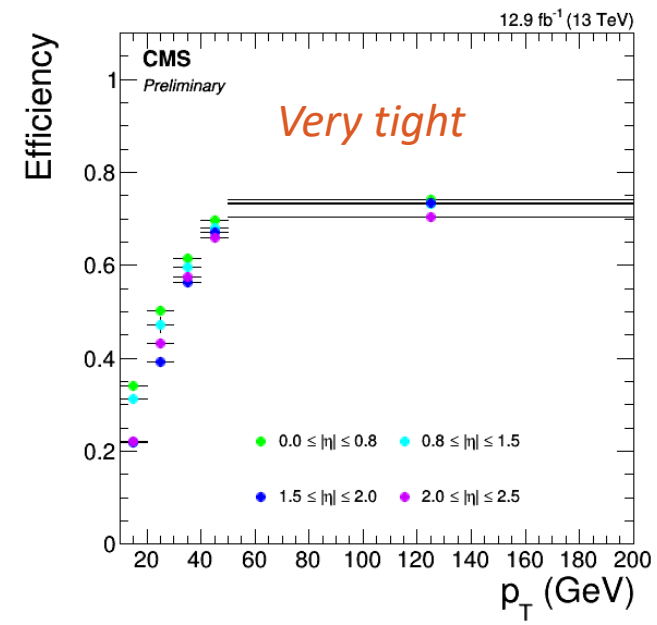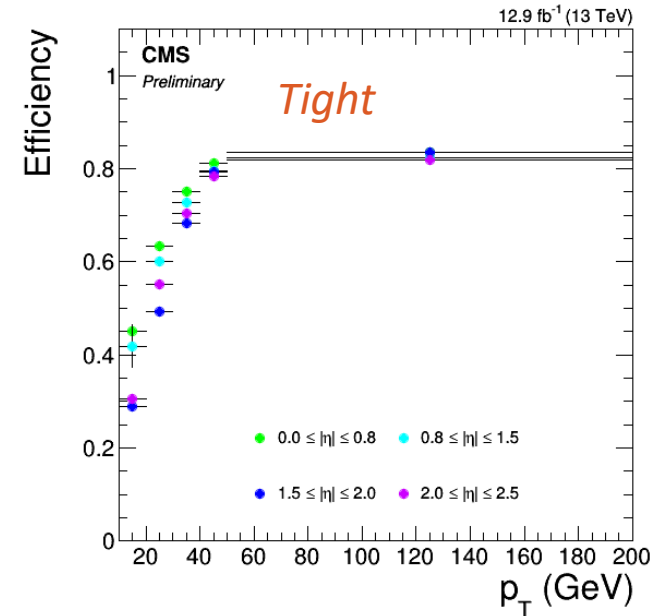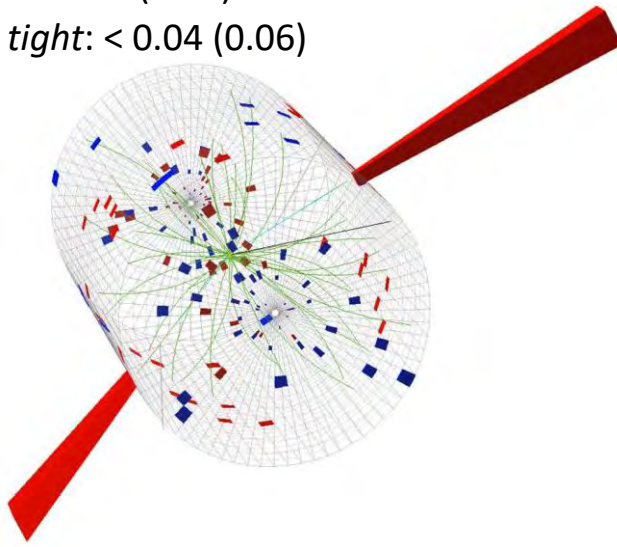
Tau Reconstruction

- Reconstructed using the hadrons plus strips (HPS) algorithm
  - Target tau decay modes
    - $h^{\pm}$, $h^{\pm}\pi^0$, $h^{\pm}\pi^0\pi^0$, $h^+h^-h^+$
  - Strips are the result of $\pi^0 \rightarrow \gamma\gamma$ with subsequent electron-positron pair production from the photon
    - New reconstruction mode in Run-2 has dynamically defined strip size
- Tau identification
  - MVA discriminator is used (Vloose working point below)
    - Inputs include isolation sums, decay mode, transverse impact parameter and significance, tau lifetime, shape variables, and electron/photon multiplicity
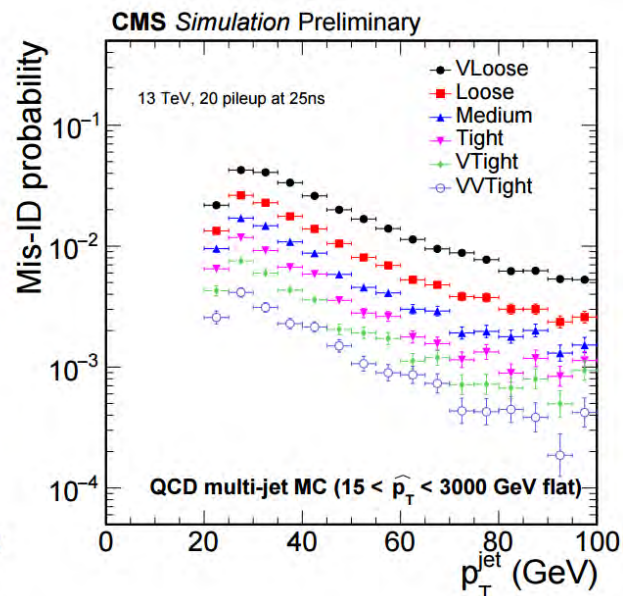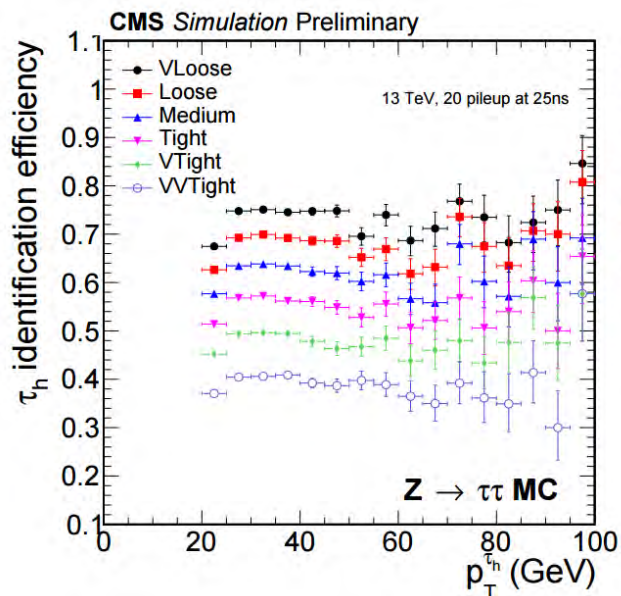
Missing Energy

- Neutrinos and potentially other beyond the standard model particles will not deposit energy in the CMS detector
  - Leads to missing energy (MET)
  - Magnitude of the negative vector sum of all PF objects
    - Missing energy can only be resolved in φ
- Pile-up also contributes to errors in the MET measurement
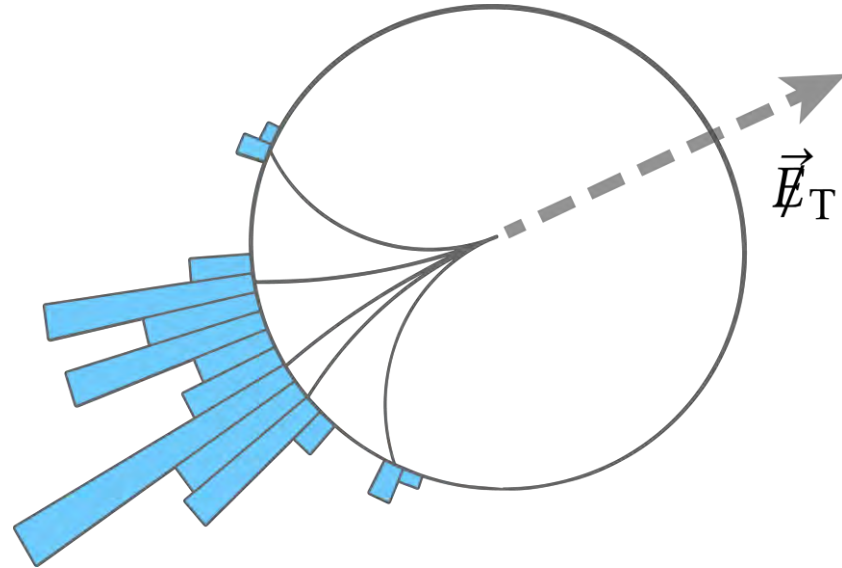
$$\vec{E}_{\mathrm{T}}^{\mathrm{Type\text{-}I}} = -\sum_{\mathrm{jet}} \vec{p}_{\mathrm{T\,jet}}^{\mathrm{JEC}} - \sum_{i\in\mathrm{uncl.}} \vec{p}_{\mathrm{T}i}$$

Jet Reconstruction

- Charged hadrons, neutral hadrons, and photons are built from PF candidates after the removal of muon and electron candidates
  - Typical jet structure is 65% charged hadrons, 25% neutral hadrons, and 10% photons
- Jets are reconstructed with the anti-k_T algorithm with distance parameter R=0.4
  - The anti-k_T algorithm is collinear and IR safe
- Jets are charged hadron subtracted (CHS)
  - Charged hadrons with tracks not associated to the primary vertex are removed
- Jet energy corrections (JEC) are applied
  - Include removal of pile-up energy, MC-truth corrections, residual corrections from dijet, Z+jet, and photon+jet data-MC comparison
- Jets from b hadrons
  - Long lifetime translates to a secondary vertex
  - Jets are tagged with a multivariate discriminator
    - CSVv2 – "Tight" working point 49% efficiency
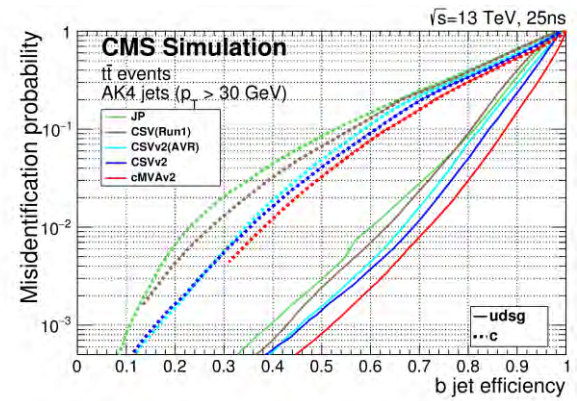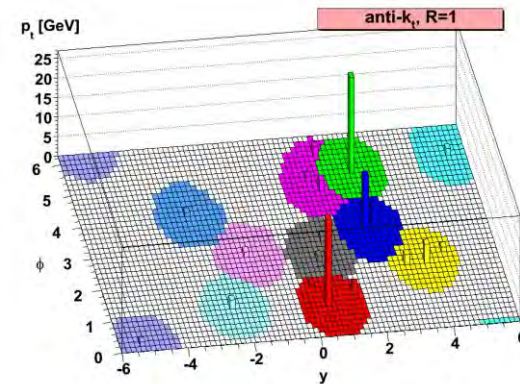
Nonprompt Background

- Prompt leptons are directly from the hard process
- The nonprompt background refers to the combination of
  - Nonprompt leptons: leptons arising from decays from other particles
  - Jets that are misidentified as leptons
- The contributions from misidentified objects are estimated using the "*tight*-to-*loose*" method
  - Measure the efficiency for a jet that passes a *loose* ID to also pass the *tight* ID in a nonprompt dominant control region

$$N_{BG}^{nonprompt} = \sum_{j>0} (-1)^{j+1} N_{jF,(n-j)P} \times \prod_{0<i\leq j} \frac{\epsilon_i^{misid}}{1 - \epsilon_i^{misid}}$$
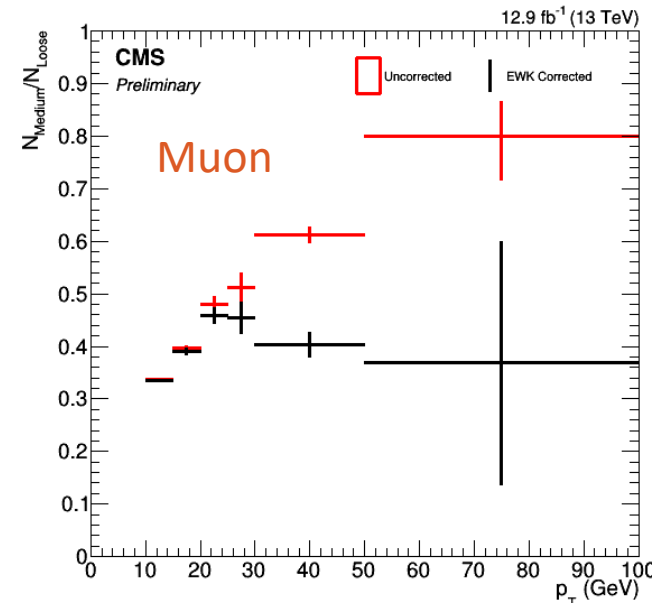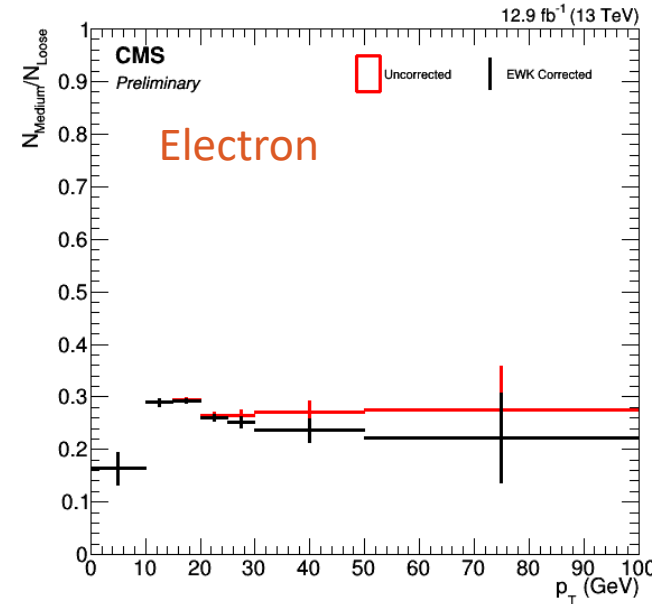
WZ CROSS SECTION MEASUREMENT

WZ Analysis Selections

- Trigger requirements
  - Single electron (muon) $p_T > 23$ (20) GeV
  - Double electron (muon) with same or different flavors with leading $p_T > 17$ (17) GeV and subleading $p_T > 12$ (8) GeV
- Topology
  - Exactly 3 *tight* leptons with pt > 10 GeV and an opposite-sign same-flavor pair
  - Veto events with an additional lepton
  - $m_{3l} > 100$ GeV
  - All lepton pairs $m_{ll} > 4$ GeV
- Z Selection
  - Leading lepton pt > 20 GeV
  - Z window of [76, 106] GeV
- W Selection
  - If electron, pass *very tight* lepton requirement
  - Lepton pt > 20 GeV
  - $E_T^{miss} > 30$ GeV
- No events with pt > 20 GeV b tagged jet
- Full selection: 142 million → 318 events
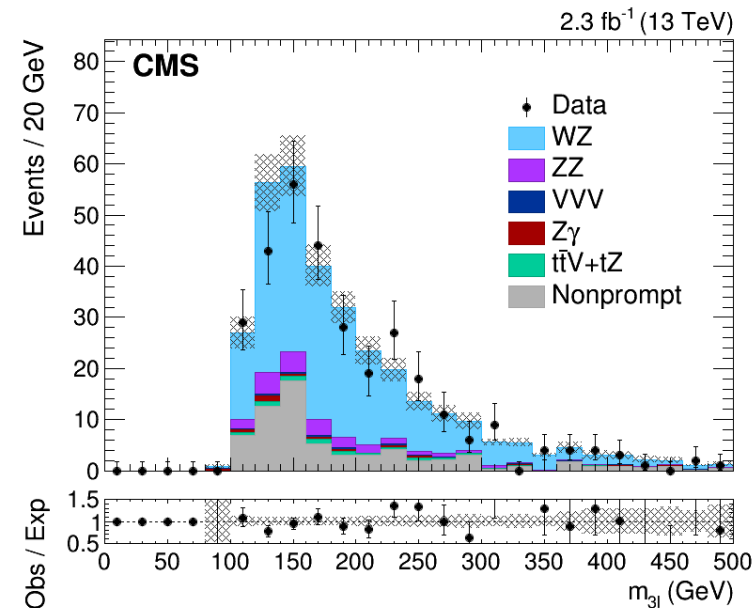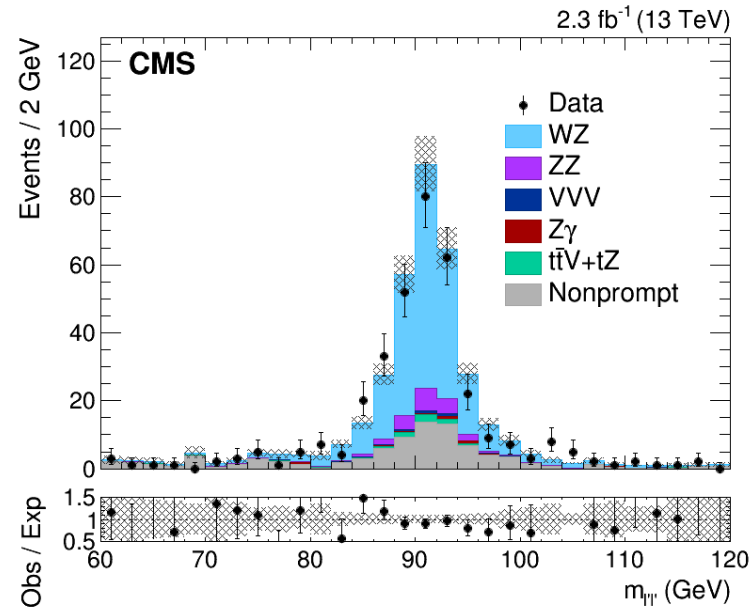
WZ Systematic Uncertainties

- Integrated luminosity
  - 2.7%
- Lepton efficiency
  - Muon: 1+0.5% (ID+Iso)
  - Electron: 2%
- Pileup
  - Minimum bias cross section: 5%

- E_T^{miss}
  - Electron energy: 0.6-1.5%
  - Muon energy: 0.2-1.5%
  - Jet energy: <3%
- b tagging
  - 2% for WZ, 7% for TTV

- Nonprompt
  - Electron: 30%
  - Muon: 30%
- Background MC uncertainties
  - ZZ: 4%
  - ttV: 15%
  - VVV: 6%
  - Zγ: 6%

Source of uncertainty	Uncertainty in the cross section
Background with nonprompt μ	5.4%
Background with nonprompt e	3.9%
b tagging	2.1%
E_T^{miss}	2.0%
Electron efficiency	1.9%
Muon efficiency	1.5%
Pileup	0.8%
ZZ cross section	0.4%
$t\bar{t}V$ cross section	negligible
$Z\gamma$ cross section	negligible
VVV cross section	negligible
Integrated luminosity	3.2%
PDF and scales	1.0%

WZ Yields

- WZ yields after all analysis selections applied
  - Expected WZ signal from POWHEG
    - Scaled to NLO cross section prediction from POWHEG
  - Prompt background from simulation
  - Nonprompt background from "*tight*-to-*loose*" method

Decay channel	Expected WZ	Background Nonprompt	Prompt	Total expected	Observed
eee	$35.9 \pm 0.6^{+1.8}_{-1.8}$	$10.6 \pm 1.7^{+3.2}_{-2.5}$	$6.6 \pm 0.6^{+0.5}_{-0.5}$	$53.1 \pm 1.9^{+3.9}_{-3.3}$	49
$ee\mu$	$50.2 \pm 0.8^{+2.4}_{-2.4}$	$14.8 \pm 3.6^{+3.9}_{-3.0}$	$8.3 \pm 0.5^{+0.6}_{-0.6}$	$73.3 \pm 3.7^{+4.8}_{-4.1}$	78
$\mu\mu e$	$56.0 \pm 0.8^{+2.5}_{-2.4}$	$21.5 \pm 3.2^{+5.0}_{-3.9}$	$9.3 \pm 0.6^{+0.8}_{-0.7}$	$86.8 \pm 3.4^{+5.8}_{-4.8}$	83
$\mu\mu\mu$	$84.0 \pm 1.0^{+3.4}_{-3.3}$	$20.0 \pm 4.9^{+6.1}_{-4.7}$	$12.4 \pm 0.5^{+0.8}_{-0.7}$	$116.3 \pm 5.0^{+7.2}_{-6.0}$	108
Total	$226 \pm 2^{+10}_{-9}$	$67 \pm 7^{+14}_{-11}$	$37 \pm 1^{+3}_{-2}$	$330 \pm 7^{+18}_{-16}$	318

WZ Cross Section

- Theoretical cross sections are calculated using POWHEG with NNPDF3.0

  - Acceptance correction from total to fiducial of 45 ± 0.4%

- Fiducial Cross Section

  - Observed:

$$\sigma_{\text{fid}}(pp \to WZ \to \ell\nu\ell'\ell') = 258 \pm 21\,(\text{stat})^{+19}_{-20}\,(\text{syst}) \pm 8\,(\text{lumi})\,\text{fb}$$

  - Theoretical: (NLO): $274^{+11}_{-8}\,(\text{scale}) \pm 4\,(\text{PDF})\,\text{fb}$

- Total Cross Section

  - Observed:

$$\sigma(pp \to WZ) = 39.9 \pm 3.2\,(\text{stat})^{+2.9}_{-3.1}\,(\text{syst}) \pm 0.4\,(\text{theo}) \pm 1.3\,(\text{lumi})\,\text{pb}$$

  - Theoretical (NLO): $42.3^{+1.4}_{-1.1}\,(\text{scale}) \pm 0.6\,(\text{PDF})\,\text{pb}$
  - Theoretical (NNLO): $50.0^{+1.1}_{-1.0}\,(\text{scale})\,\text{pb}$

Fiducial region

- Z mass window [60, 120]
- Lepton $p_T > 20, 10, 20$ GeV and $|\eta| < 2.5$
- $m_{ll} > 4$ GeV

WZ Cross Section vs $\sqrt{s}$

- CMS 7 and 8 TeV
  - [71, 111]
  - 2% correction
- ATLAS
  - [66, 116]
  - 1% correction
- CMS 13 TeV
  - [60, 120]

DOUBLY-CHARGED HIGGS SEARCH

42
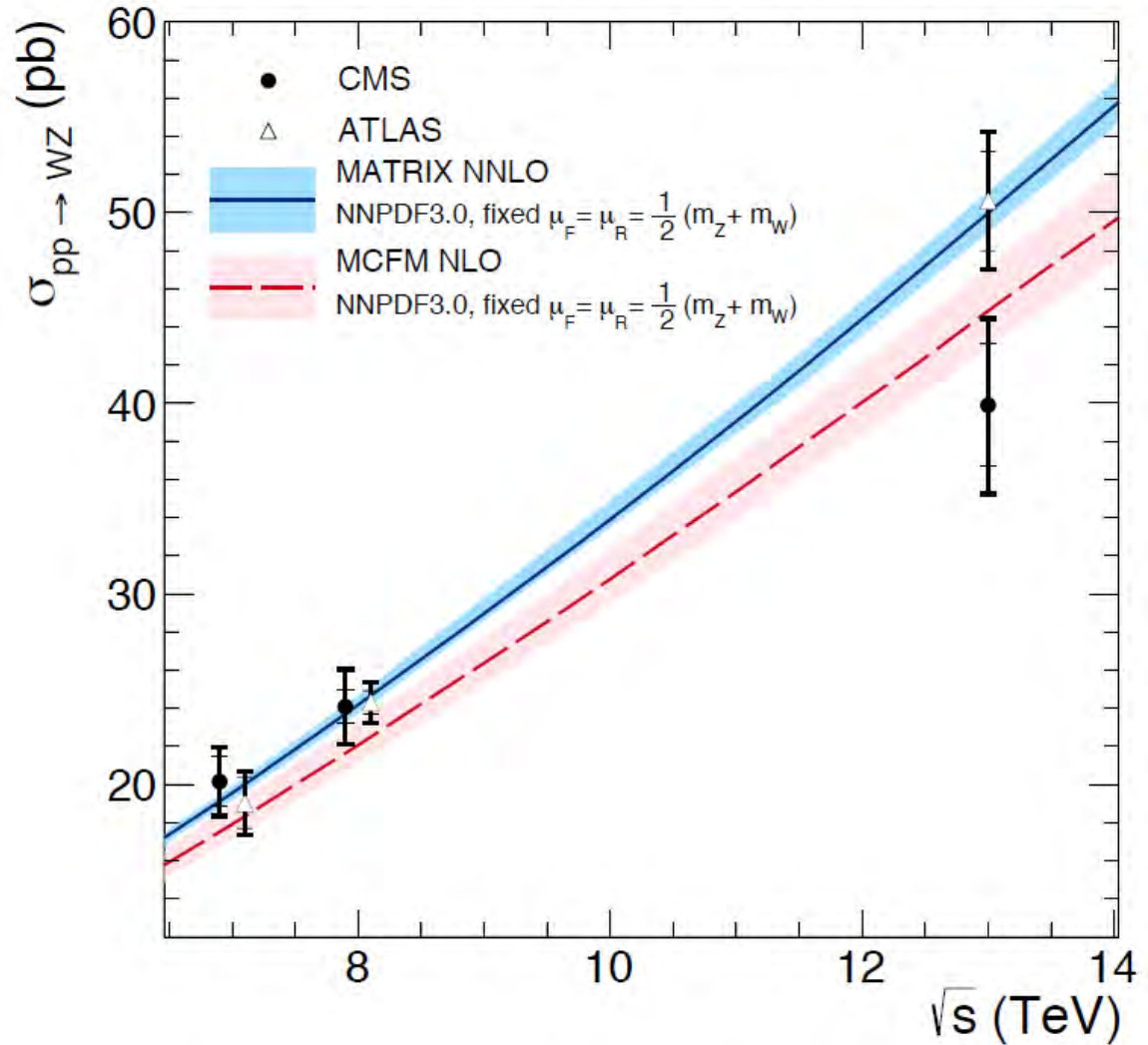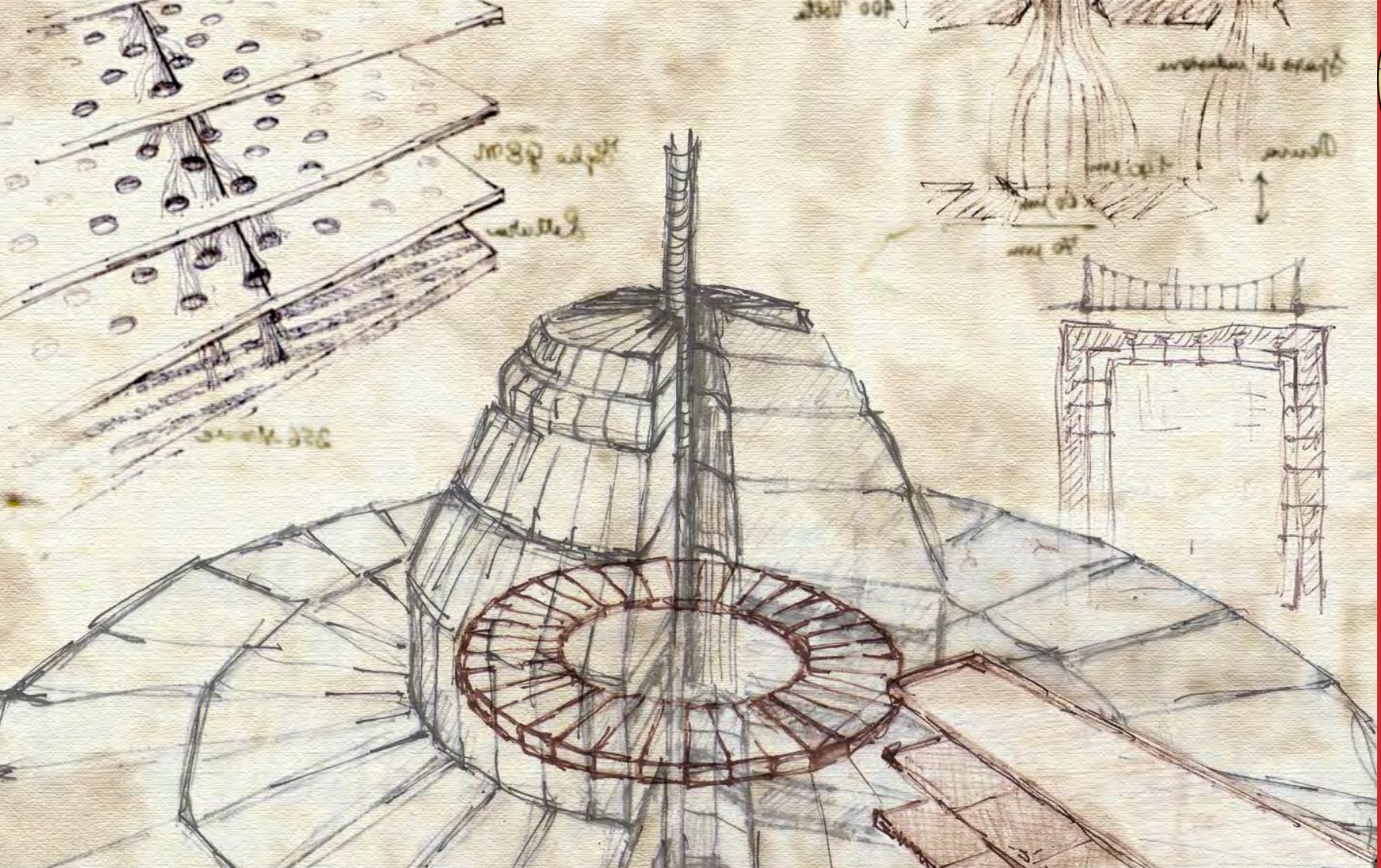
Φ⁺⁺ Signal Simulation

- Pair and associated production modes simulated with PYTHIA8 and CalcHEP, respectively
- Both types of signal samples do not allow the decay to WW
- Cross sections are NLO for all signals shown here
  - k-factors typically ~1.25 for LO -> NLO

Pair Production
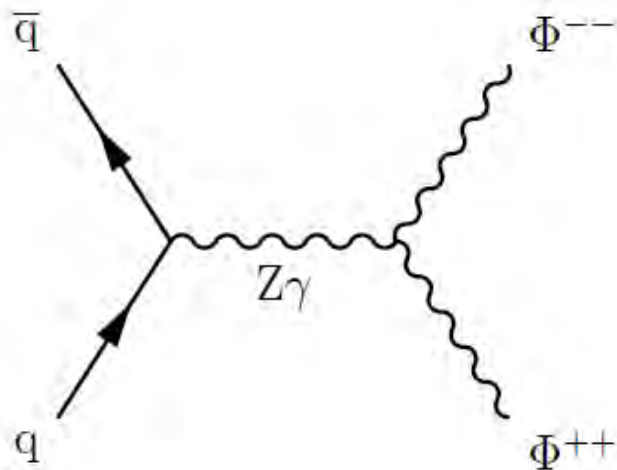
Associated Production
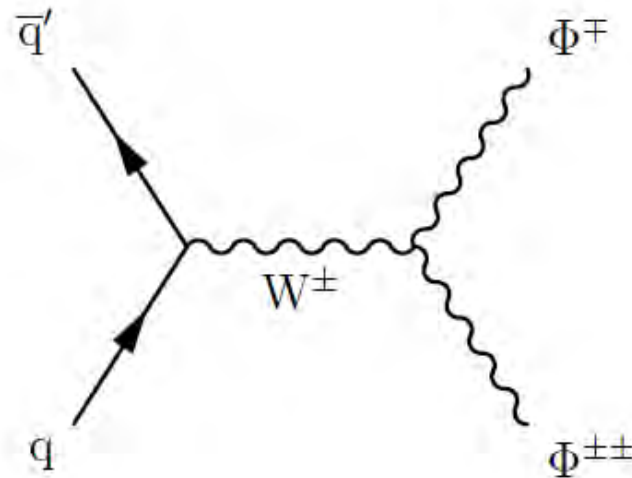
Φ^{++} Event Selection - *Preselection*

- Trigger requirements: the OR of
  - Single electron (muon)
    - $p_T > 25$ (22) GeV
  - Double electron (muon) with same or different flavors
    - Leading $p_T > 23$ (17) GeV
    - Subleading $p_T > 12$ (8) GeV
  - Double tau trigger
    - $p_T > 35$ GeV for both
- Three or four leptons with charge requirement of ++−, −−+, or ++−−
- In case of three leptons, no other isolation light leptons (hadronic taus) with $p_T > 10$ (20) GeV
- All dilepton pairs with $m_{ll} > 12$ GeV
- Fiducial definition
  - Electron / muon / hadronic tau
    - $p_T > 10 / 10 / 20$ GeV
    - $|\eta| < 2.5 / 2.4 / 2.3$
  - One or more light leptons: leading light lepton $p_T > 30$ GeV
  - Two or more light leptons: subleading light lepton $p_T > 20$ GeV
  - Zero light leptons: two leading hadronic taus $p_T > 40$ GeV

Channel	Preselection Yield
$\ell^\pm \ell^\pm \ell^\mp$	6734
$\ell^\pm \ell^\pm \tau^\mp$	329
$\ell^\pm \tau^\pm \ell^\mp$	76887
$\ell^\pm \tau^\pm \tau^\mp$	3908
$\tau^\pm \tau^\pm \ell^\mp$	2786
$\tau^\pm \tau^\pm \tau^\mp$	905
$\ell^+ \ell^+ \ell^- \ell^-$	223
$\ell^+ \ell^+ \ell^- \tau^-$	78
$\ell^+ \ell^+ \tau^- \tau^-$	4
$\ell^+ \tau^+ \ell^- \tau^-$	223
$\ell^+ \tau^+ \tau^- \tau^-$	23
$\tau^+ \tau^+ \tau^- \tau^-$	1

Invariant Mass Distribution

- Invariant mass distribution after *preselection* for the three and four light lepton final states
- A sample signal distribution for a mass hypothesis of 500 GeV is shown

45
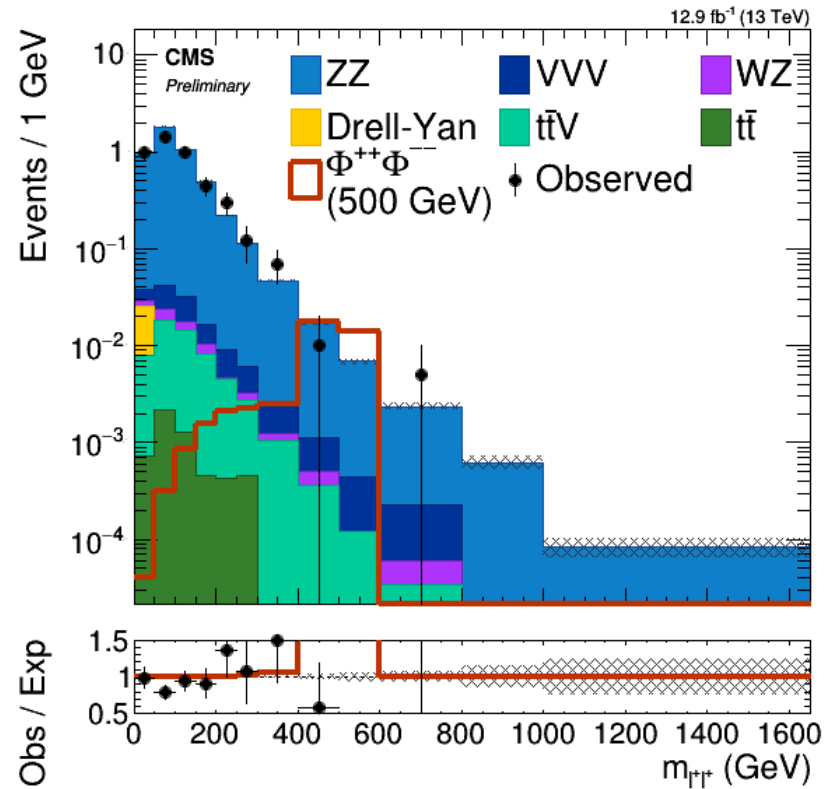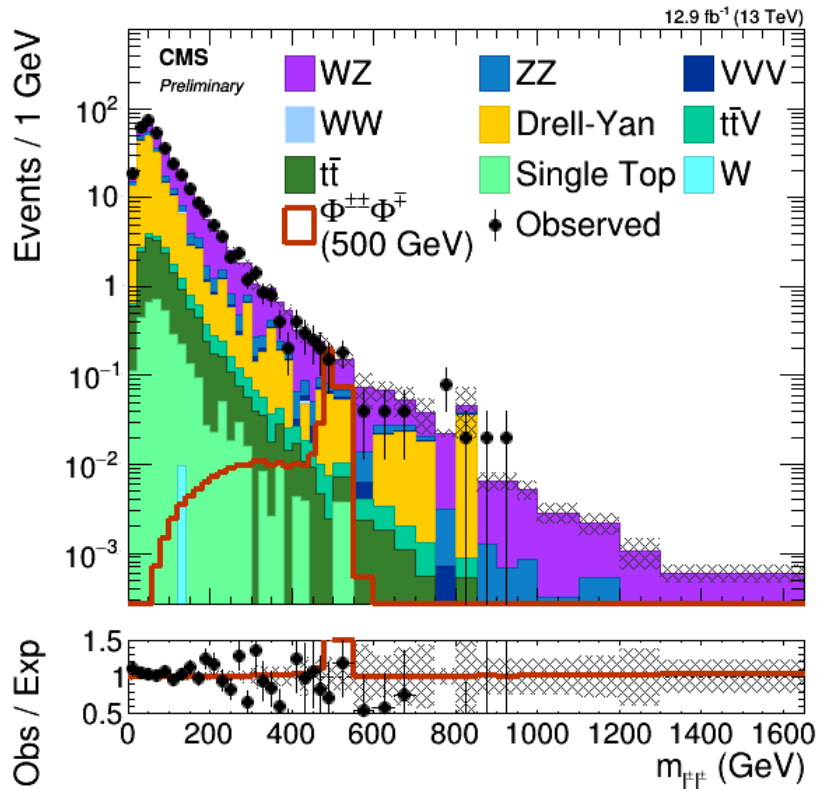
Φ++ Analysis Categories

- The analysis categories are separated by the number of taus associated to the Φ++

- Background estimation is modified based on category
  - All light leptons or categories with a real Z decaying to light leptons are estimated fully from MC
  - Others are estimated with a combination of MC and nonprompt (NP) via the fake efficiency method discussed before

3l Channel	BG Est	4l Channel	BG Est
$l^+l^+l^-$	MC	$l^+l^+l^-l^-$	MC
$l^+l^+\tau^-$	MC + NP	$l^+l^+l^-\tau^-$	MC
$l^+\tau^+l^-$	MC	$l^+l^+\tau^-\tau^-$	MC + NP
$l^+\tau^+\tau^-$	MC + NP	$l^+\tau^+l^-\tau^-$	MC
$\tau^+\tau^+l^-$	MC + NP	$l^+\tau^+\tau^-\tau^-$	MC + NP
$\tau^+\tau^+\tau^-$	MC + NP	$\tau^+\tau^+\tau^-\tau^-$	MC + NP

Mass Dependent Selections

- From the *preselection*, five variables are used to increase signal sensitivity

  - S_T = scalar sum of lepton p_T
  - Difference between "best Z" and PDG Z mass
  - ΔR between same sign leptons
  - E_T^{miss} (three lepton final state only)
  - Same sign invariant mass

- Selections are optimized based on the figure of merit S/sqrt(S+B)

Three lepton

Variable	$ee, e\mu, \mu\mu$	$e\tau, \mu\tau$	$\tau\tau$
S_T	$> 0.99 \cdot m_{\Phi++} - 35\,\mathrm{GeV}$	$> 1.15 \cdot m_{\Phi++} + 2\,\mathrm{GeV}$	$> 0.98 \cdot m_{\Phi++} + 91\,\mathrm{GeV}$
$\|m_{\ell+\ell-} - m_Z\|$	$> 10\,\mathrm{GeV}$	$> 20\,\mathrm{GeV}$	$> 25\,\mathrm{GeV}$
E_T^{miss}	$-$	$> 20\,\mathrm{GeV}$	$> 50\,\mathrm{GeV}$
$\Delta R(\ell^\pm \ell'^\pm)$	$-$	< 3.2	$< m_{\Phi++}/380 + 1.86\ (m_{\Phi++} \leq 400)$ $< m_{\Phi++}/750 + 2.37\ (m_{\Phi++} > 400)$
Mass window	$[0.9, 1.1] \cdot m_{\Phi++}\,\mathrm{GeV}$	$[0.4, 1.1] \cdot m_{\Phi++}\,\mathrm{GeV}$	$[0.3, 1.1] \cdot m_{\Phi++}\,\mathrm{GeV}$

Four lepton

Variable	$ee, e\mu, \mu\mu$	$e\tau, \mu\tau$	$\tau\tau$
S_T	$> 1.23 \cdot m_{\Phi++} + 54\,\mathrm{GeV}$	$> 0.88 \cdot m_{\Phi++} + 73\,\mathrm{GeV}$	$> 0.46 \cdot m_{\Phi++} + 108\,\mathrm{GeV}$
$\|m_{\ell+\ell-} - m_Z\|$	$-$	$> 10\,\mathrm{GeV}$	$> 25\,\mathrm{GeV}$
$\Delta R(\ell^\pm \ell'^\pm)$	$-$	$-$	$< m_{\Phi++}/1400 + 2.43$
Mass window	$[0.9, 1.1] \cdot m_{\Phi++}\,\mathrm{GeV}$	$[0.4, 1.1] \cdot m_{\Phi++}\,\mathrm{GeV}$	$[0.3, 1.1] \cdot m_{\Phi++}\,\mathrm{GeV}$

Sideband Method

- Background estimation in the final signal region is performed using an alpha sideband method
  - α and α' are defined as below and estimated with MC + nonprompt
    - N_{pre} : *preselection* with the NOT of the mass window and the NOT of the other mass dependent selections
    - N_{SB} : with the mass dependent selections and the NOT of the mass window
    - N_{SR} : with the AND of the mass dependent selections and the mass window
  - The contribution N^{exp} is then estimated from data in the preselection

$$\alpha = \frac{N_{SR}}{N_{pre}} \qquad \alpha' = \frac{N_{SB}}{N_{pre}}$$

$$N_{SR}^{exp} = \alpha \cdot (N_{pre}^{Data} + 1)$$

$$N_{SB}^{exp} = \alpha' \cdot (N_{pre}^{Data} + 1)$$
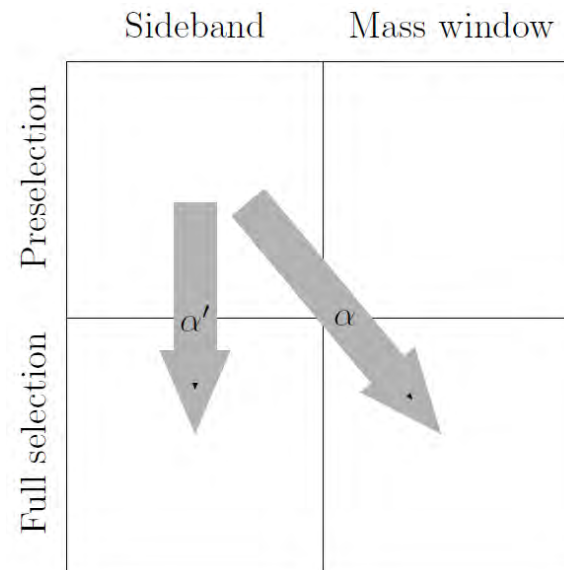
Φ^{++} Systematic Uncertainties

- Luminosity
  - 6.2 %
- Trigger
  - 0.5 %
- Lepton identification
  - 2-6 % per lepton
- Pileup minimum bias cross section
  - 5 %
- Electron energy
  - 0.6 (1.5) % in barrel (endcap)

- Muon energy
  - 0.2 (1.5) % for p_T < (≥) 100 GeV
- Tau energy
  - 3 %
- Charge identification
  - 1-4 (2.2) % for electrons (taus)
- Signal cross section
  - 15 %
- Alpha method
  - 10 %

Uncertainty source	Uncertainty in the 95% CLs upper limit
Luminosity	0.6-6.2%
Trigger	0.5%
Pileup	< 0.1%
Electron identification	0.1-3.3%
Muon identification	0.1-1.7%
Tau identification	0.5-4.6%
Charge identification	0.4-6.5%
Signal cross section	3-14%
Background estimation method	10-100%

Φ^{++} Limit Setting

- Limits are set using a modified frequentist confidence levels (CLs) method
- Simultaneous fit in two bins per channel
  - Sideband (SB) and signal region (SR)
- Systematic uncertainties are input as nuisance parameters
  - Alpha method modeled with a Gamma distribution
  - Other uncertainties modelled with log-normal distribution
- Limits are reported for three analysis scenarios and 10 benchmarks
  - Scenarios
    - Associated production only
    - Pair production only
    - Combination
  - Benchmarks
    - Six 100% decay hypotheses (ee, eμ, μμ, eτ, μτ, ττ)
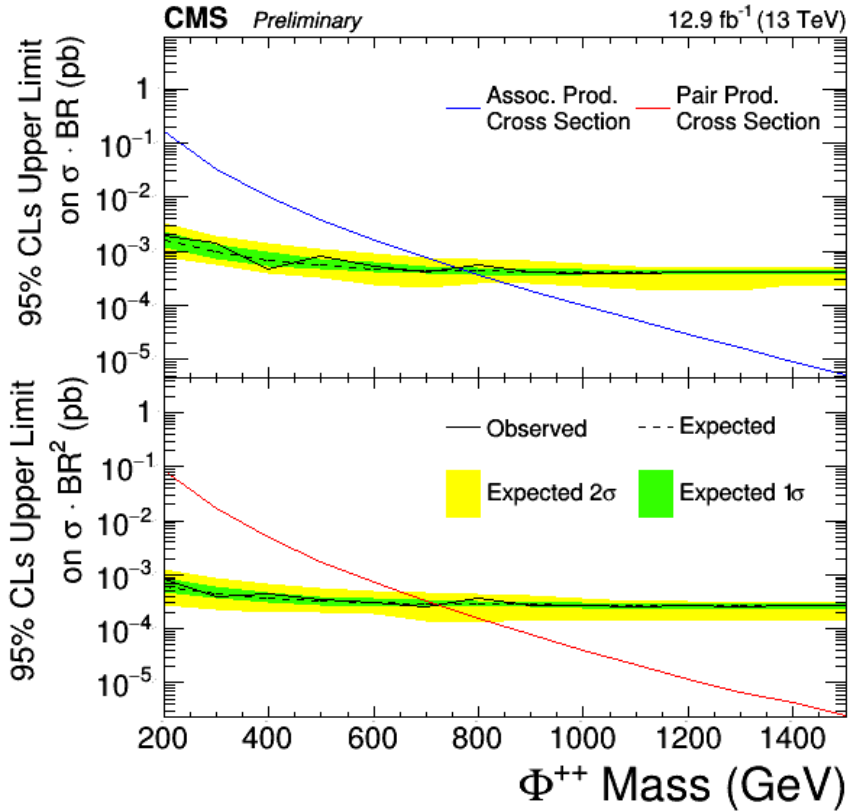   - Four benchmarks targeting neutrino mass hypotheses

Limits on 100% $\Phi^{++} \rightarrow \mu\mu$

Upper limit per production mode

Combined upper limit
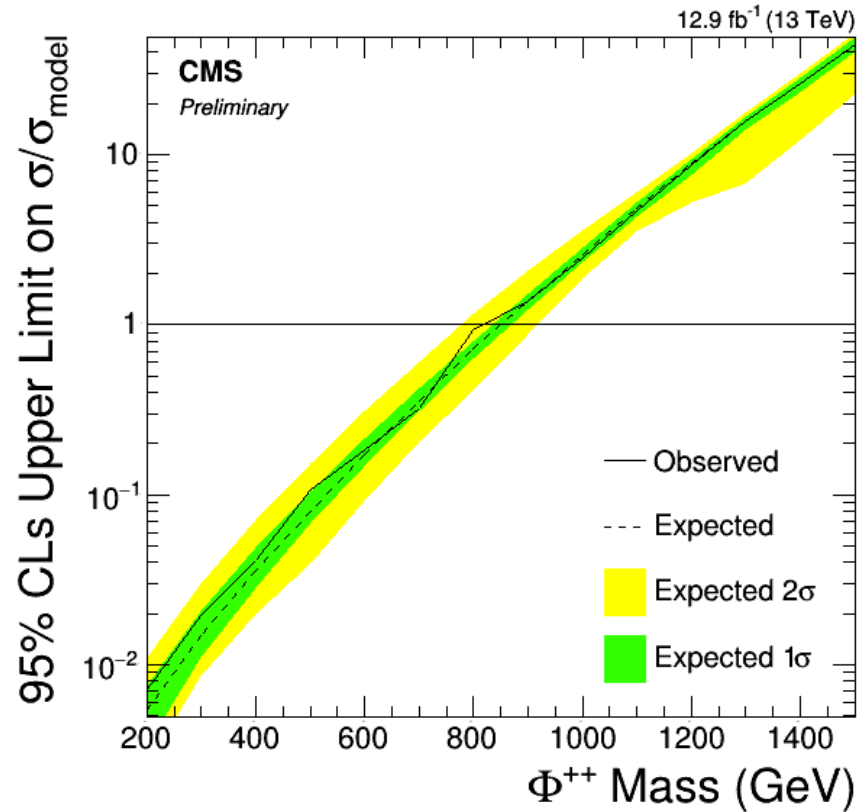
Φ^{++} Benchmarks

- Limits are set for six 100% branching fraction assumptions and four benchmarks targeting several neutrino mass hypotheses
  - Benchmark 1: Tri-bi-maximal normal hierarchy
  - Benchmark 2: Tri-bi-maximal inverted hierarchy
  - Benchmark 3: Degenerate mass spectrum of 0.2 eV
  - Benchmark 4: Equal branching fractions

Benchmark	Branching fraction					
	ee	$e\mu$	$e\tau$	$\mu\mu$	$\mu\tau$	$\tau\tau$
Benchmark 1	0	0.01	0.01	0.30	0.38	0.30
Benchmark 2	1/2	0	0	1/8	1/4	1/8
Benchmark 3	1/3	0	0	1/3	0	1/3
Benchmark 4	1/6	1/6	1/6	1/6	1/6	1/6

Φ⁺⁺ Excluded Regions

CONCLUSION

54
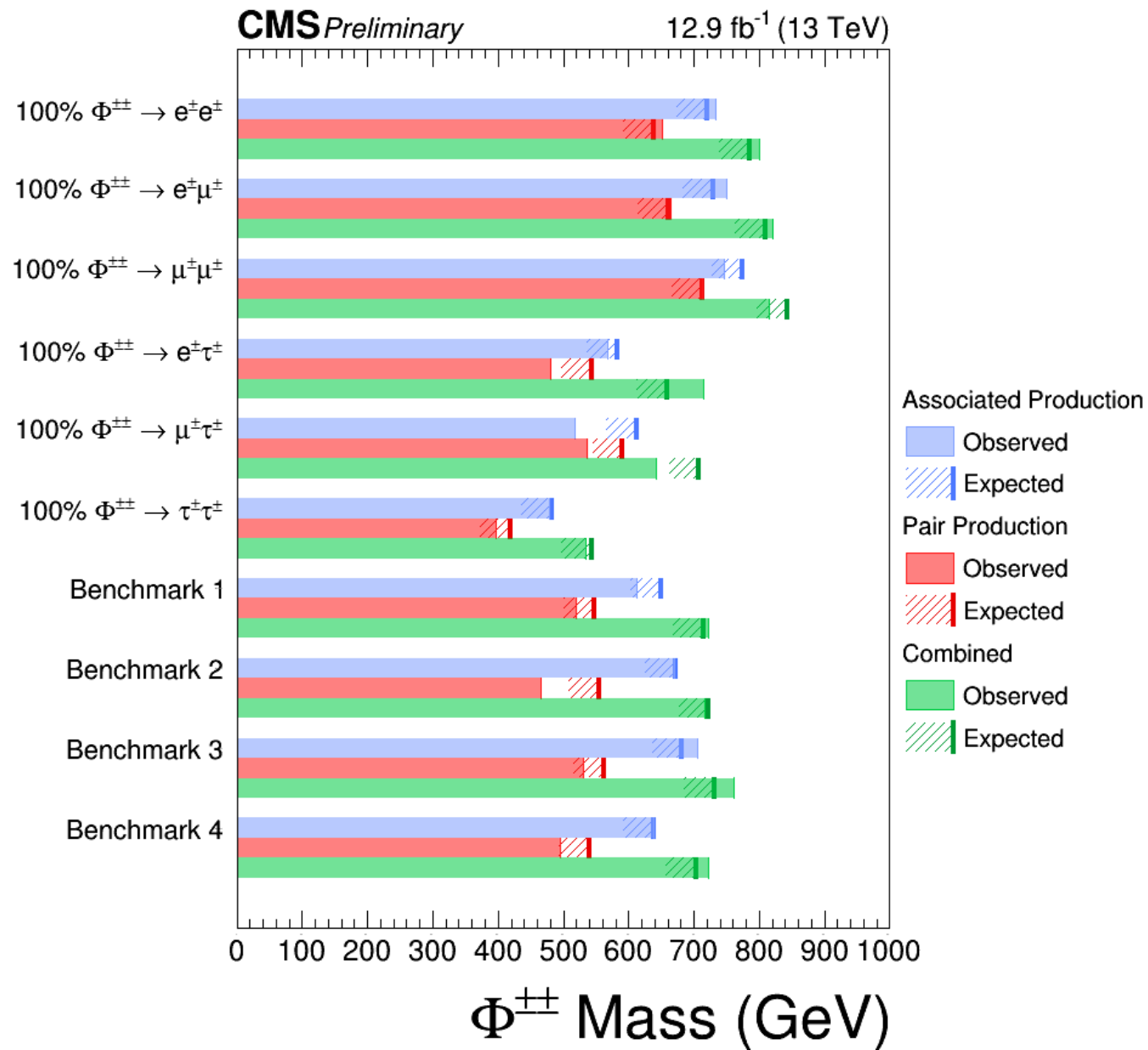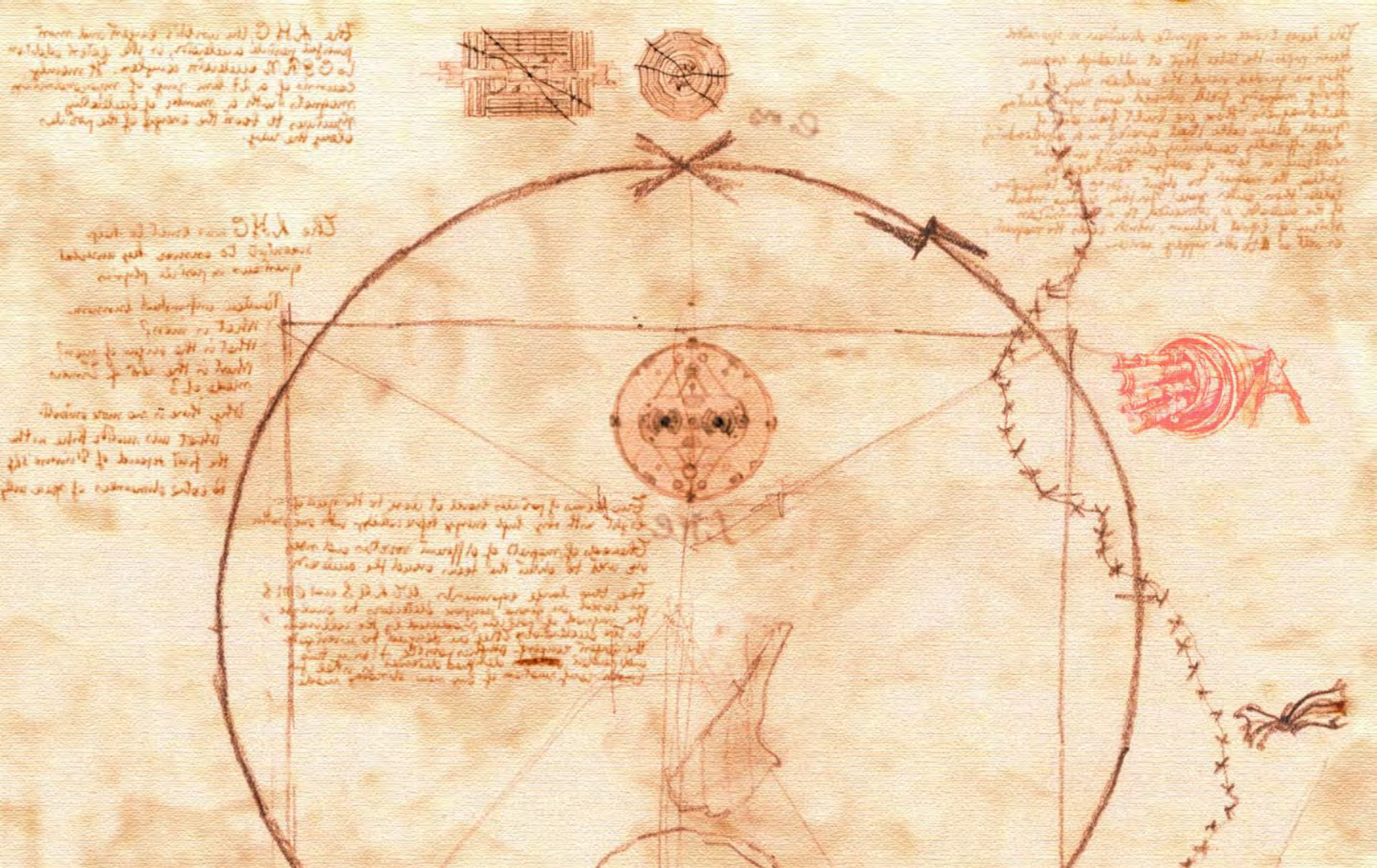
Conclusion

- Made the first measurement of the WZ 13 TeV cross section with 2.3 fb^{-1} of data

$$\sigma(pp \to WZ) = 39.9 \pm 3.2\,(\text{stat})^{+2.9}_{-3.1}\,(\text{syst}) \pm 0.4\,(\text{theo}) \pm 1.3\,(\text{lumi})\,\text{pb}$$

- Performed a search for a doubly-charged Higgs boson with 12.9 fb^{-1} of 13 TeV data

  - Increased the limits on the presence of a doubly-charged Higgs boson in both the pair production (PP) and associated production (AP) modes
  - Previous limits: light leptons ~600 GeV, 1 tau ~450 GeV, 2 tau ~200 GeV

| Benchmark	AP [GeV]	PP [GeV]	Combined [GeV]
100% $\Phi^{\pm\pm} \to ee$	734 (720)	652 (639)	800 (785)
100% $\Phi^{\pm\pm} \to e\mu$	750 (729)	665 (660)	820 (810)
100% $\Phi^{\pm\pm} \to \mu\mu$	746 (774)	712 (712)	816 (843)
100% $\Phi^{\pm\pm} \to e\tau$	568 (582)	481 (543)	714 (658)
100% $\Phi^{\pm\pm} \to \mu\tau$	518 (613)	537 (591)	643 (708)
100% $\Phi^{\pm\pm} \to \tau\tau$	479 (483)	396 (419)	535 (544)
Benchmark 1	613 (649)	519 (548)	723 (715)
Benchmark 2	670 (671)	465 (554)	716 (723)
Benchmark 3	706 (682)	531 (562)	761 (732)
Benchmark 4	639 (639)	496 (539)	722 (704)

Outlook

- WZ cross section shows tension with the NNLO prediction
  - ATLAS has a corresponding measurement that favors the NNLO prediction: $50.0^{+1.1}_{-1.0}\,(\text{scale})\,\text{pb}$

    CMS: $\sigma(pp \to WZ) = 39.9 \pm 3.2\,(\text{stat})^{+2.9}_{-3.1}\,(\text{syst}) \pm 0.4\,(\text{theo}) \pm 1.3\,(\text{lumi})\,\text{pb}$

    ATLAS: $\sigma(pp \to WZ) = 50.6 \pm 2.6\,(\text{stat}) \pm 2.0\,(\text{syst}) \pm 0.9\,(\text{theo}) \pm 1.2\,(\text{lumi})\,\text{pb}$

  - Both measurements can have reduced uncertainties with more data
- Differential cross section measurements that can exceed 8 TeV precision already possible with 2016 dataset
- Run-2 dataset: expect > 100 fb^{-1}
  - Evidence for VBS WZ production possible by the end of Run-2
- The doubly-charged Higgs search benefitted from increase in production cross section from 8 TeV to 13 TeV

	ee	eµ	µµ	eτ	µτ	ττ
12.9 fb^{-1}	785	810	843	658	708	544
100 fb^{-1}	1120	1160	1220	990	1010	870
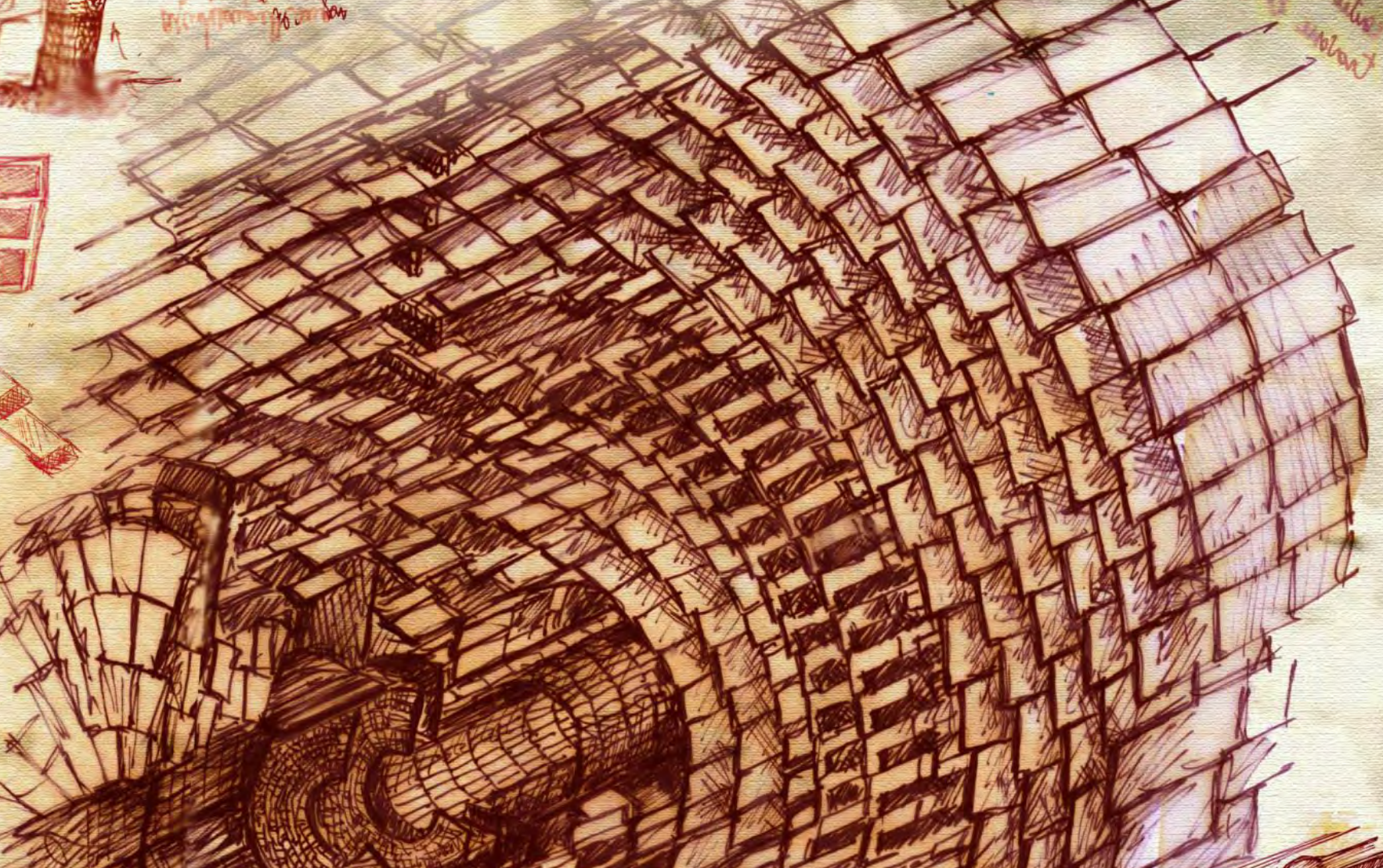
BACKUP

57

LHC Performance

$$L = \frac{N_b^2 n_b f_{rev} \gamma_r}{4\pi \eta_n \beta^*} F \quad F = 1/\sqrt{1 + \left(\frac{\theta_c \sigma_z}{2\sigma^*}\right)^2}$$
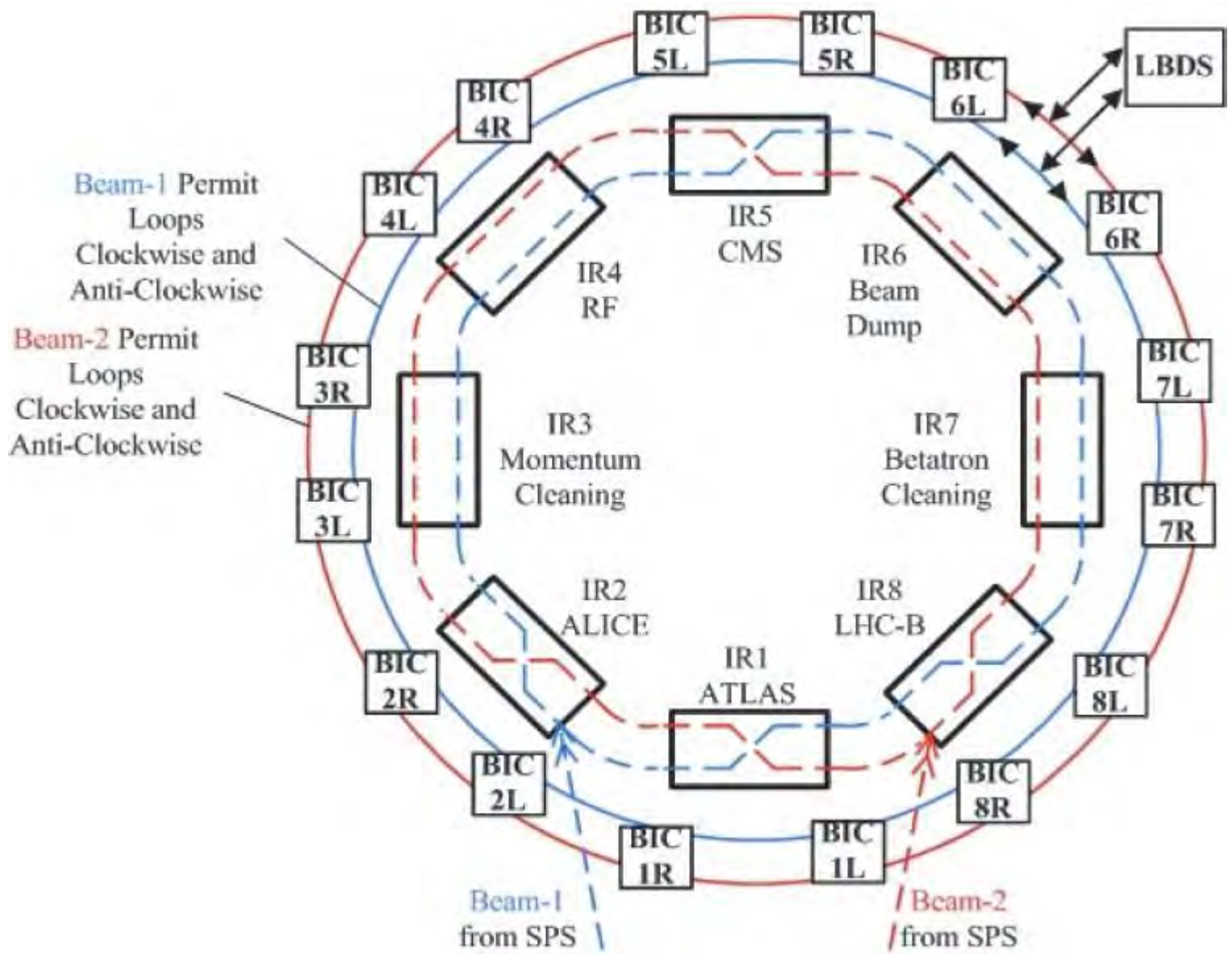
$$\eta \equiv -\ln\left[\tan\left(\frac{\theta}{2}\right)\right]$$

$$y \equiv \frac{1}{2} \ln\left(\frac{E + p_L}{E - p_L}\right)$$

	Run 1			Run 2		Design
Year	2010	2011	2012	2015	2016	—
Beam energy [TeV]	3.5	3.5	4	6.5	6.5	7
Bunch spacing [ns]	150	50	50	25	25	25
Colliding bunches per beam	348	1331	1368	2232	2208	2808
Beta* [m]	3.5	1.0	0.6	0.8	0.4	0.55
Protons per bunch [10^{11}]	1.2	1.5	1.7	1.15	1.25	1.15
Emittance [mm mrad]	2.2	2.3	2.5	3.5	3.0	3.75
Peak inst. lumi. [$10^{34}\,\mathrm{cm}^{-2}\,\mathrm{s}^{-1}$]	0.02	0.35	0.77	0.52	1.53	1
Peak collisions per bunch	4	17	37	22	49	
Integrated lumi. [fb^{-1}]	0.04	6.1	23.3	4.2	41.1	—

LHC Layout

LHC Dipole

LHC DIPOLE : STANDARD CROSS-SECTION

CERN AC/DI/MM - HE107 - 30 04 1999

- ALIGNMENT TARGET
- MAIN QUADRIPOLE BUS-BARS
- HEAT EXCHANGER PIPE
- SUPERINSULATION
- SUPERCONDUCTING COILS
- BEAM PIPE
- VACUUM VESSEL
- BEAM SCREEN
- AUXILIARY BUS-BARS
- SHRINKING CYLINDER / HE I-VESSEL
- THERMAL SHIELD (55 to 75K)
- NON-MAGNETIC COLLARS
- IRON YOKE (COLD MASS, 1.9K)
- DIPOLE BUS-BARS
- SUPPORT POST
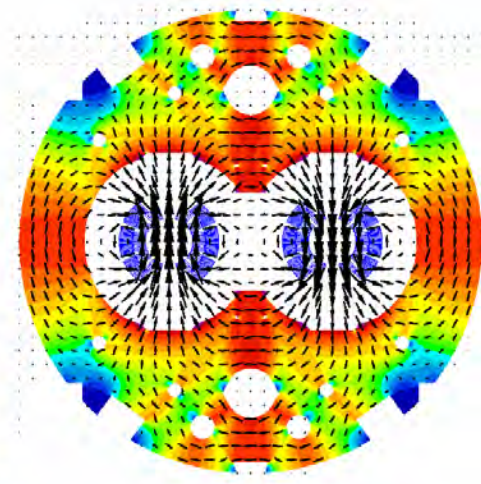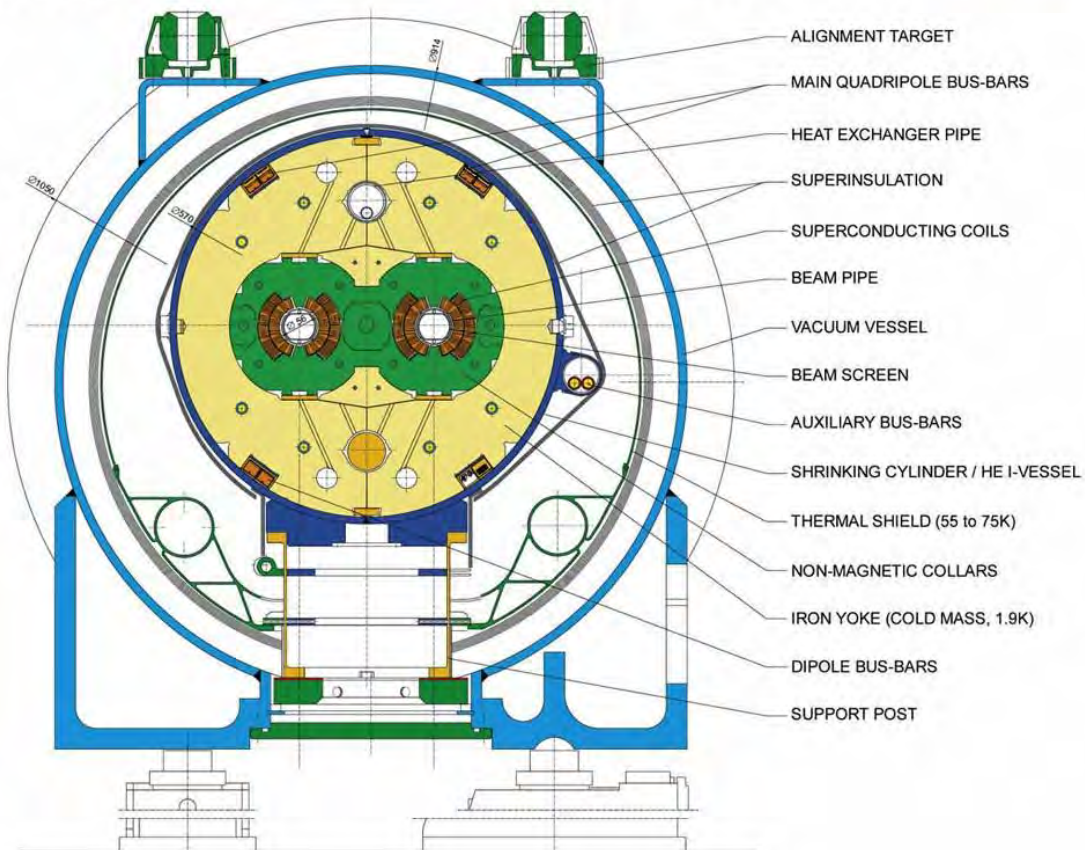
Solenoid and p_T Measurement

- The central feature of CMS is the large 3.8 T solenoid magnet
  - Length: 12.5 m, diameter: 6.3 M
  - Cooled to 4.7 K
- Drove the design of the rest of the detector systems
  - All calorimetry inside solenoid for good energy resolution
- Good p_T measurement of charged particles in tracker and muon system due to strong magnetic field
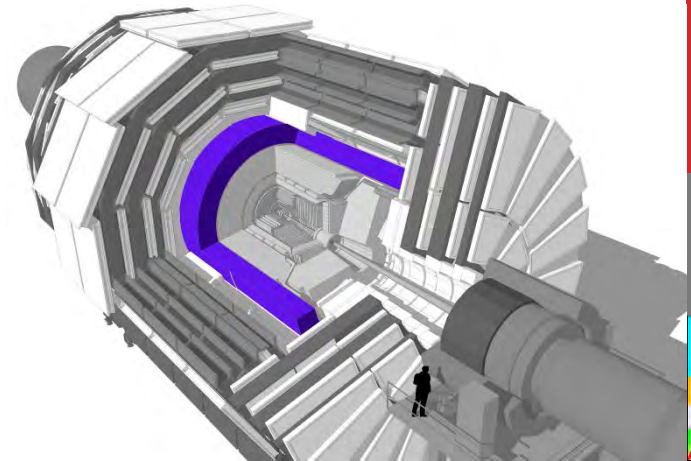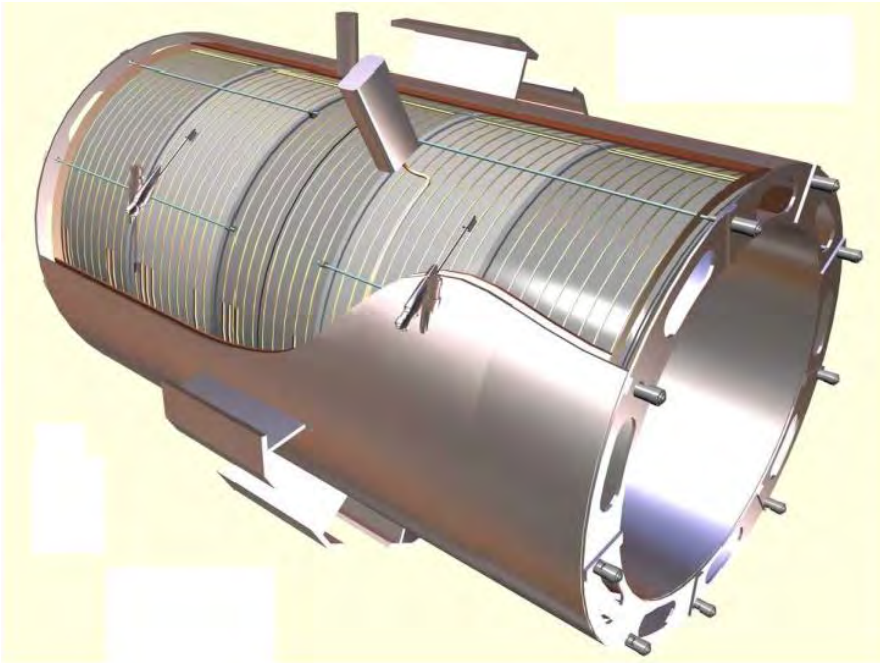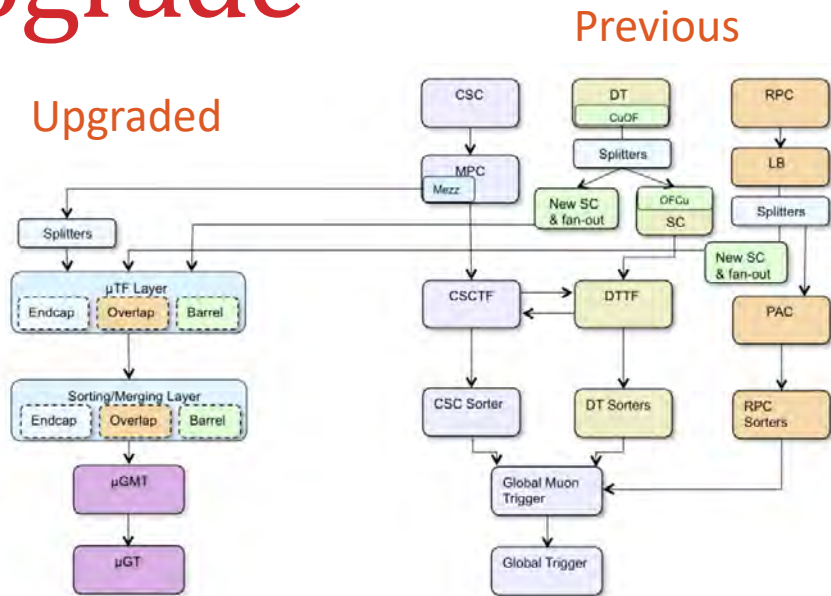
The L1 Trigger Upgrade

- L1 trigger in 2015
  - Muon trigger with detector level track finders from Run-1
  - Calorimeter trigger consists of partial upgrade from Run-1 configuration
- L1 trigger in 2016
  - Muon trigger upgraded to regional track finders
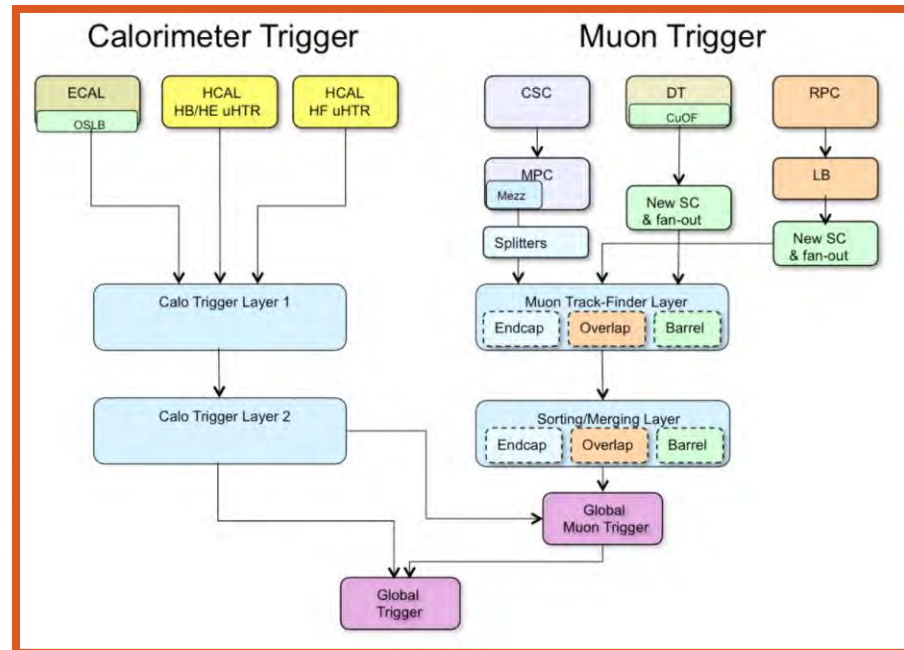 - Calorimeter trigger fully upgraded
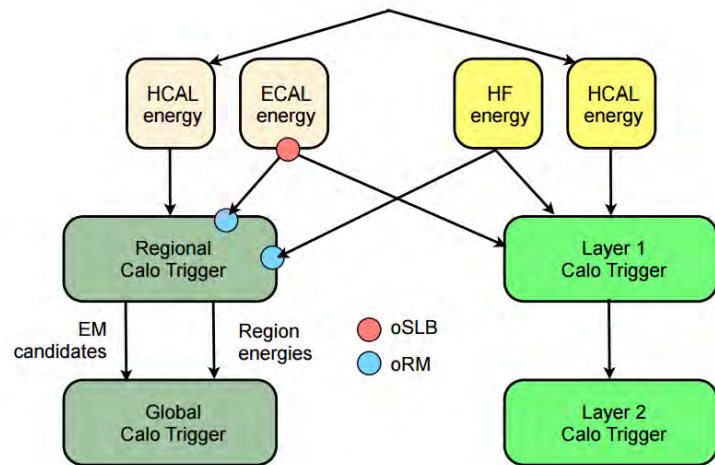
Upgraded

Previous   Upgraded

62

Pile-up

- To achieve large integrated luminosity, many collisions occur at each bunch crossing
  - This leads to pile-up, many uninteresting QCD interactions that act as a background to the primary interaction that triggered the event
  - Particle flow (via the excellent pixel detector) mitigates tracks from secondary vertices and energy deposits associated to these tracks
  - Energy deposits not associated to tracks (neutral particles) are more difficult
  - At the analysis level, require objects from primary vertex to reduce pile-up effects

protons

protons
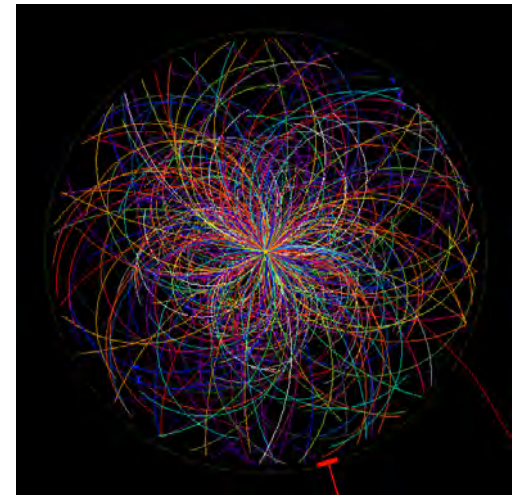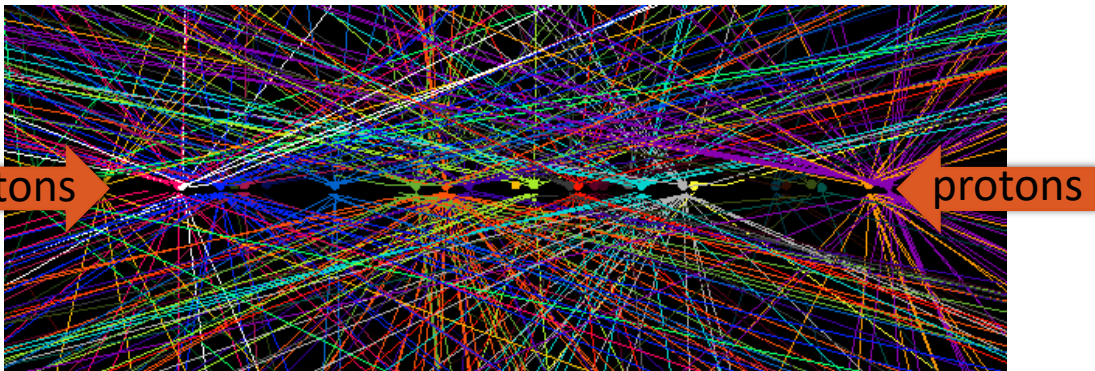
Parton Showering, Hadronization

- Parton showering is the process by which additional initial state (ISR) or final state (FSR) particles are produced in addition to the hard process
  - Typically performed in a subsequent generator, PYTHIA8
  - Radiated matrix element particles matched to parton showers to avoid double counting
- Hadronization is the process by which particles with color charge become hadrons
  - PYTHIA8 uses the Lund string model
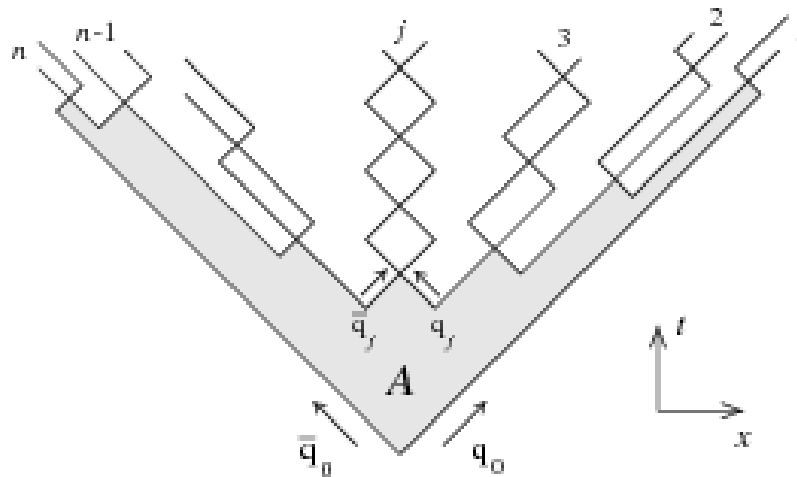
PDF Data
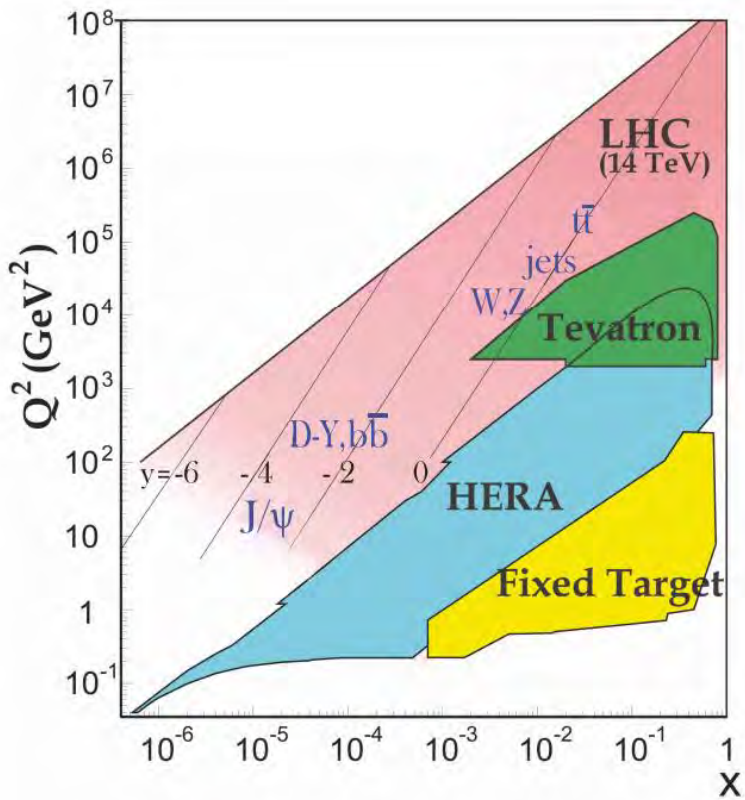
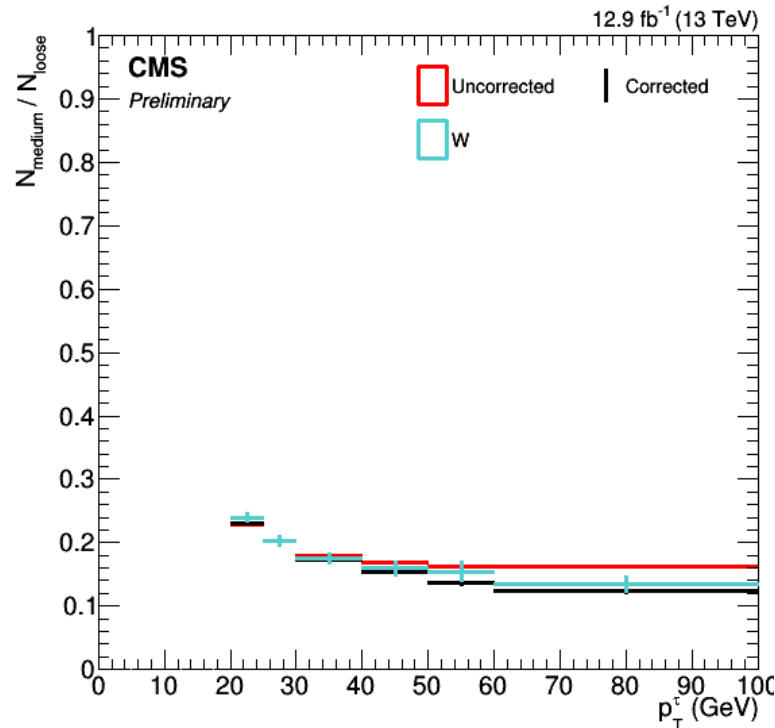| Process	Subprocess	Partons	x range
$\ell^{\pm} \{p, n\} \to \ell^{\pm} X$	$\gamma^* q \to q$	$q, \bar{q}, g$	$x \gtrsim 0.01$
$\ell^{\pm} n/p \to \ell^{\pm} X$	$\gamma^* d/u \to d/u$	d/u	$x \gtrsim 0.01$
$pp \to \mu^+ \mu^- X$	$u\bar{u}, d\bar{d} \to \gamma^*$	$\bar{q}$	$0.015 \lesssim x \lesssim 0.35$
$pn/pp \to \mu^+ \mu^- X$	$(u\bar{d})/(u\bar{u}) \to \gamma^*$	$\bar{d}/\bar{u}$	$0.015 \lesssim x \lesssim 0.35$
$\nu(\bar{\nu}) N \to \mu^-(\mu^+) X$	$W^* q \to q'$	$q, \bar{q}$	$0.01 \lesssim x \lesssim 0.5$
$\nu N \to \mu^- \mu^+ X$	$W^* s \to c$	s	$0.01 \lesssim x \lesssim 0.2$
$\bar{\nu} N \to \mu^- \mu^+ X$	$W^* \bar{s} \to \bar{c}$	$\bar{s}$	$0.01 \lesssim x \lesssim 0.2$
$e^{\pm} p \to e^{\pm} X$	$\gamma^* q \to q$	$g, q, \bar{q}$	$10^{-4} \lesssim x \lesssim 0.1$
$e^+ p \to \bar{\nu} X$	$W^+ \{d, s\} \to \{u, c\}$	d, s	$x \gtrsim 0.01$
$e^{\pm} p \to e^{\pm} c\bar{c}X, e^{\pm} b\bar{b}X$	$\gamma^* c \to c, \gamma^* g \to c\bar{c}$	c, b, g	$10^{-4} \lesssim x \lesssim 0.01$
$e^{\pm} p \to \ \text{jet}+X$	$\gamma^* g \to q\bar{q}$	g	$0.01 \lesssim x \lesssim 0.1$
$p\bar{p}, pp \to \ \text{jet}+X$	$gg, qg, qq \to 2j$	g, q	$0.00005 \lesssim x \lesssim 0.5$
$p\bar{p} \to (W^{\pm} \to \ell^{\pm} \nu) X$	$ud \to W^+, \bar{u}\bar{d} \to W^-$	$u, d, \bar{u}, \bar{d}$	$x \gtrsim 0.05$
$pp \to (W^{\pm} \to \ell^{\pm} \nu) X$	$u\bar{d} \to W^+, d\bar{u} \to W^-$	$u, d, \bar{u}, \bar{d}, g$	$x \gtrsim 0.001$
$p\bar{p}(pp) \to (Z \to \ell^+ \ell^-) X$	$uu, dd, ..(u\bar{u}, ..) \to Z$	$u, d, ..(g)$	$x \gtrsim 0.001$
$pp \to W^- c, \ W^+ \bar{c}$	$gs \to W^- c$	$s, \bar{s}$	$x \sim 0.01$
$pp \to (\gamma^* \to \ell^+ \ell^-) X$	$u\bar{u}, d\bar{d}, .. \to \gamma^*$	$\bar{q}, g$	$x \gtrsim 10^{-5}$
$pp \to b\bar{b} X, \ t\bar{t}X$	$gg \to b\bar{b}, \ t\bar{t}$	g	$x \gtrsim 10^{-5}, 10^{-2}$
$pp \to \text{exclusive } J/\psi, \ \Upsilon$	$\gamma^*(gg) \to J/\psi, \ \Upsilon$	g	$x \gtrsim 10^{-5}, 10^{-4}$
$pp \to \gamma X$	$gq \to \gamma q, g\bar{q} \to \gamma \bar{q}$	g	$x \gtrsim 0.005$

65

Electron/Muon Fake Efficiencies

- Efficiencies measured as a function of p_T and eta
- Electroweak contributions in the dijet control region estimated from MC are subtracted
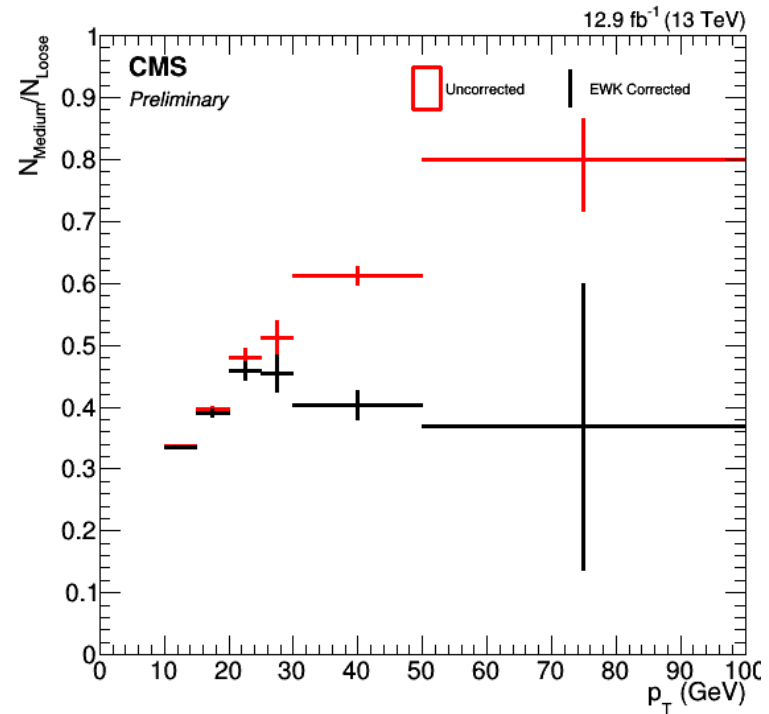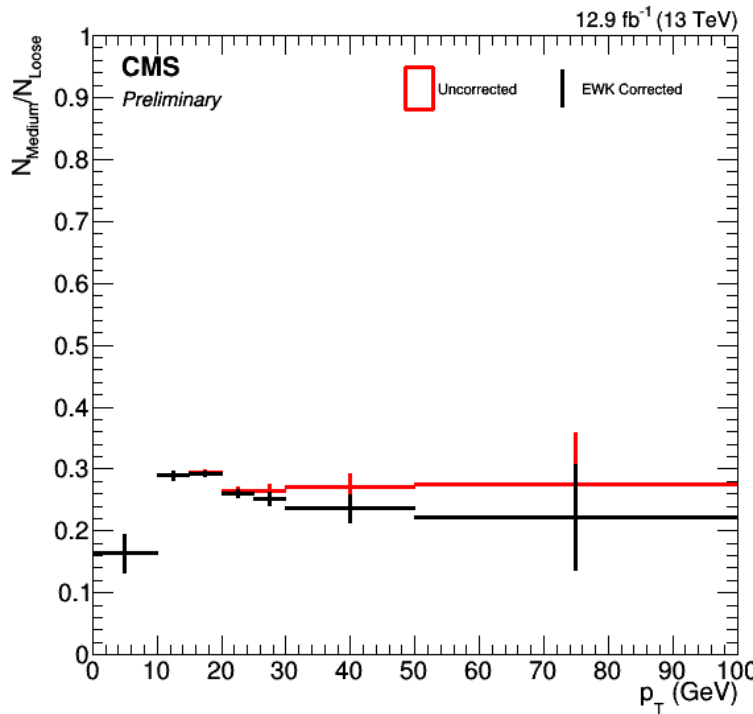
Tau Fake Efficiencies

- Similar method for taus
- Calculated in a W+jet control region with the W decaying leptonically to a muon
- Electroweak contribution corrected via MC
- As cross check, efficiency calculated via W+jets MC sample as well
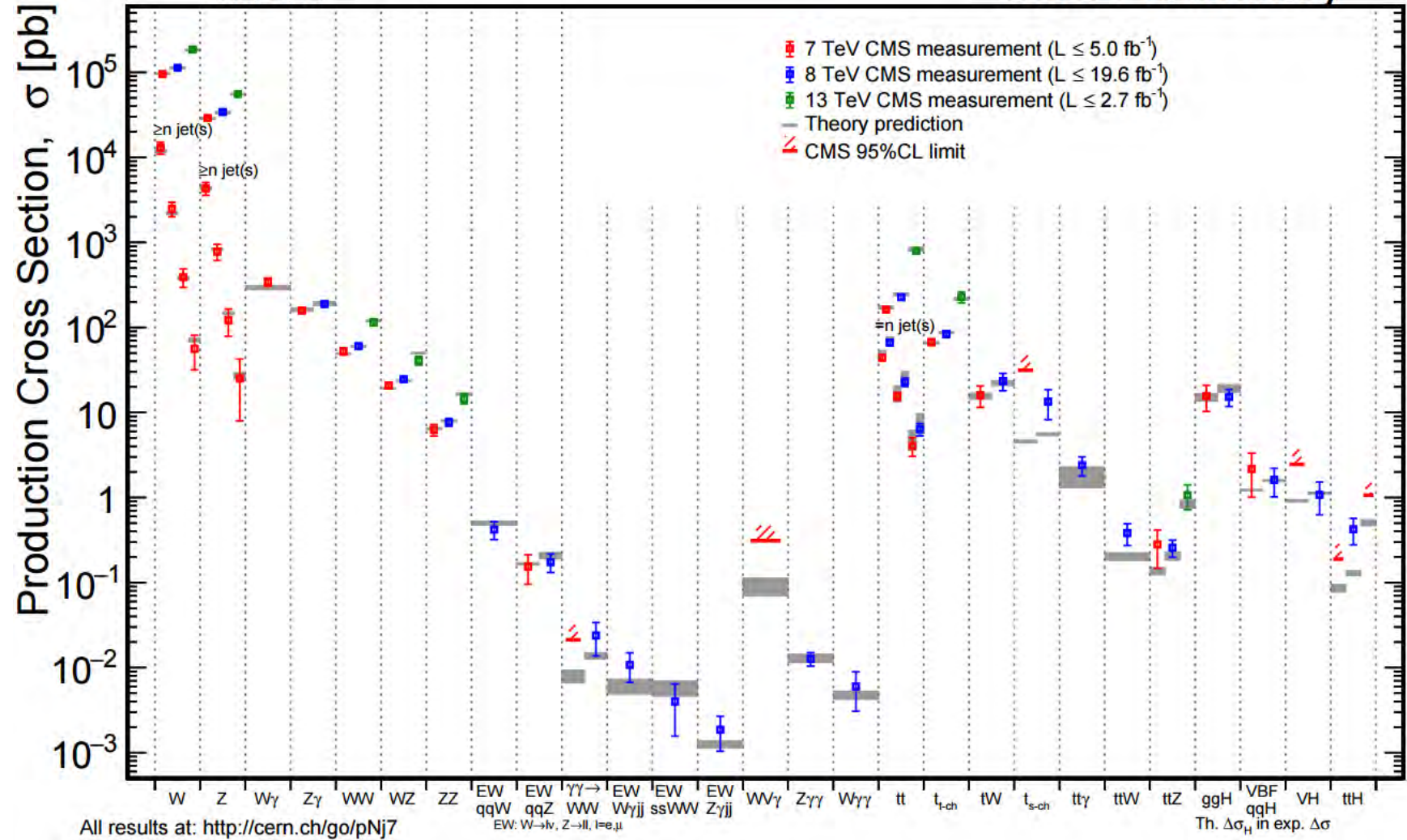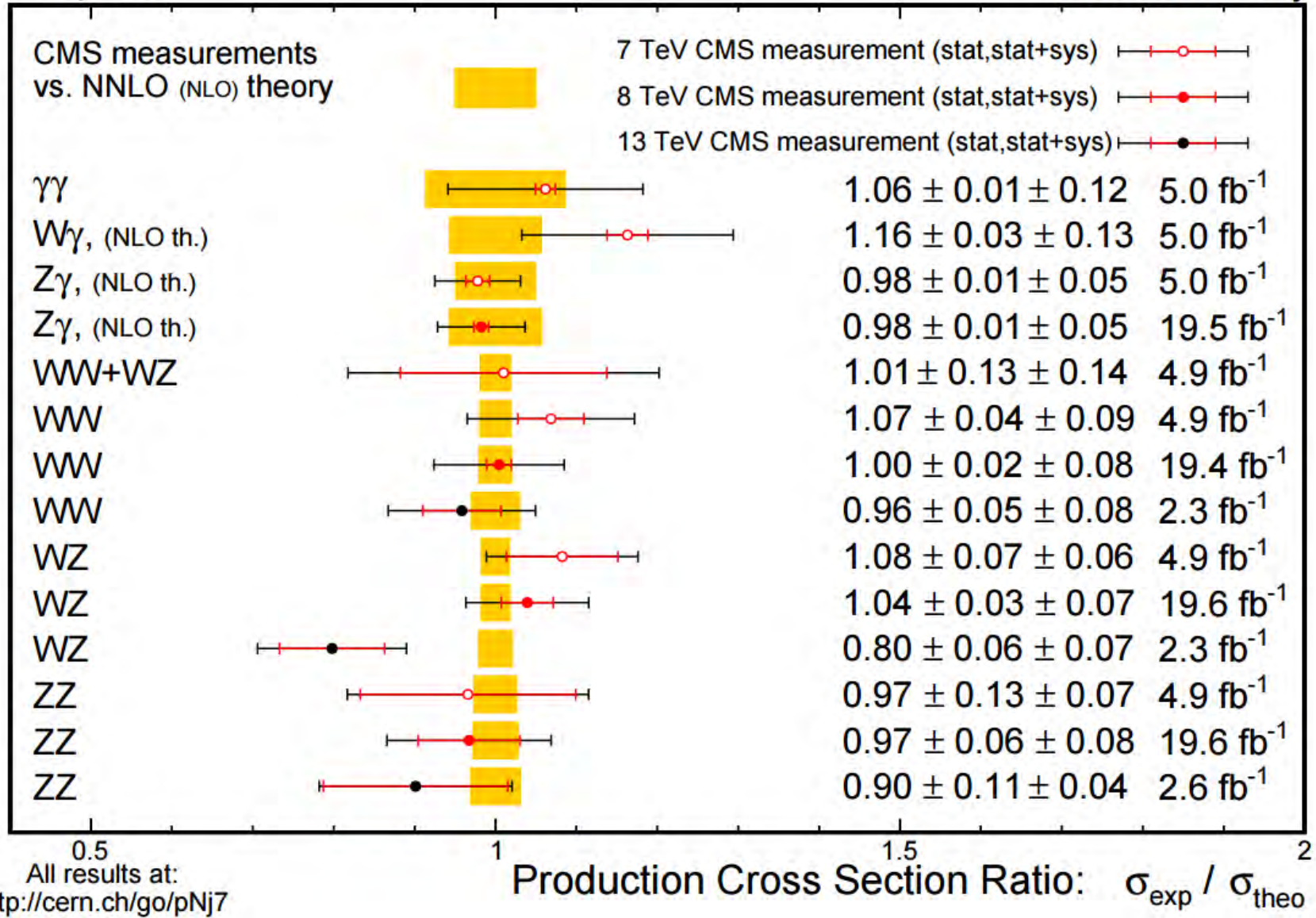 - Good agreement

SM Cross Sections (CMS)

Diboson Cross Sections (CMS)

July 2016 — CMS Preliminary

CMS measurements vs. NNLO (NLO) theory

	7 TeV CMS measurement (stat,stat+sys)
	8 TeV CMS measurement (stat,stat+sys)
	13 TeV CMS measurement (stat,stat+sys)

|	$\sigma_{exp}/\sigma_{theo}$	Luminosity
$\gamma\gamma$	$1.06 \pm 0.01 \pm 0.12$	5.0 fb^{-1}
$W\gamma$, (NLO th.)	$1.16 \pm 0.03 \pm 0.13$	5.0 fb^{-1}
$Z\gamma$, (NLO th.)	$0.98 \pm 0.01 \pm 0.05$	5.0 fb^{-1}
$Z\gamma$, (NLO th.)	$0.98 \pm 0.01 \pm 0.05$	19.5 fb^{-1}
WW+WZ	$1.01 \pm 0.13 \pm 0.14$	4.9 fb^{-1}
WW	$1.07 \pm 0.04 \pm 0.09$	4.9 fb^{-1}
WW	$1.00 \pm 0.02 \pm 0.08$	19.4 fb^{-1}
WW	$0.96 \pm 0.05 \pm 0.08$	2.3 fb^{-1}
WZ	$1.08 \pm 0.07 \pm 0.06$	4.9 fb^{-1}
WZ	$1.04 \pm 0.03 \pm 0.07$	19.6 fb^{-1}
WZ	$0.80 \pm 0.06 \pm 0.07$	2.3 fb^{-1}
ZZ	$0.97 \pm 0.13 \pm 0.07$	4.9 fb^{-1}
ZZ	$0.97 \pm 0.06 \pm 0.08$	19.6 fb^{-1}
ZZ	$0.90 \pm 0.11 \pm 0.04$	2.6 fb^{-1}

All results at:
http://cern.ch/go/pNj7

Production Cross Section Ratio: $\sigma_{exp}/\sigma_{theo}$

Nonprompt Uncertainty

- Uncertainty on nonprompt background derived in Drell—Yan and tt control regions
  - Drell—Yan: Same as signal region with E_T^{miss} cut inverted and W lepton $p_T > 10$ GeV
  - tt: Same as signal region with Z window veto in [81, 101] GeV, at least one b-tagged jet, and W lepton $p_T > 10$ GeV
- The final signal region has 75% Drell—Yan and 25% tt
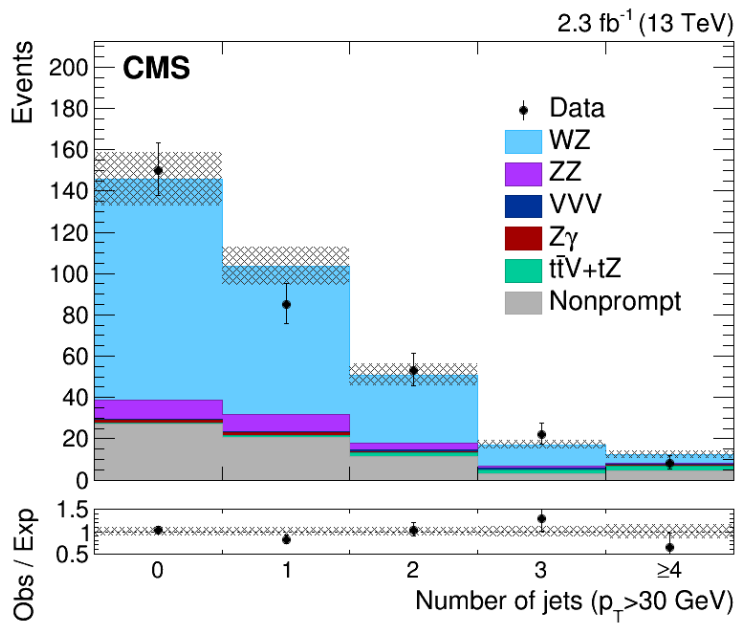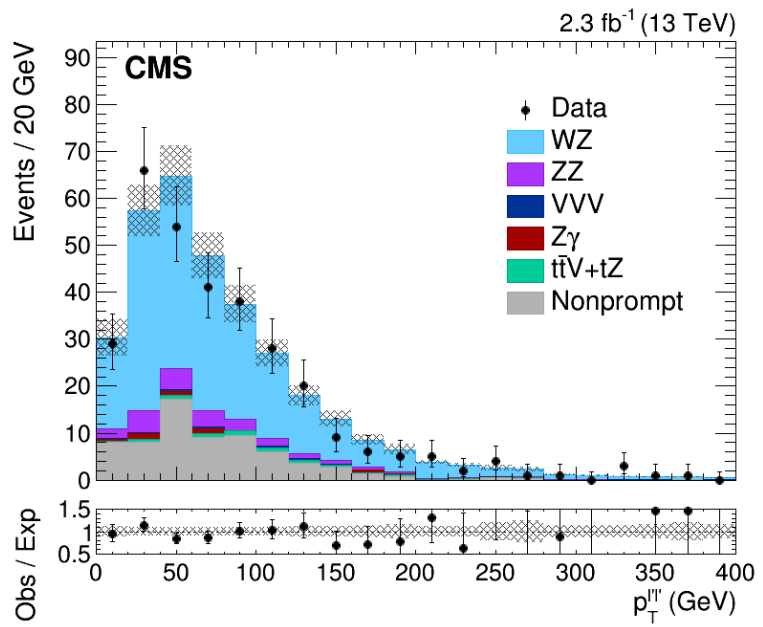 - Correspond to 30% uncertainty in nonprompt
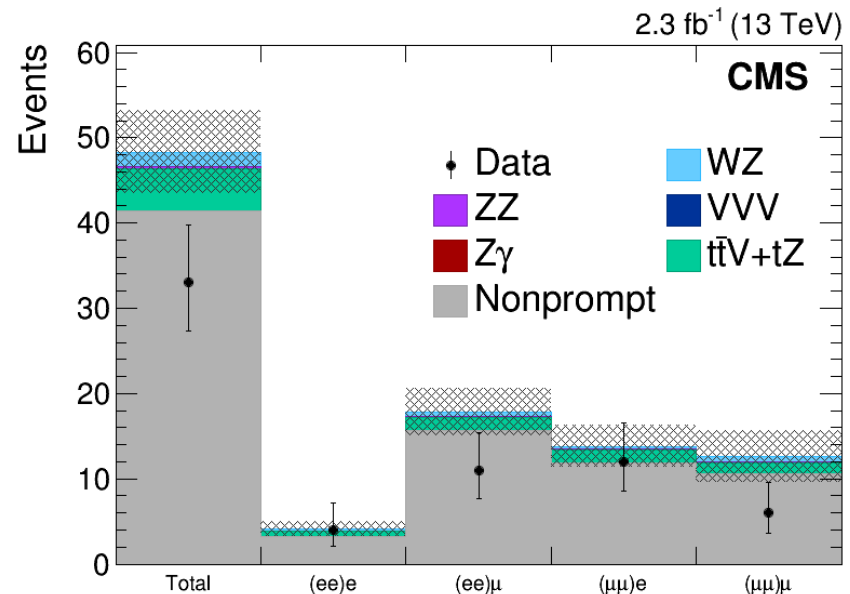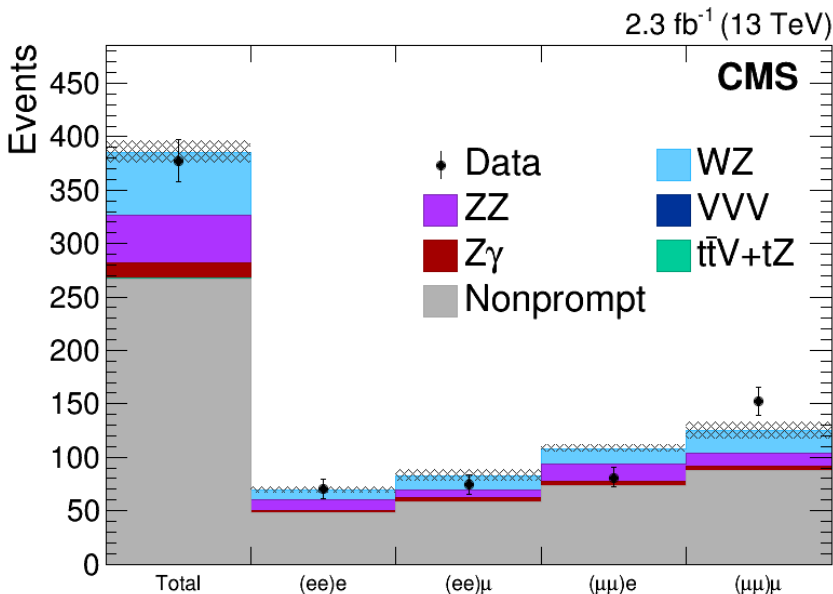
WZ Distributions (1)
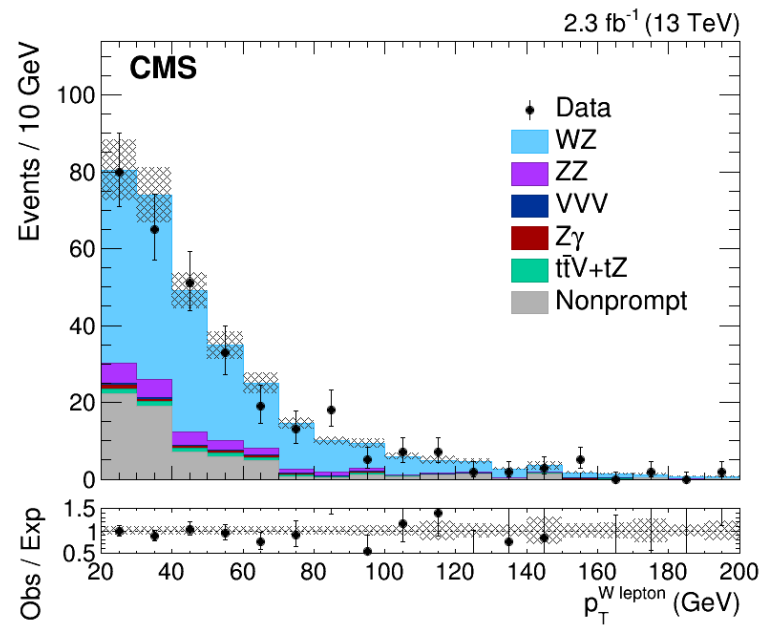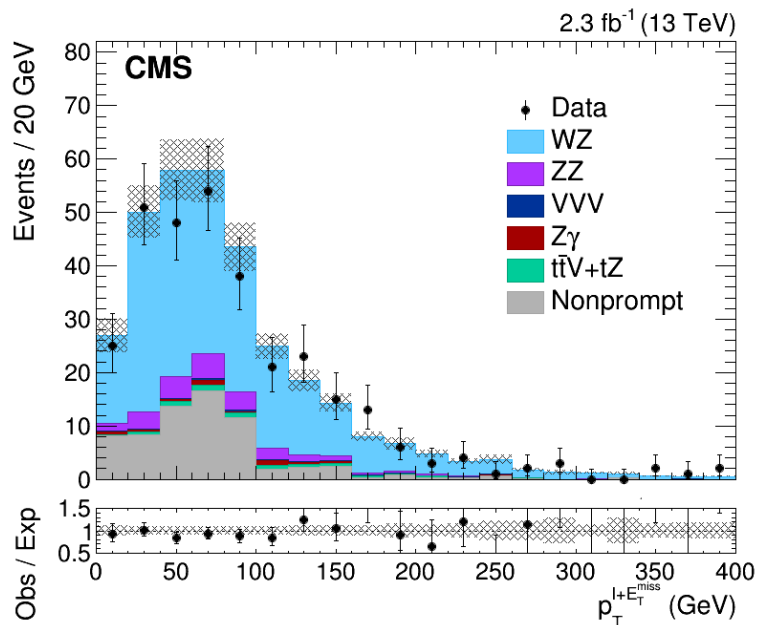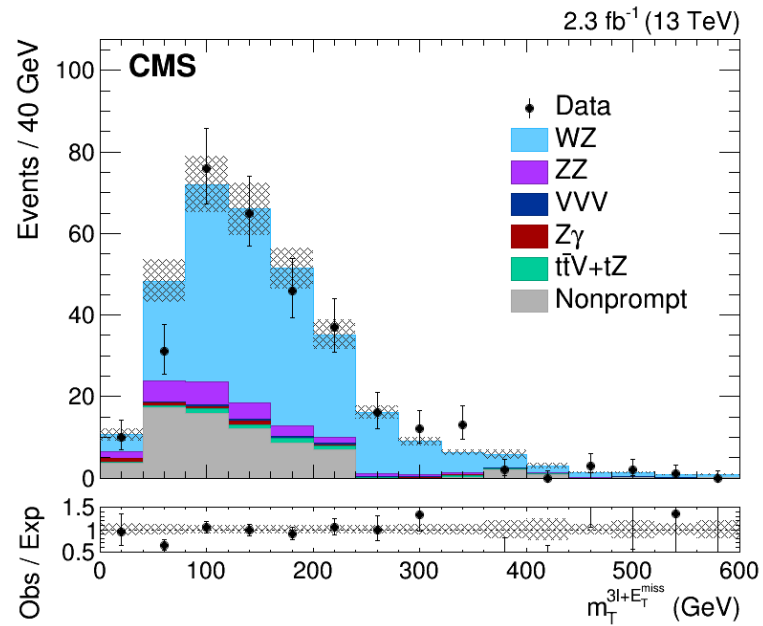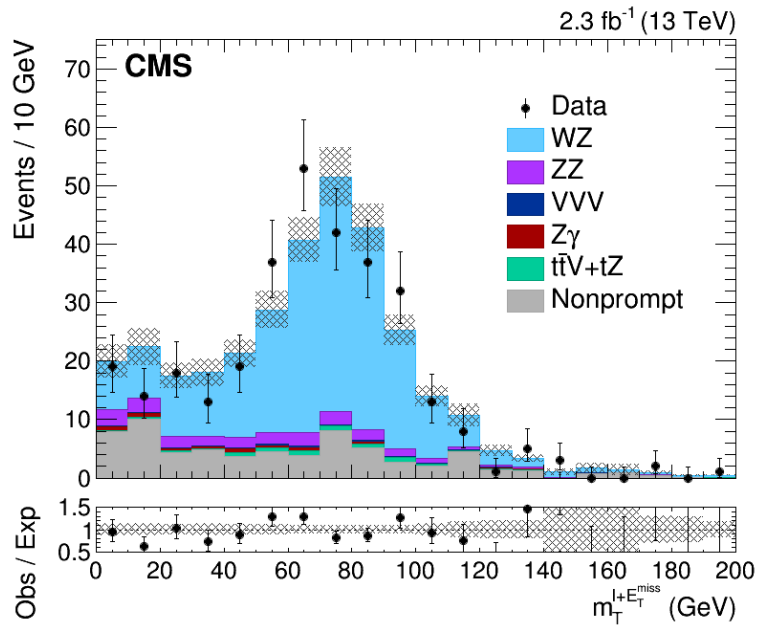
WZ Distributions (2)

WZ Per Channel MC Comparison

- The cross section is reported for two regions

Selection	Final state	Cross section (fb)	
		MCFM	POWHEG
$M_Z \in [60, 120]$ GeV	eee	$153.0^{+6.5}_{-3.1} \pm 2.2$	$152.9^{+5.2}_{-4.4} \pm 2.1$
	$ee\mu$	$153.0^{+6.5}_{-3.1} \pm 2.2$	$153.7^{+5.3}_{-4.4} \pm 2.1$
	$\mu\mu e$	$153.0^{+6.5}_{-3.1} \pm 2.2$	$154.7^{+5.3}_{-4.4} \pm 2.1$
	$\mu\mu\mu$	$153.0^{+6.5}_{-3.1} \pm 2.2$	$153.6^{+5.3}_{-4.4} \pm 2.1$
Fiducial region	eee	$68.58^{+2.61}_{-2.17} \pm 0.99$	$69.18^{+2.61}_{-2.17} \pm 0.94$
	$ee\mu$	$68.58^{+2.61}_{-2.17} \pm 0.99$	$68.97^{+2.61}_{-2.17} \pm 0.94$
	$\mu\mu e$	$68.58^{+2.61}_{-2.17} \pm 0.99$	$69.77^{+2.64}_{-2.20} \pm 0.94$
	$\mu\mu\mu$	$68.58^{+2.61}_{-2.17} \pm 0.99$	$69.46^{+2.65}_{-2.20} \pm 0.94$

Fiducial region
- Z mass window [60, 120]
- Lepton p_T > 20, 10, 20 GeV and $|\eta|$ < 2.5
- m_{ll} > 4 GeV

- Theoretical cross sections are calculated using POWHEG with NNPDF3.0

  - Acceptance correction from total to fiducial of 45 ± 0.4%

	Final state			
	$\mu\mu\mu$	$\mu\mu e$	$ee\mu$	eee
Acceptance (MCFM)	$44.84^{+0.21}_{-0.60}$	$44.84^{+0.21}_{-0.60}$	$44.84^{+0.21}_{-0.60}$	$44.84^{+0.21}_{-0.60}$
Acceptance (POWHEG)	$45.22^{+0.19}_{-0.17}$	$45.10^{+0.18}_{-0.14}$	$44.86^{+0.17}_{-0.14}$	$45.24^{+0.18}_{-0.15}$
Efficiency (POWHEG)	54.5	37.4	34.5	25.4
Acceptance $\times$ Efficiency	$24.6^{+0.1}_{-0.1}$	$16.9^{+0.1}_{-0.1}$	$15.5^{+0.1}_{-0.1}$	$11.5^{+0.1}_{-0.1}$

Neutrino Mixing

- Atmospheric, solar, reactor, and accelerator neutrino oscillation experiments have shown neutrinos do have mass
  - Three mixing angles θ_{12}, θ_{13}, and θ_{23} and one CP violating phase δ
  - Three masses m_1, m_2, and m_3
- Atmospheric oscillation experiments cannot measure sign of the splitting
  - Gives rise to two possible orderings, normal and inverted hierarchy
- The mixing angles have also been measured
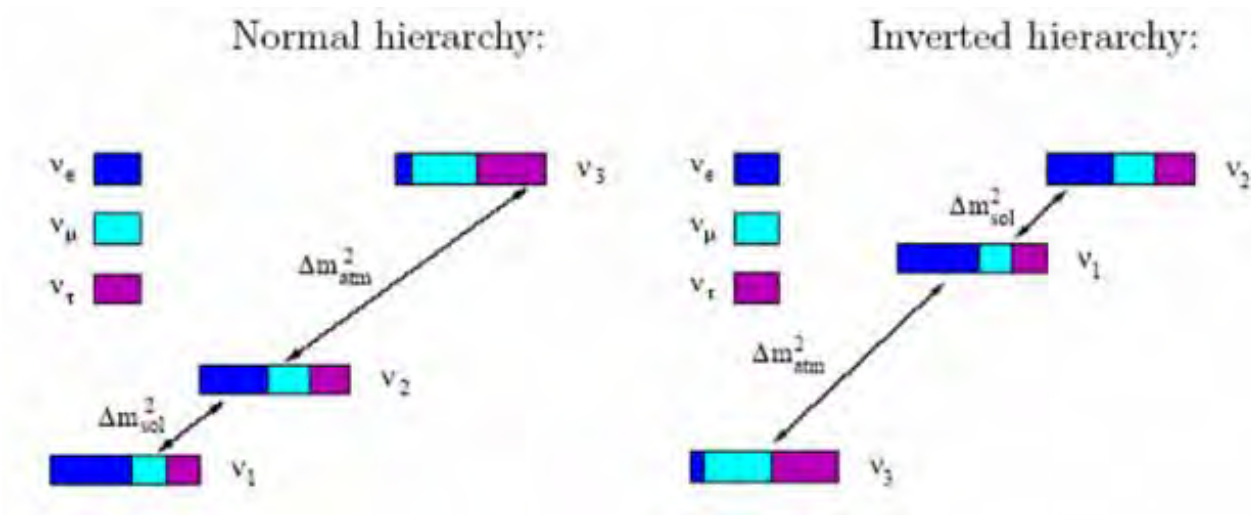
Neutrino Mixing Parameters

- Known neutrino parameters including mixing angles and atmospheric and solar mass splittings

$$\sin^2(\theta_{12}) = 0.308 \pm 0.017$$

$$\sin^2(\theta_{23}) = 0.437^{+0.033}_{-0.023}\, (0.455^{+0.039}_{-0.031})$$

$$\sin^2(\theta_{13}) = 0.0234^{+0.0020}_{-0.0019}\, (0.0240^{+0.0019}_{-0.0022})$$

$$\Delta m^2_{atm} = \Delta m^2_{31}$$

$$\Delta m^2_{\odot} = \Delta m^2_{21}$$

$$\Delta m^2_{21} = 7.54^{+0.26}_{-0.22} \times 10^{-5}\,\mathrm{eV}$$

$$|\Delta m^2| = 2.43 \pm 0.06\,(2.38 \pm 0.06) \times 10^{-3}\,\mathrm{eV}$$

$$\begin{pmatrix} \nu_e \\ \nu_\mu \\ \nu_\tau \end{pmatrix} = U \begin{pmatrix} \nu_1 \\ \nu_2 \\ \nu_3 \end{pmatrix}$$

$$\delta/\pi = 1.39^{+0.38}_{-0.27}\,(1.31^{+0.29}_{-0.33})$$

$$\Delta m^2 = m_3^2 - (m_2^2 + m_1^2)/2$$

$$U = \begin{pmatrix} c_{12}c_{13} & s_{12}c_{13} & s_{13}e^{-i\delta} \\ -s_{12}c_{23} - c_{12}s_{23}s_{13}e^{i\delta} & c_{12}c_{23} - s_{12}s_{23}s_{13}e^{i\delta} & s_{23}c_{13} \\ s_{12}s_{23} - c_{12}c_{23}s_{13}e^{i\delta} & -c_{12}s_{23} - s_{12}c_{23}s_{13}e^{i\delta} & c_{23}c_{13} \end{pmatrix} \begin{pmatrix} 1 & 0 & 0 \\ 0 & e^{i\alpha_{21}/2} & 0 \\ 0 & 0 & e^{i\alpha_{31}/2} \end{pmatrix}$$

Neutrino Experiments

- Oscillation experiments
  - Solar: ν_e from nuclear fusion
  - Atmospheric: ν_μ, $\overline{\nu}_\mu$ from cosmic ray colliding with nuclei in the atmosphere
  - Reactor: $\overline{\nu}_e$ from nuclear reactor fission
  - Accelerator: ν_μ from decays of mesons produced from collisions of a beam with a target
- Neutrinoless double beta decay
  - If neutrinos are Majorana-like
  - Can probe mass scale, Majorana phase, mass hierarchy
- Electron spectrum from tritium beta decay
  - Measure the electron-neutrino mass
  - Upper limit: $m(\nu_e) < 2.05$ eV
- Cosmological data
  - Sum of neutrino masses < 0.23 eV
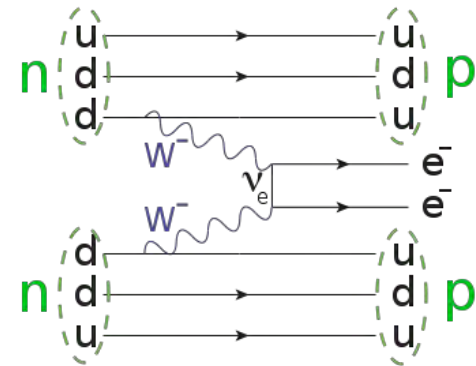
BSM Neutrino Models

- Right-handed neutrino
  - Masses arise via Yukawa couplings like other SM fermions
- Type-I seesaw
  - Singlet neutrinos have large Majorana masses (10^{14} GeV)
  - Suppress neutrino mass via seesaw mechanism
- Type-II seesaw
  - Higgs triplet added to Higgs doublet
  - Masses proportional to Yukawa couplings of the leptons to the doubly-charged Higgs boson

$$M_Z^2 = \frac{(g^2 + g'^2)(v_d^2 + 4v_t^2)}{4} = \frac{g^2(v_d^2 + 4v_t^2)}{4\cos^2\theta_W}$$

$$M_W^2 = \frac{g^2(v_d^2 + 2v_t^2)}{4}$$

CMS

Neutrino Parameters from Φ^{++}

- Tri-bi-maximal mixing

$$\sin^2\theta_{12} = \frac{1}{3}\ ,\ \ \sin^2\theta_{23} = \frac{1}{2}\ ,\ \ \sin^2\theta_{13} = 0$$

- Neutrino hierarchy
  - $C_1 > 1$: normal
  - $C_1 < 1$: inverted
  - $C_1 \approx 1$: degenerate

$$C_1 \equiv \frac{2\mathrm{BR}_{\mu\mu} + \mathrm{BR}_{\mu\tau} - \mathrm{BR}_{ee}}{\mathrm{BR}_{ee} + \mathrm{BR}_{e\mu}} = \frac{-m_1^2 + m_2^2 + 3m_3^2}{2m_1^2 + m_2^2}$$

- Lightest neutrino
  - m_1: normal
  - m_3: inverted

$$m_1^2 = \frac{\Delta m_{sol}^2 (4 - C_1) + 3\Delta m_{atm}^2}{3(C_1 - 1)}$$

$$m_3^2 = \frac{\Delta m_{sol}^2 (1 + 2C_1) - 3C_1 \Delta m_{atm}^2}{3(C_1 - 1)}$$
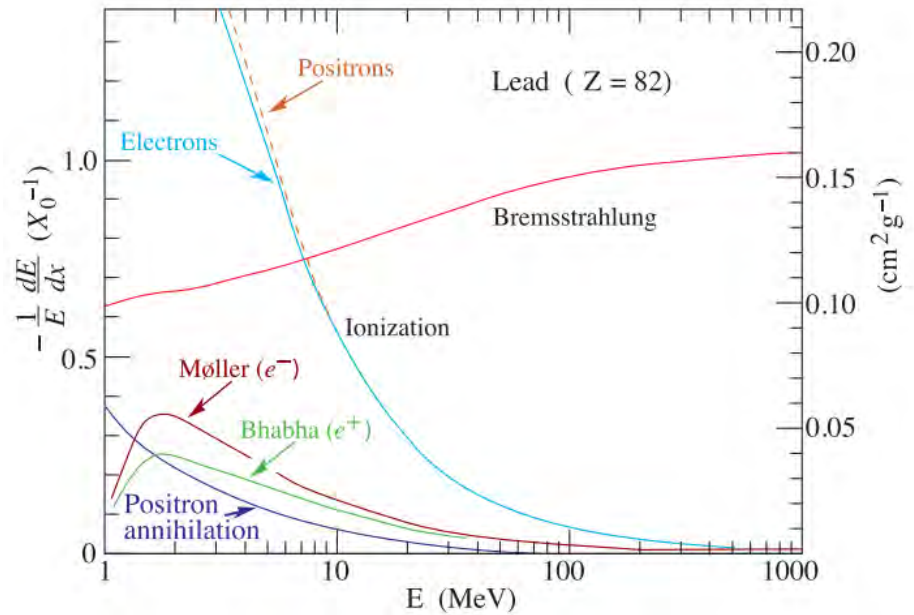
- Non-zero θ_{13}

$$C_1' \equiv \frac{2\mathrm{BR}_{\mu\mu} + 2\mathrm{BR}_{\tau\tau} + 2\mathrm{BR}_{\mu\tau} - 2\mathrm{BR}_{ee}}{2\mathrm{BR}_{ee} + \mathrm{BR}_{e\mu} + \mathrm{BR}_{e\tau}} = \frac{-m_1^2 + m_2^2 + 3m_3^2}{2m_1^2 + m_2^2} + \mathcal{O}(\sin^2\theta_{13})$$
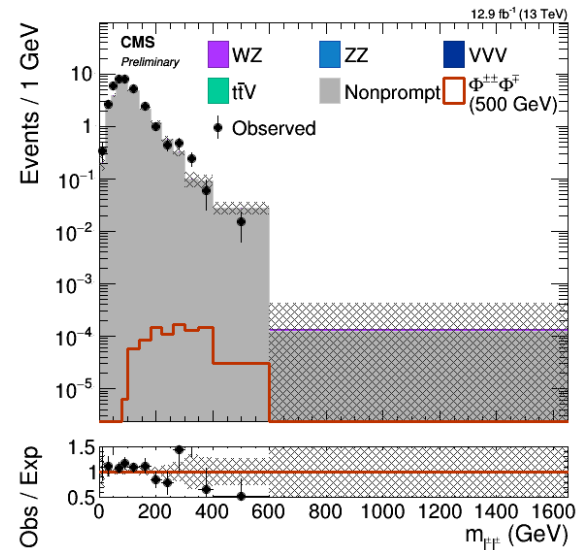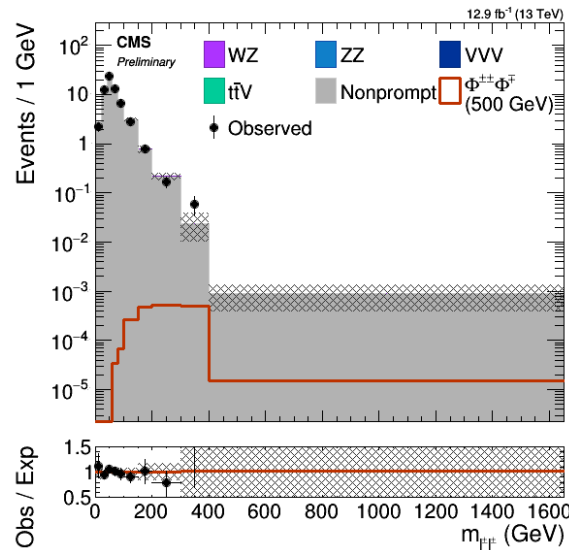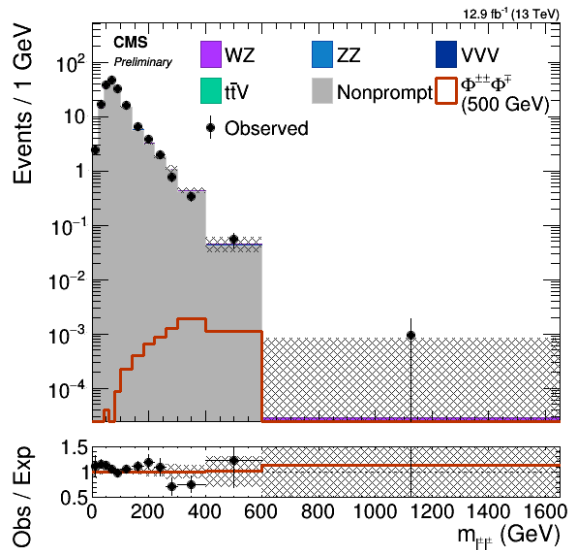
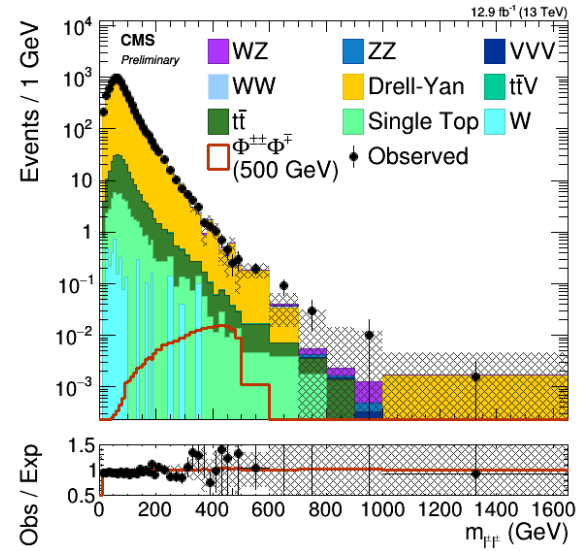- Majorana phases can be similarly found

Energy Losses

- Electrons in lead
- Muons in copper
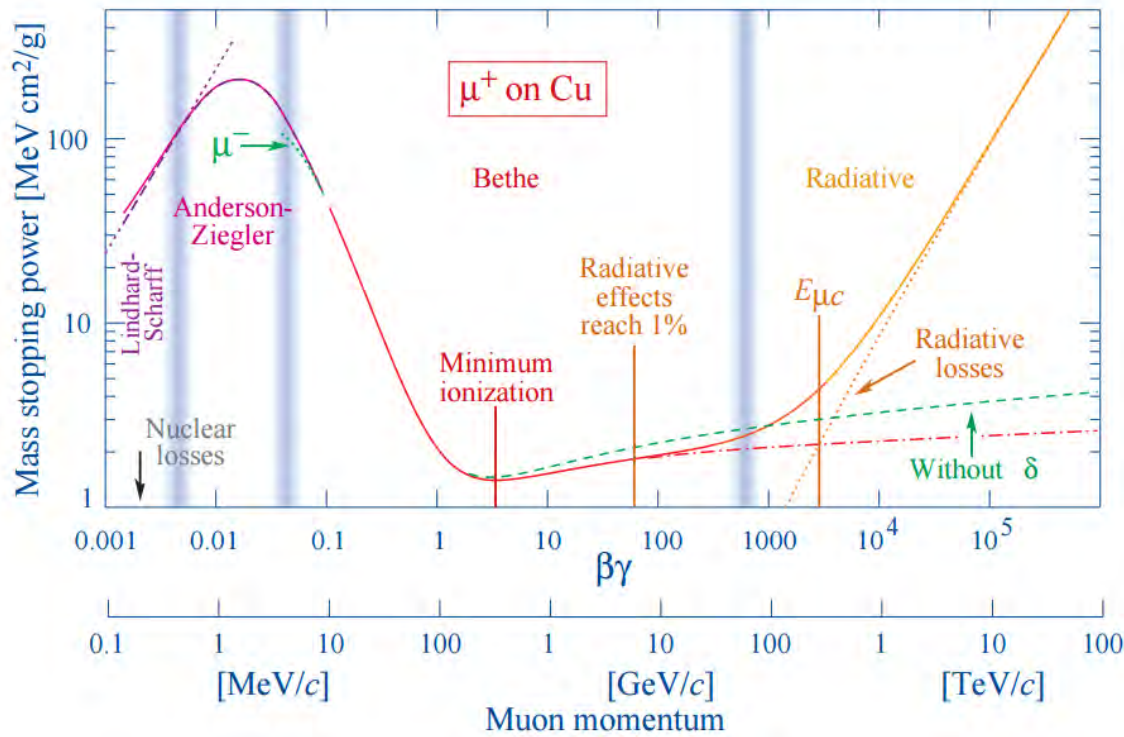
Same Sign Invariant Mass – 3l
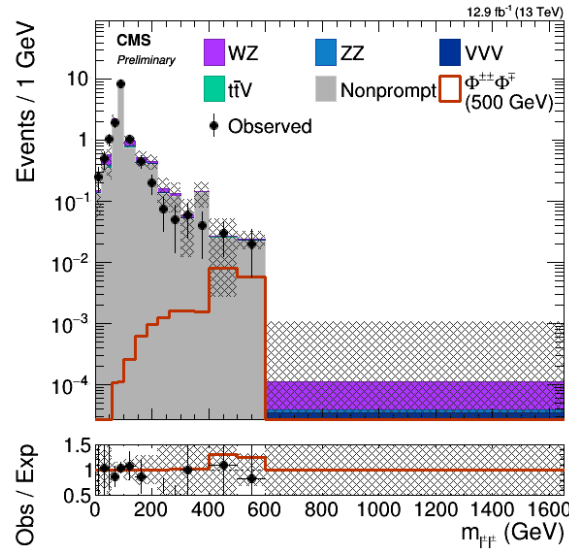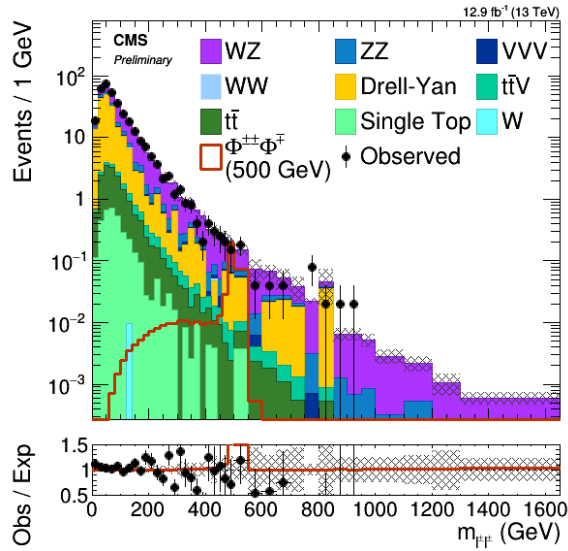
Same Sign Invariant Mass – 4l
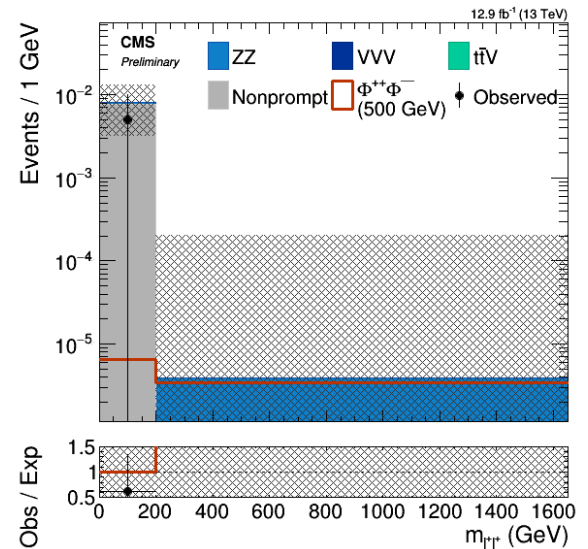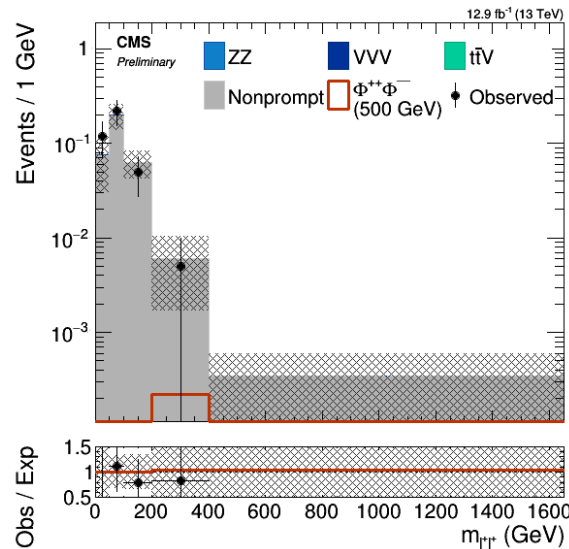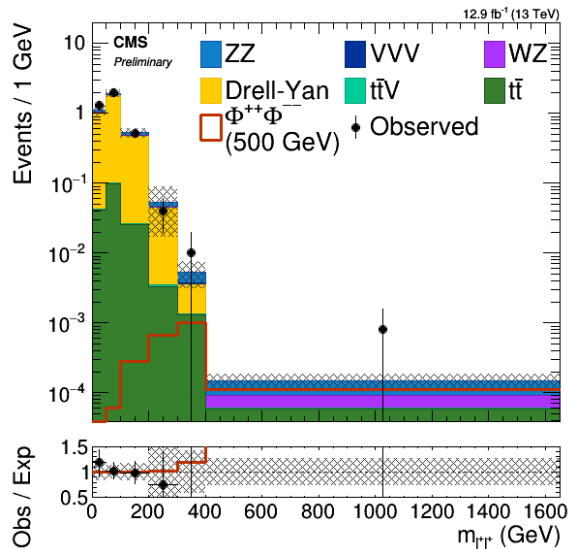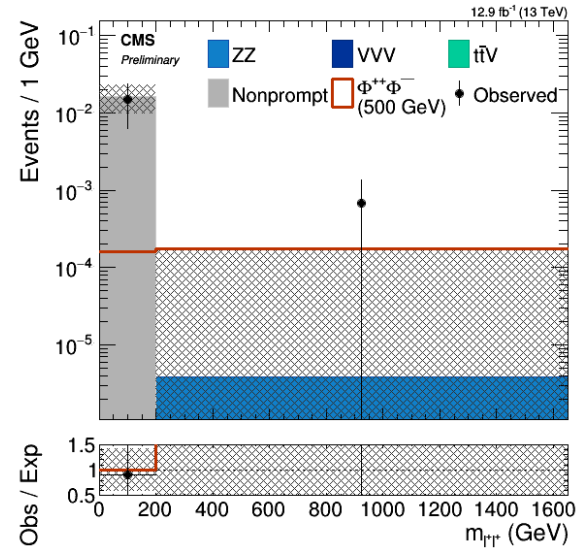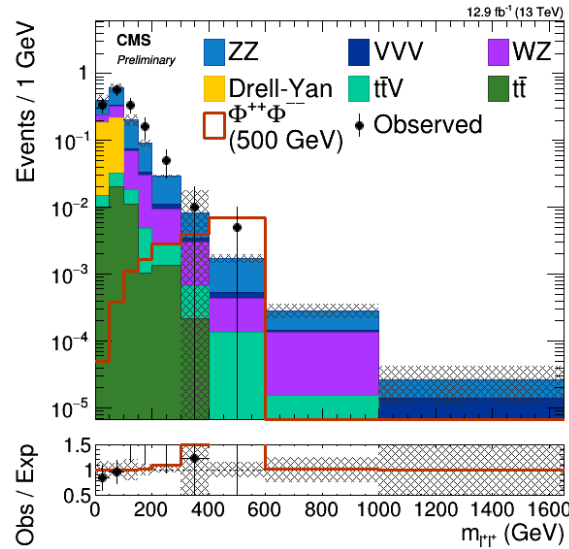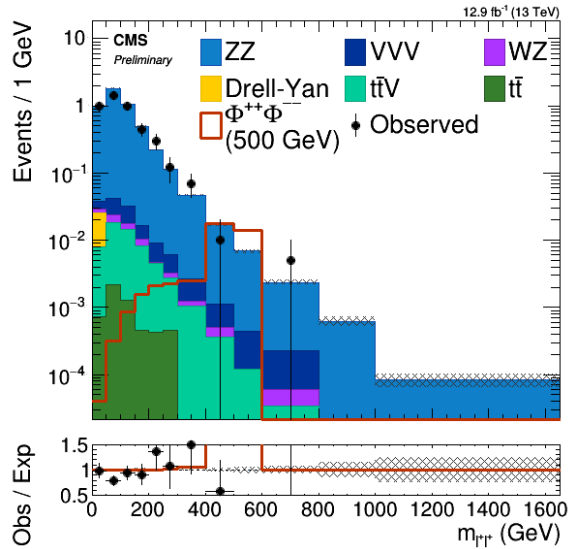
Yields for 500 GeV

Benchmark	Channel	Assoc. Prod.	Pair Prod.	Background	Obs.
100% $\Phi \to ee$	$\ell^{\pm}\ell^{\pm}\ell^{\mp}$	$1.54^{+0.28}_{-0.25} \times 10^1$	$3.87^{+0.71}_{-0.64} \times 10^0$	$2.02^{+0.97}_{-0.69} \times 10^0$	2
	$\ell^{\pm}\ell^{\pm}\tau^{\mp}$	$2.28^{+0.43}_{-0.39} \times 10^0$	—	$3.48^{+2.65}_{-1.56} \times 10^{-1}$	0
	$\ell^+\ell^+\ell^-\ell^-$	—	$6.81^{+1.39}_{-1.26} \times 10^0$	$5.23^{+1.14}_{-1.12} \times 10^{-2}$	0
100% $\Phi \to e\mu$	$\ell^{\pm}\ell^{\pm}\ell^{\mp}$	$1.83^{+0.32}_{-0.28} \times 10^1$	$4.00^{+0.70}_{-0.62} \times 10^0$	$5.19^{+2.22}_{-1.65} \times 10^0$	5
	$\ell^{\pm}\ell^{\pm}\tau^{\mp}$	$2.79^{+0.51}_{-0.46} \times 10^0$	—	$4.20^{+2.70}_{-1.92} \times 10^{-1}$	0
	$\ell^+\ell^+\ell^-\ell^-$	—	$9.19^{+1.66}_{-1.49} \times 10^0$	$1.22^{+0.19}_{-0.18} \times 10^{-1}$	0
100% $\Phi \to e\tau$	$\ell^{\pm}\ell^{\pm}\ell^{\mp}$	$3.11^{+0.55}_{-0.49} \times 10^0$	$1.21^{+0.23}_{-0.20} \times 10^0$	$6.62^{+2.02}_{-1.60} \times 10^0$	10
	$\ell^{\pm}\ell^{\pm}\tau^{\mp}$	$4.21^{+0.81}_{-0.73} \times 10^{-1}$	$1.37^{+0.34}_{-0.30} \times 10^{-1}$	$3.16^{+2.10}_{-1.34} \times 10^{-1}$	0
	$\ell^{\pm}\tau^{\pm}\ell^{\mp}$	$4.76^{+0.88}_{-0.79} \times 10^0$	$1.70^{+0.33}_{-0.30} \times 10^0$	$2.35^{+1.38}_{-0.96} \times 10^0$	0
	$\ell^{\pm}\tau^{\pm}\tau^{\mp}$	$7.04^{+1.38}_{-1.25} \times 10^{-1}$	$2.35^{+0.55}_{-0.49} \times 10^{-1}$	$1.47^{+1.48}_{-0.75} \times 10^{-1}$	0
	$\ell^+\ell^+\ell^-\ell^-$	—	$5.43^{+1.17}_{-1.05} \times 10^{-1}$	$8.57^{+1.51}_{-1.43} \times 10^{-1}$	0
	$\ell^+\ell^+\ell^-\tau^-$	—	$7.91^{+1.61}_{-1.46} \times 10^{-1}$	$5.99^{+2.70}_{-2.48} \times 10^{-2}$	0
	$\ell^+\tau^+\ell^-\tau^-$	—	$1.08^{+0.23}_{-0.20} \times 10^0$	$2.12^{+1.18}_{-0.85} \times 10^{-2}$	1
100% $\Phi \to \mu\mu$	$\ell^{\pm}\ell^{\pm}\ell^{\mp}$	$2.19^{+0.37}_{-0.32} \times 10^1$	$4.07^{+0.68}_{-0.60} \times 10^0$	$1.14^{+0.33}_{-0.28} \times 10^0$	3
	$\ell^{\pm}\ell^{\pm}\tau^{\mp}$	$3.35^{+0.60}_{-0.54} \times 10^0$	—	$4.23^{+4.45}_{-2.46} \times 10^{-2}$	0
	$\ell^+\ell^+\ell^-\ell^-$	—	$1.40^{+0.23}_{-0.21} \times 10^1$	$9.03^{+2.90}_{-2.37} \times 10^{-2}$	0
100% $\Phi \to \mu\tau$	$\ell^{\pm}\ell^{\pm}\ell^{\mp}$	$3.67^{+0.64}_{-0.57} \times 10^0$	$1.66^{+0.31}_{-0.28} \times 10^0$	$6.94^{+2.53}_{-1.95} \times 10^0$	9
	$\ell^{\pm}\ell^{\pm}\tau^{\mp}$	$5.00^{+0.95}_{-0.85} \times 10^{-1}$	$8.35^{+2.39}_{-1.95} \times 10^{-2}$	$3.64^{+2.31}_{-1.47} \times 10^{-1}$	0
	$\ell^{\pm}\tau^{\pm}\ell^{\mp}$	$5.82^{+1.04}_{-0.93} \times 10^0$	$2.47^{+0.45}_{-0.41} \times 10^0$	$8.86^{+3.87}_{-2.89} \times 10^{-1}$	3
	$\ell^{\pm}\tau^{\pm}\tau^{\mp}$	$8.62^{+1.67}_{-1.50} \times 10^{-1}$	$1.33^{+0.35}_{-0.30} \times 10^{-1}$	$2.42^{+2.44}_{-1.24} \times 10^{-1}$	0
	$\ell^+\ell^+\ell^-\ell^-$	—	$7.02^{+1.35}_{-1.21} \times 10^{-1}$	$1.52^{+0.33}_{-0.29} \times 10^0$	1
	$\ell^+\ell^+\ell^-\tau^-$	—	$1.09^{+0.21}_{-0.19} \times 10^0$	$1.18^{+0.40}_{-0.37} \times 10^{-1}$	0
	$\ell^+\tau^+\ell^-\tau^-$	—	$1.61^{+0.35}_{-0.31} \times 10^0$	$9.74^{+4.55}_{-3.40} \times 10^{-3}$	0
100% $\Phi \to \tau\tau$	$\ell^{\pm}\ell^{\pm}\ell^{\mp}$	$5.20^{+0.98}_{-0.87} \times 10^{-1}$	$3.72^{+1.49}_{-1.09} \times 10^{-2}$	$5.81^{+2.09}_{-1.63} \times 10^0$	9
	$\ell^{\pm}\ell^{\pm}\tau^{\mp}$	$4.67^{+1.35}_{-1.09} \times 10^{-2}$	$9.81^{+2.79}_{-2.28} \times 10^{-2}$	$8.11^{+6.75}_{-3.99} \times 10^{-1}$	0
	$\ell^{\pm}\tau^{\pm}\ell^{\mp}$	$1.71^{+0.32}_{-0.29} \times 10^0$	$1.75^{+0.48}_{-0.41} \times 10^{-1}$	$1.34^{+0.57}_{-0.36} \times 10^0$	1
	$\ell^{\pm}\tau^{\pm}\tau^{\mp}$	$2.01^{+0.45}_{-0.40} \times 10^{-1}$	$3.31^{+0.77}_{-0.69} \times 10^{-1}$	$3.13^{+2.53}_{-1.30} \times 10^{-1}$	0
	$\tau^{\pm}\tau^{\pm}\ell^{\mp}$	$1.41^{+0.27}_{-0.25} \times 10^0$	$1.10^{+0.31}_{-0.26} \times 10^{-1}$	$1.83^{+1.00}_{-0.58} \times 10^{-1}$	0
	$\tau^{\pm}\tau^{\pm}\tau^{\mp}$	$1.72^{+0.41}_{-0.37} \times 10^{-1}$	$2.65^{+0.69}_{-0.61} \times 10^{-1}$	$1.25^{+0.70}_{-0.48} \times 10^{-1}$	0
	$\ell^+\ell^+\ell^-\ell^-$	—	$2.17^{+1.07}_{-0.67} \times 10^{-2}$	$2.29^{+0.37}_{-0.34} \times 10^0$	3
	$\ell^+\ell^+\ell^-\tau^-$	—	$7.72^{+2.42}_{-1.87} \times 10^{-2}$	$1.51^{+0.48}_{-0.44} \times 10^{-1}$	0
	$\ell^+\ell^+\tau^-\tau^-$	—	$6.94^{+2.37}_{-1.91} \times 10^{-2}$	$1.55^{+1.77}_{-1.33} \times 10^{-4}$	0
	$\ell^+\tau^+\ell^-\tau^-$	—	$2.55^{+0.60}_{-0.52} \times 10^{-1}$	$6.50^{+2.11}_{-2.02} \times 10^{-2}$	0
	$\ell^+\tau^+\tau^-\tau^-$	—	$1.87^{+0.53}_{-0.46} \times 10^{-1}$	$4.93^{+2.11}_{-1.95} \times 10^{-2}$	0
	$\tau^+\tau^+\tau^-\tau^-$	—	$1.55^{+0.58}_{-0.49} \times 10^{-1}$	$5.54^{+4.33}_{-4.18} \times 10^{-3}$	0

Generator channel	3ℓ reconstructed channel						4ℓ reconstructed channel						Total
	$\ell^\pm\ell^\pm\ell^\mp$	$\ell^\pm\ell^\pm\tau^\mp$	$\ell^\pm\tau^\pm\ell^\mp$	$\ell^\pm\tau^\pm\tau^\mp$	$\tau^\pm\tau^\pm\ell^\mp$	$\tau^\pm\tau^\pm\tau^\mp$	$\ell^+\ell^+\ell^-\ell^-$	$\ell^+\ell^+\ell^-\tau^-$	$\ell^+\ell^+\tau^-\tau^-$	$\ell^+\tau^+\ell^-\tau^-$	$\ell^+\tau^+\tau^-\tau^-$	$\tau^+\tau^+\tau^-\tau^-$	
eee	41.4	—	—	—	—	—	—	—	—	—	—	—	41.4
$ee\mu$	47.2	—	—	—	—	—	—	—	—	—	—	—	47.2
$ee\tau$	10.4	13.9	—	—	—	—	—	—	—	—	—	—	24.3
$e\mu e$	46.0	—	—	—	—	—	—	—	—	—	—	—	46.0
$e\mu\mu$	54.8	—	—	—	—	—	—	—	—	—	—	—	54.8
$e\mu\tau$	11.6	15.9	—	—	—	—	—	—	—	—	—	—	27.5
$e\tau e$	9.6	—	13.2	—	—	—	—	—	—	—	—	—	22.8
$e\tau\mu$	11.4	—	15.6	—	—	—	—	—	—	—	—	—	27.0
$e\tau\tau$	1.7	2.9	2.7	4.4	—	—	—	—	—	—	—	—	11.6
$\mu\mu e$	55.0	—	—	—	—	—	—	—	—	—	—	—	55.0
$\mu\mu\mu$	64.7	—	—	—	—	—	—	—	—	—	—	—	64.7
$\mu\mu\tau$	14.4	18.9	—	—	—	—	—	—	—	—	—	—	33.3
$\mu\tau e$	11.1	—	15.3	—	—	—	—	—	—	—	—	—	26.4
$\mu\tau\mu$	13.0	—	18.5	—	—	—	—	—	—	—	—	—	31.5
$\mu\tau\tau$	2.1	3.2	3.0	5.2	—	—	—	—	—	—	—	—	13.4
$\tau\tau e$	1.6	—	5.1	—	3.8	—	—	—	—	—	—	—	10.5
$\tau\tau\mu$	1.7	—	5.8	—	4.9	—	—	—	—	—	—	—	12.5
$\tau\tau\tau$	0.2	0.3	0.5	1.4	0.5	1.1	—	—	—	—	—	—	4.0
$eeee$	3.9	—	—	—	—	—	28.9	—	—	—	—	—	32.7
$eee\mu$	5.7	—	—	—	—	—	32.8	—	—	—	—	—	38.5
$eee\tau$	11.9	1.4	2.4	—	—	—	8.4	11.6	—	—	—	—	35.6
$ee\mu\mu$	7.3	—	—	—	—	—	38.7	—	—	—	—	—	46.0
$ee\mu\tau$	13.4	0.8	2.6	—	—	—	9.7	13.4	—	—	—	—	40.0
$ee\tau\tau$	7.0	7.8	1.2	—	0.7	—	2.2	6.4	4.7	—	—	—	30.0
$e\mu e\mu$	7.1	—	—	—	—	—	36.5	—	—	—	—	—	43.6
$e\mu e\tau$	13.0	1.6	1.9	—	—	—	9.8	13.1	—	—	—	—	39.4
$e\mu\mu\mu$	8.4	—	—	—	—	—	43.5	—	—	—	—	—	51.9
$e\mu\mu\tau$	15.9	0.9	2.2	—	—	—	11.2	14.5	—	—	—	—	44.7
$e\mu\tau\tau$	8.0	8.6	1.2	—	0.6	—	2.6	6.7	4.9	—	—	—	32.6
$e\tau e\tau$	6.2	0.7	7.2	1.0	—	—	2.6	6.8	—	4.0	—	—	28.5
$e\tau\mu\mu$	15.0	1.8	1.9	—	—	—	11.7	15.1	—	—	—	—	45.5
$e\tau\mu\tau$	7.2	0.6	8.6	0.8	—	—	2.7	7.8	—	5.7	—	—	33.4
$e\tau\tau\tau$	1.6	1.7	3.6	2.2	1.0	0.1	0.7	2.7	1.1	2.5	1.7	—	19.0
$\mu\mu\mu\mu$	9.2	—	—	—	—	—	51.7	—	—	—	—	—	60.9
$\mu\mu\mu\tau$	17.4	1.0	2.1	—	—	—	13.5	17.3	—	—	—	—	51.2
$\mu\mu\tau\tau$	9.2	10.7	0.9	—	0.5	—	2.9	9.0	5.8	—	—	—	39.0
$\mu\tau\mu\tau$	8.3	0.4	10.6	0.6	—	—	3.0	9.3	—	5.9	—	—	38.1
$\mu\tau\tau\tau$	1.8	1.8	3.9	2.8	1.4	0.0	0.8	3.1	1.4	2.8	2.1	—	21.8
$\tau\tau\tau\tau$	0.2	0.5	0.8	1.5	0.5	1.2	0.1	0.9	0.6	1.1	1.6	0.7	9.6

Limits on 100% Φ⁺⁺ → ee

Limits on 100% $\Phi^{++} \to e\mu$

Limits on 100% Φ⁺⁺ → μμ

Limits on 100% $\Phi^{++} \rightarrow e\tau$

Limits on 100% $\Phi^{++} \rightarrow \mu\tau$

Limits on 100% $\Phi^{++} \rightarrow \tau\tau$
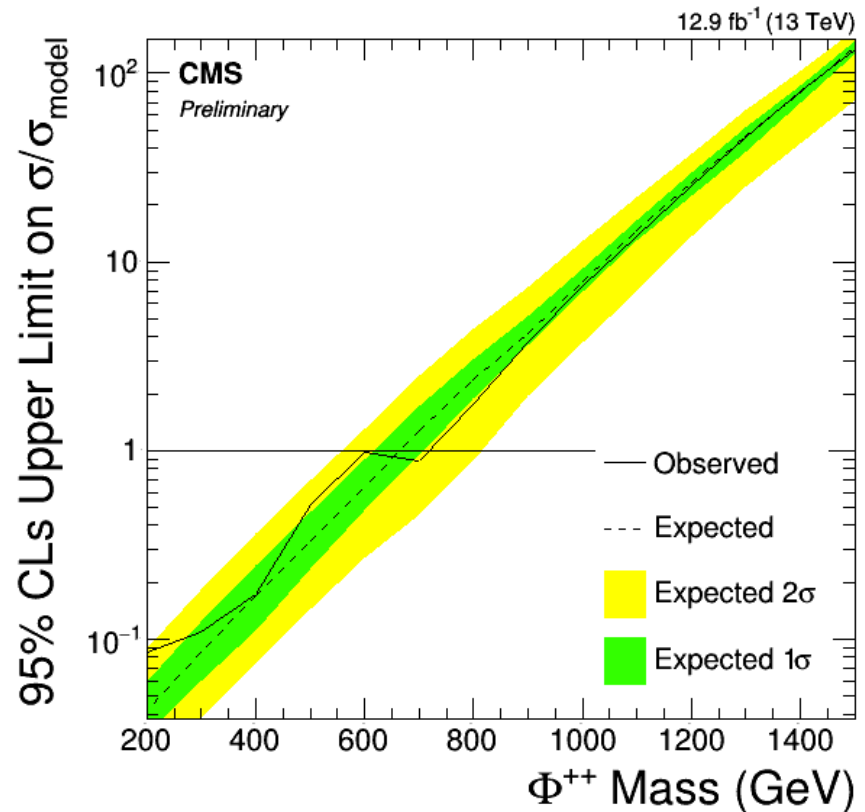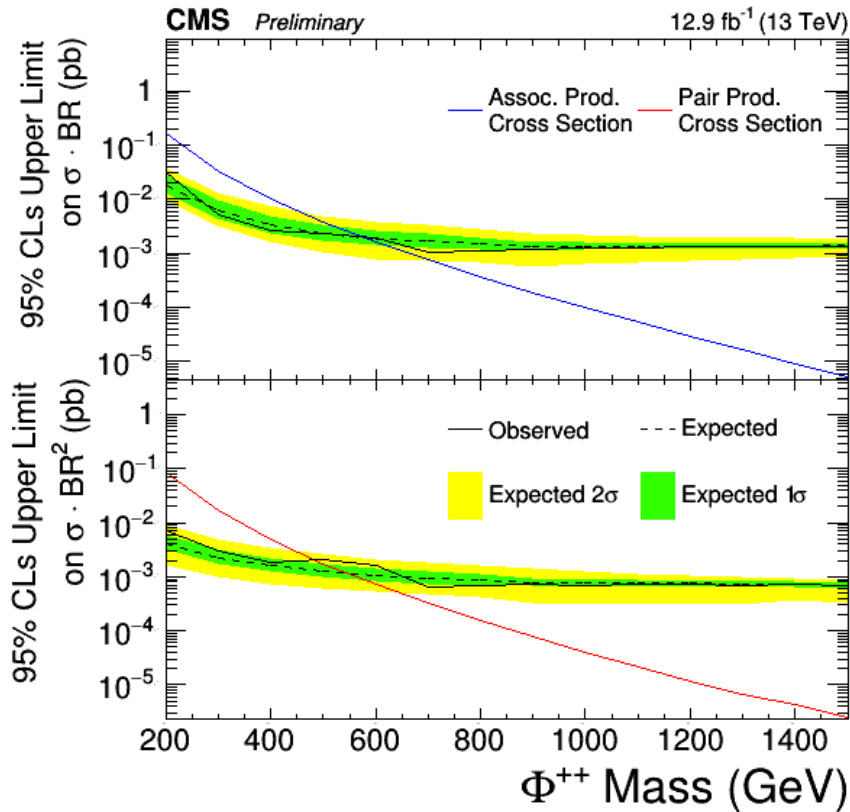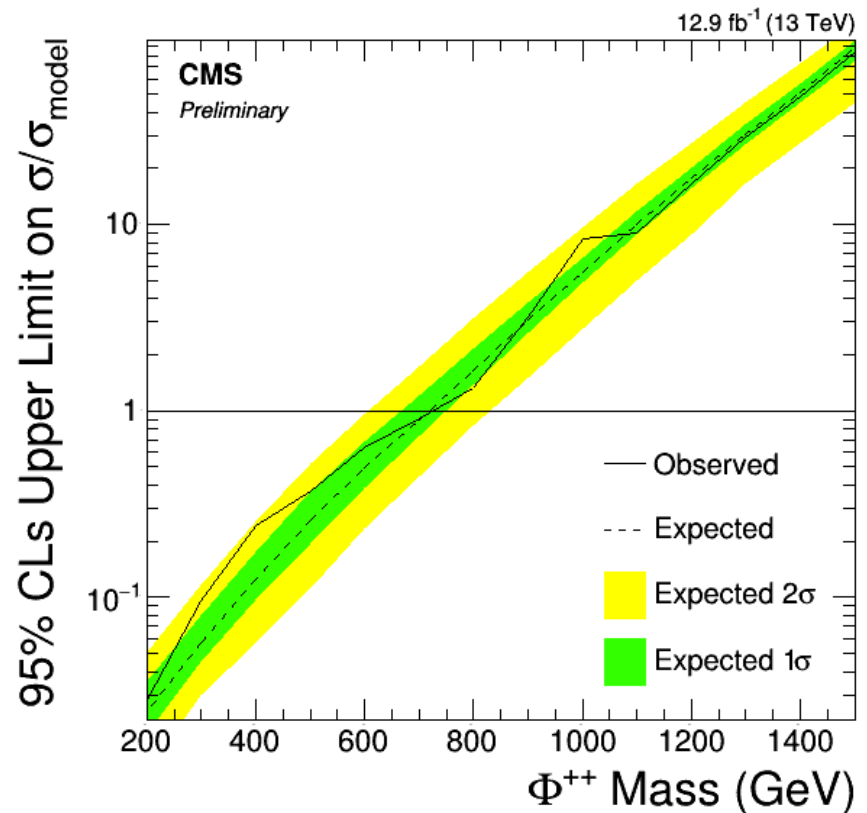
Limits on Benchmark 1
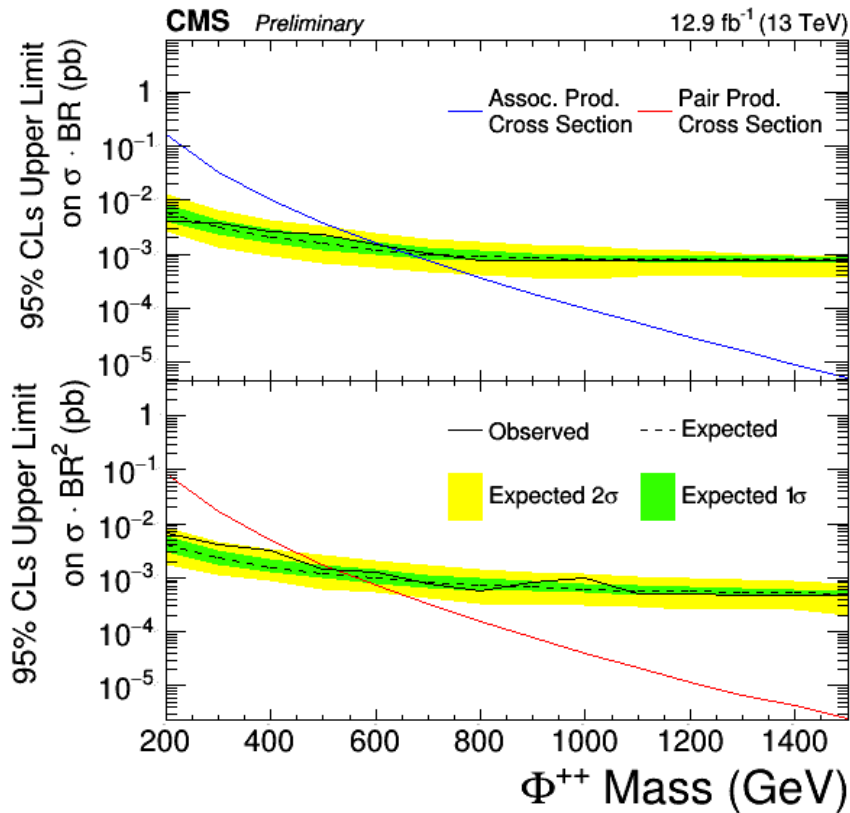
Limits on Benchmark 2

Limits on Benchmark 3
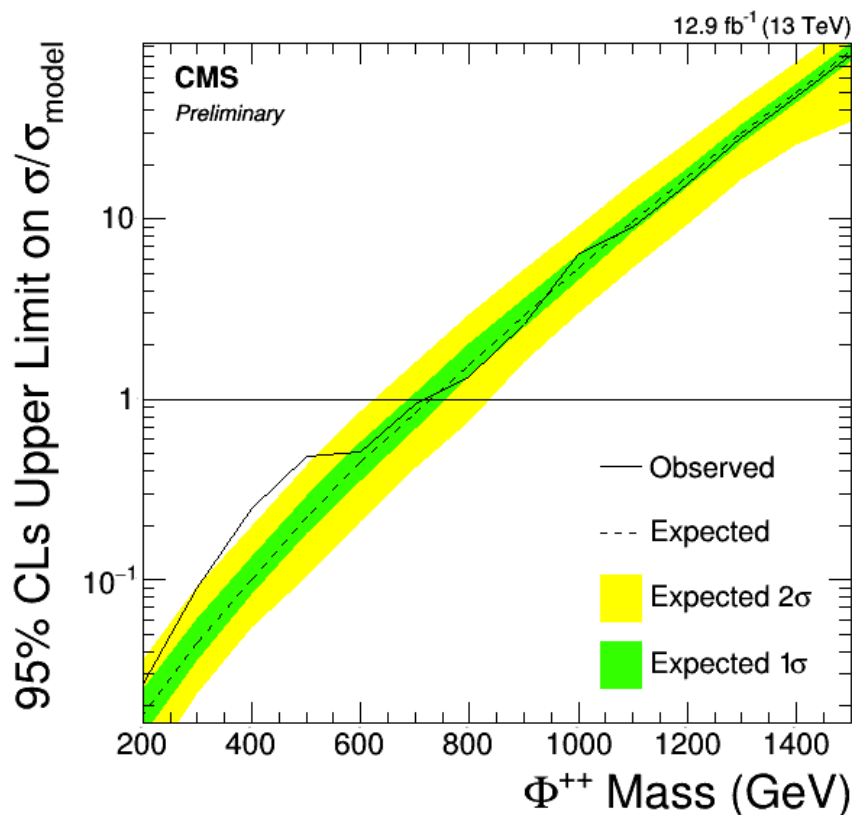
Devin Taylor   January 19, 2017

Limits on Benchmark 4
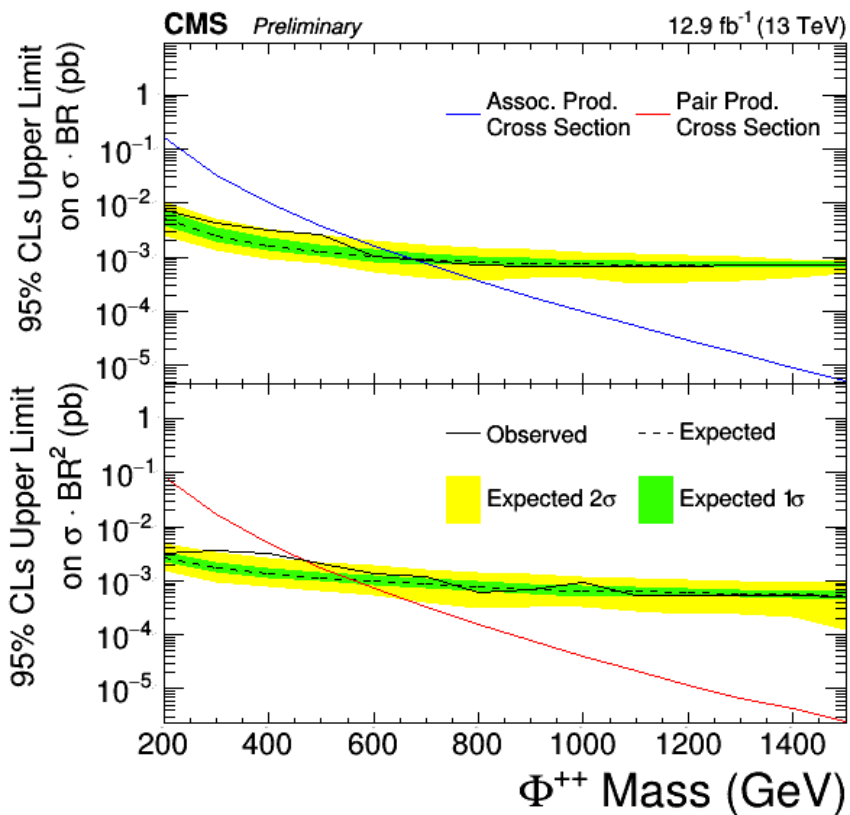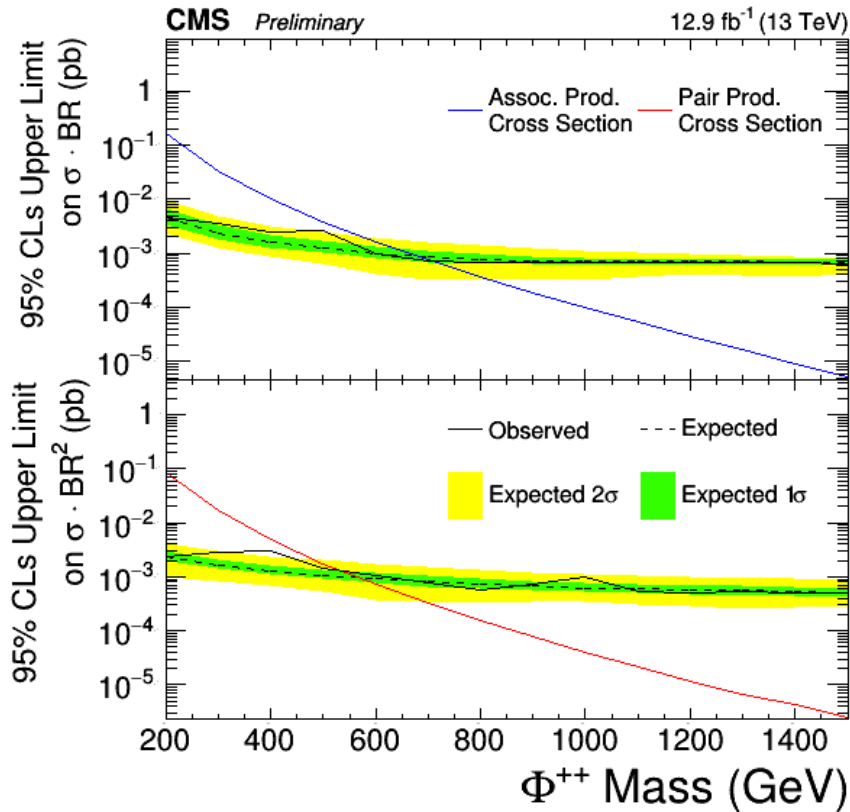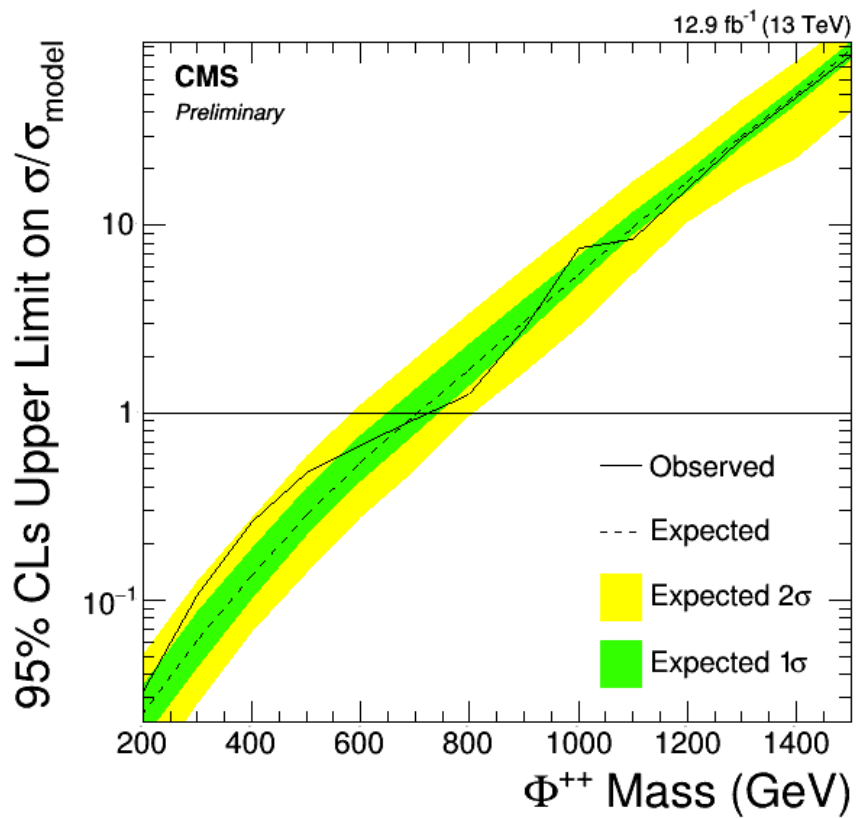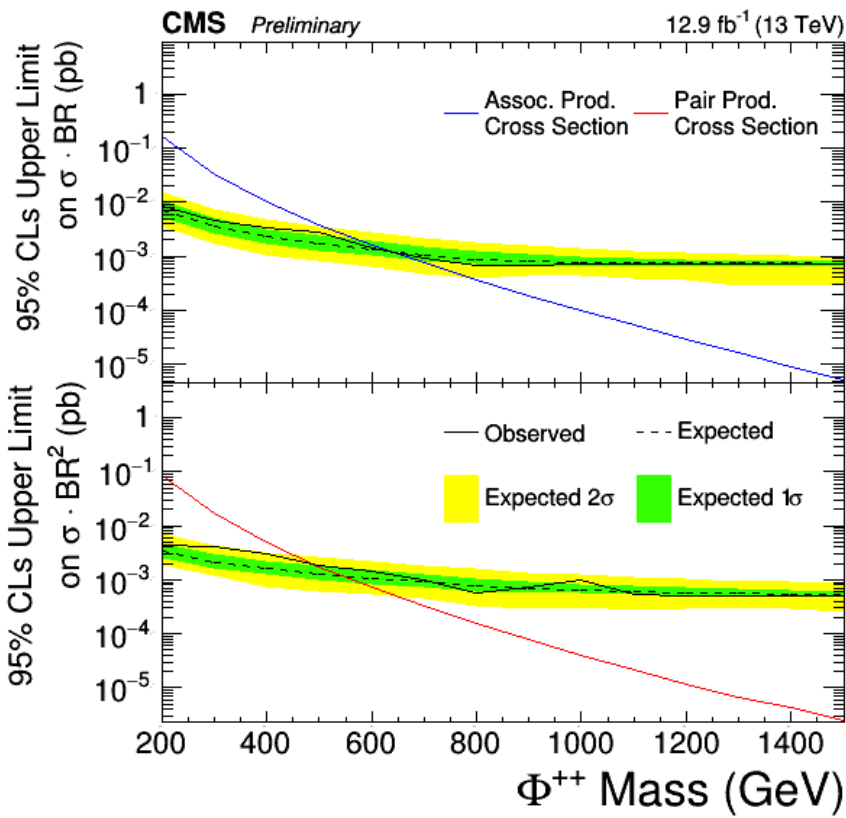
Excluded with Previous Results
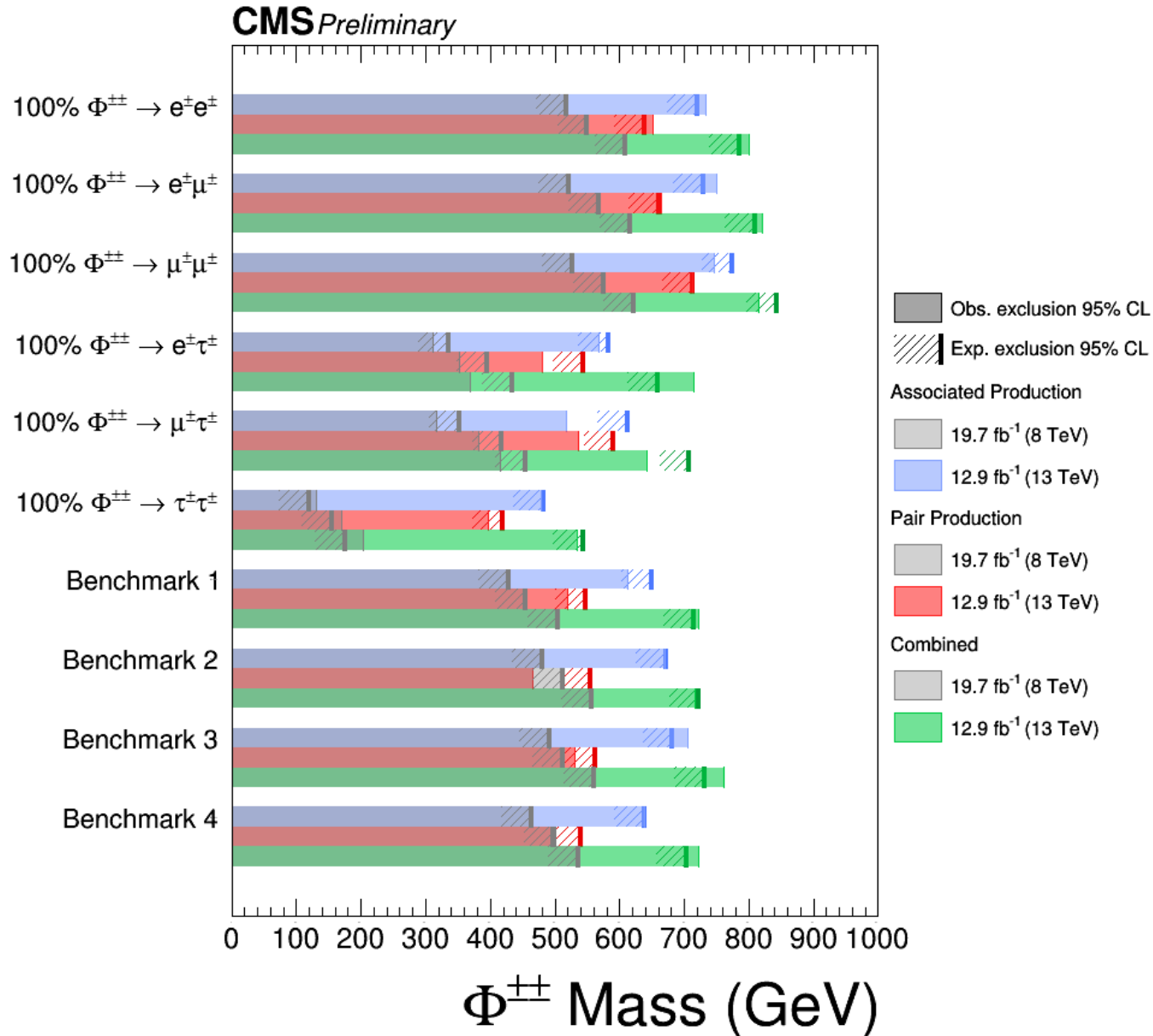
Comparison to Prior Results

- Comparison of Associated (AP) and Pair (PP) Production limits to previous results from ATLAS and cMS

Scenario	CMS PP	New PP	ATLAS PP	CMS AP	New AP
$BR(\Phi^{\pm\pm} \rightarrow e^{\pm}e^{\pm}) = 100\%$	550 (550)	652 (639)	551 (553)	517 (517)	734 (720)
$BR(\Phi^{\pm\pm} \rightarrow e^{\pm}\mu^{\pm}) = 100\%$	569 (568)	665 (660)	468 (487)	521 (521)	750 (729)
$BR(\Phi^{\pm\pm} \rightarrow e^{\pm}\tau^{\pm}) = 100\%$	353 (395)	481 (543)	–	312 (336)	568 (582)
$BR(\Phi^{\pm\pm} \rightarrow \mu^{\pm}\mu^{\pm}) = 100\%$	576 (575)	712 (712)	516 (543)	526 (526)	746 (774)
$BR(\Phi^{\pm\pm} \rightarrow \mu^{\pm}\tau^{\pm}) = 100\%$	381 (418)	537 (591)	–	316 (352)	518 (613)
$BR(\Phi^{\pm\pm} \rightarrow \tau^{\pm}\tau^{\pm}) = 100\%$	169 (155)	396 (419)	–	130 (120)	479 (483)